University of Ferrara

INFN
Istituto Nazionale di Fisica Nucleare

Exploring the multidimensional structure of the nucleon

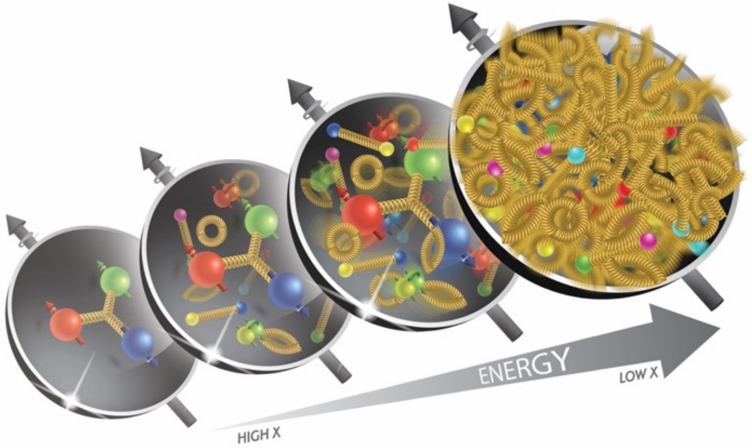

L. L. Pappalardo
(pappalardo@fe.infn.it)

Understanding the proton and its structure

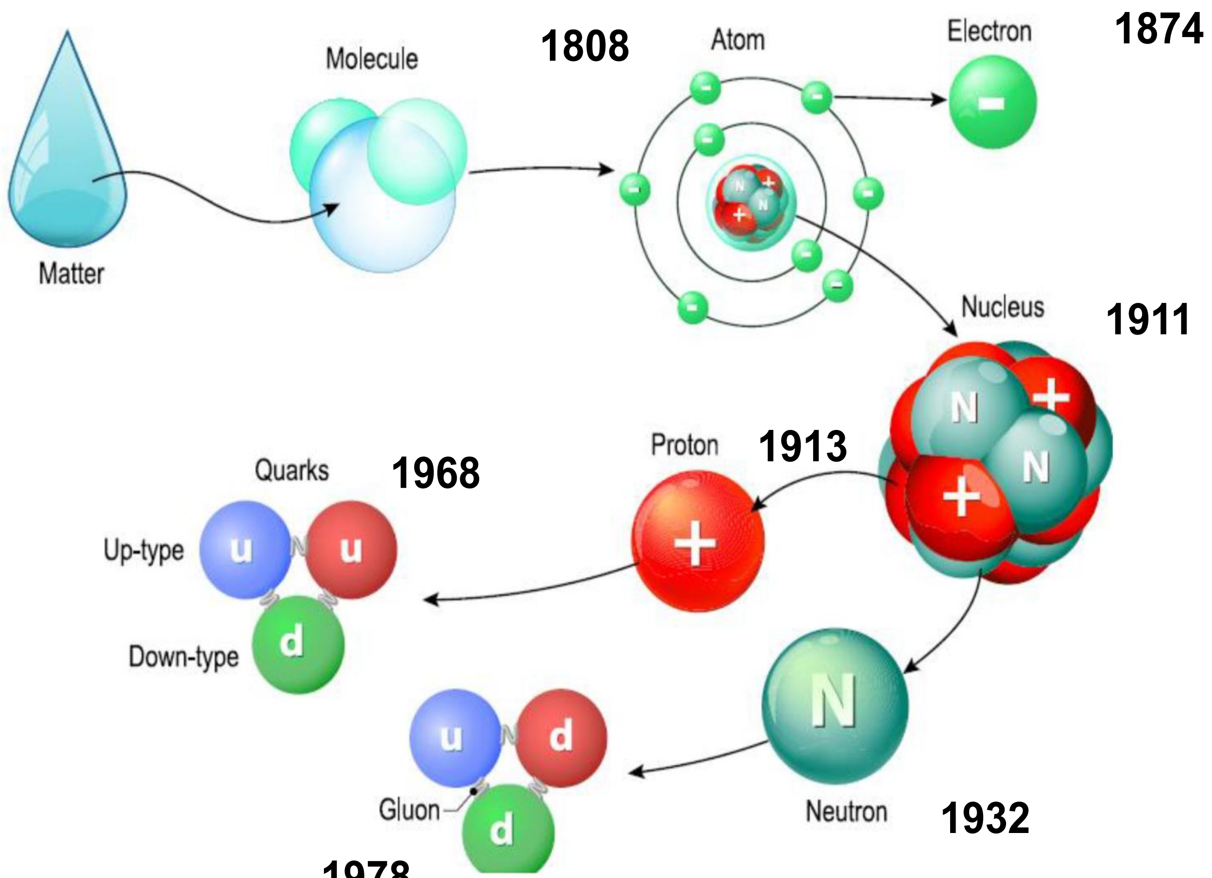

Courtesy R. Ent

Structure of matter: 2 centuries of investigations and discoveries!

We have reached what we consider **the most fundamental level of nature**

Understanding the proton and its structure

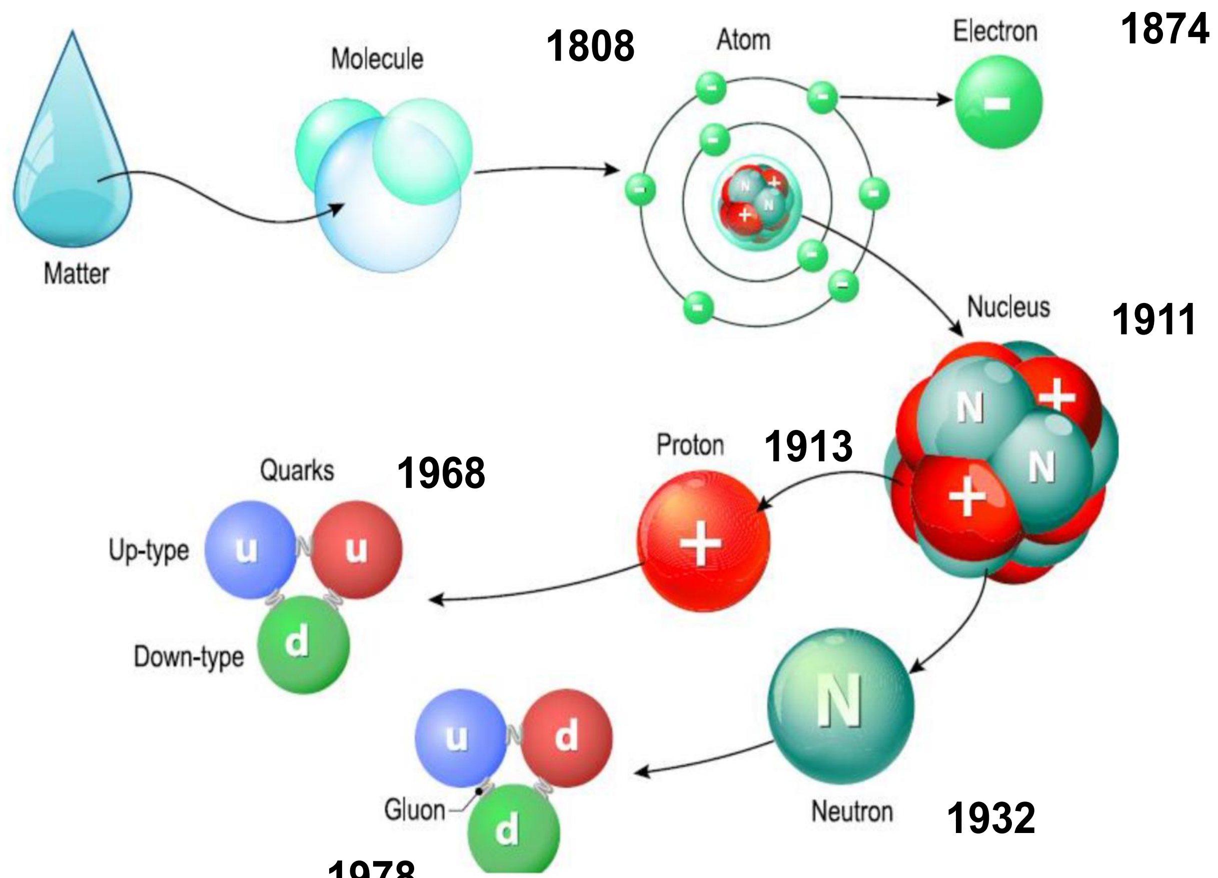

Courtesy R. Ent

Structure of matter: 2 centuries of investigations and discoveries!

We have reached what we consider **the most fundamental level of nature**

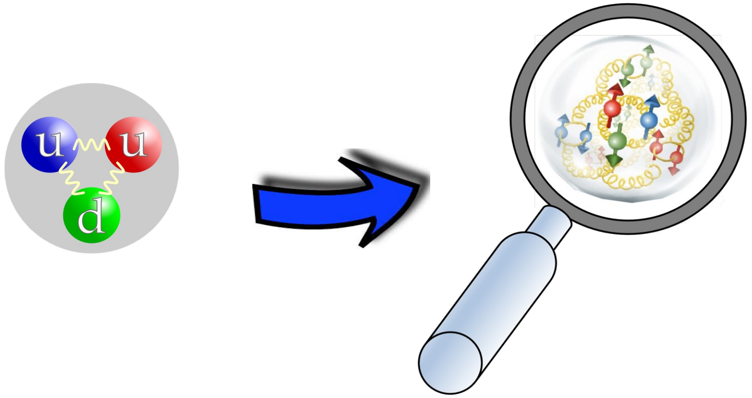

But the nucleon is not just a bound state of 3 quarks! Rather it appears as a **complex system of valence and sea quarks, and gluons interacting with each-other and moving relative to each-other.**

Understanding the proton and its structure

Key question: how do the basic properties of the nucleon (mass, charge, spin, magnetic moment, etc.) emerge from this gurgling microscopic world?

➔ need to access the effective degrees of freedom and study their interactions at large distances

Understanding the proton and its structure

Key question: how do the basic properties of the nucleon (mass, charge, spin, magnetic moment, etc.) emerge from this gurgling microscopic world?

➔ need to access the effective degrees of freedom and study their interactions at large distances

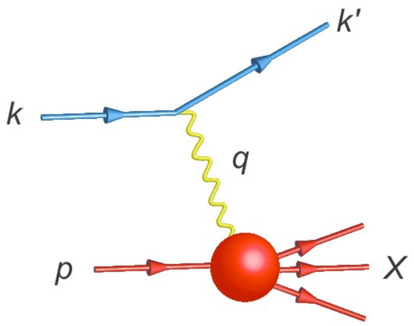

Since the late ’60s, **Deep Inelastic Scattering** has proven to be the most suitable process to access these d.o.f. and study their complex dynamics within nucleons.

Understanding the proton and its structure

Key question: how do the basic properties of the nucleon (mass, charge, spin, magnetic moment, etc.) emerge from this gurgling microscopic world?

➔ need to access the effective degrees of freedom and study their interactions at large distances

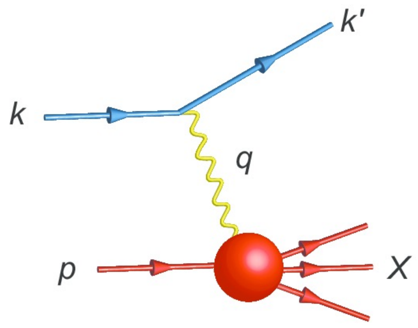

Since the late ’60s, **Deep Inelastic Scattering** has proven to be the most suitable process to access these d.o.f. and study their complex dynamics within nucleons.

Parton model: description in terms of PDFs in a frame where the nucleon moves very fast and **all transverse d.o.f. are neglected**.

The nucleon appears as a **bunch of co-linearly moving partons**, each carrying a fraction x of the nucleon momentum.

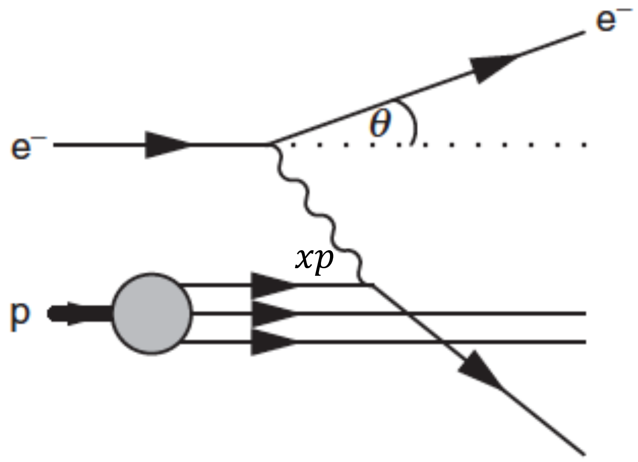

The proton collinear structure

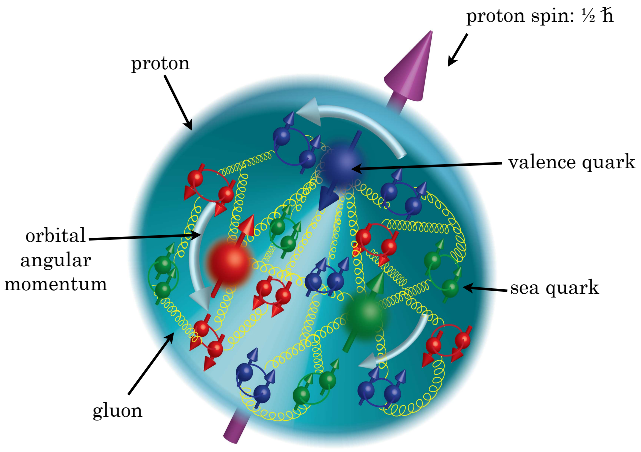

Figure courtesy of: "Electron Ion Collider: The Next QCD Frontier. Understanding the glue that binds us all". arXiv:1212.1701

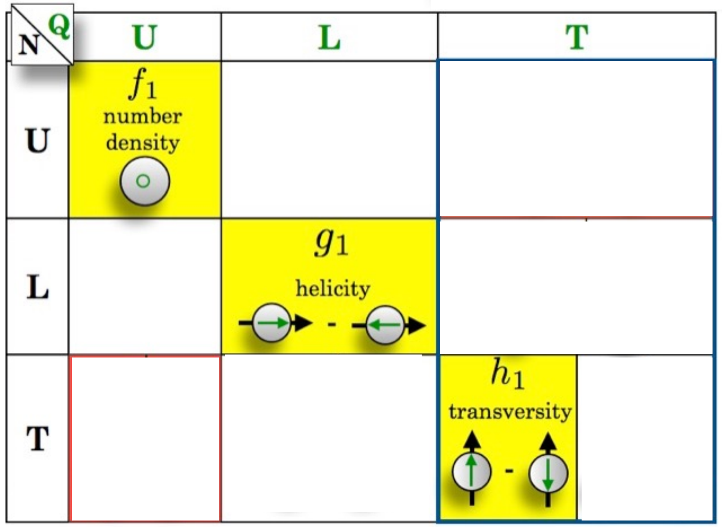

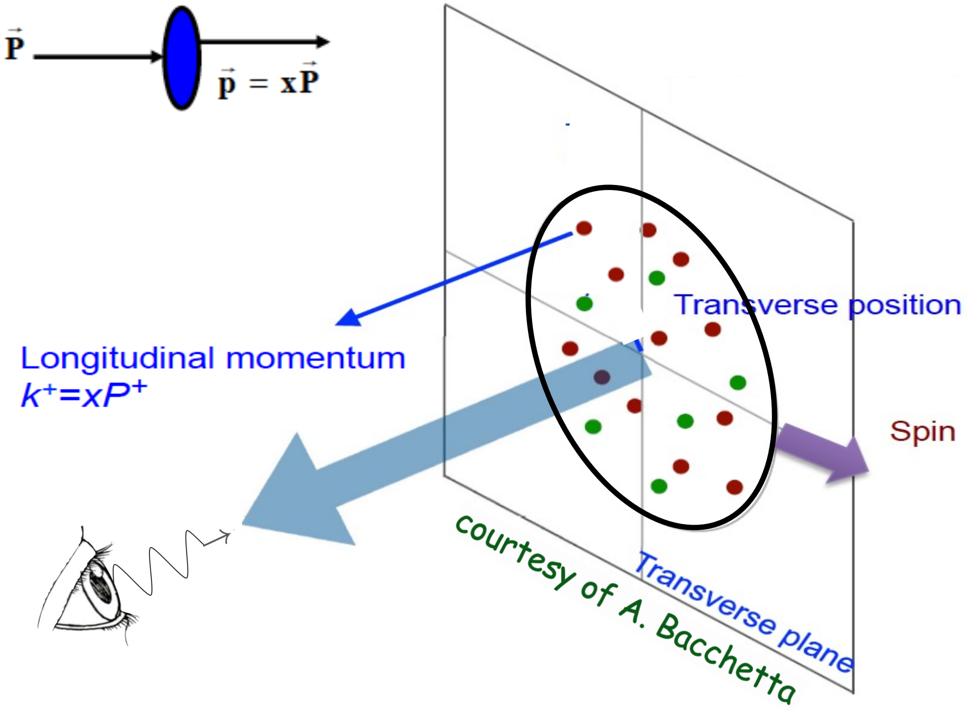

The proton collinear structure

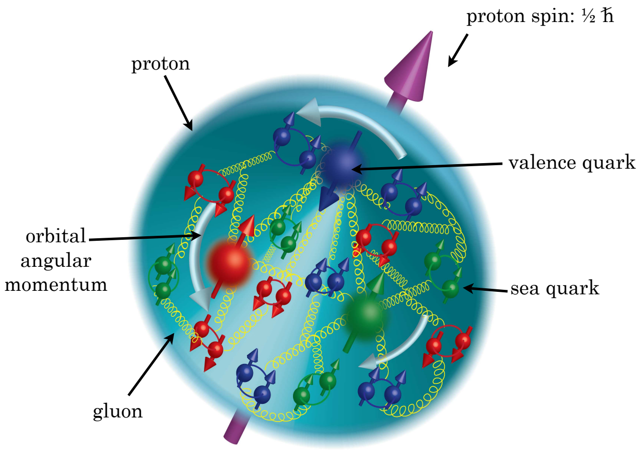

Figure courtesy of: "Electron Ion Collider: The Next QCD Frontier. Understanding the glue that binds us all". arXiv:1212.1701

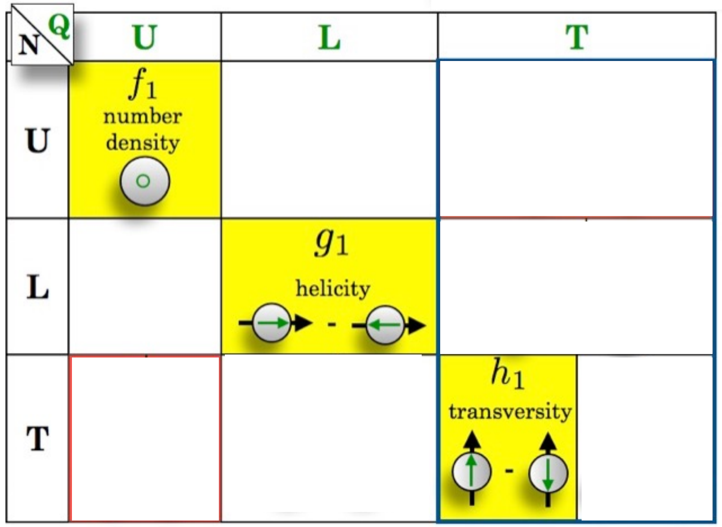

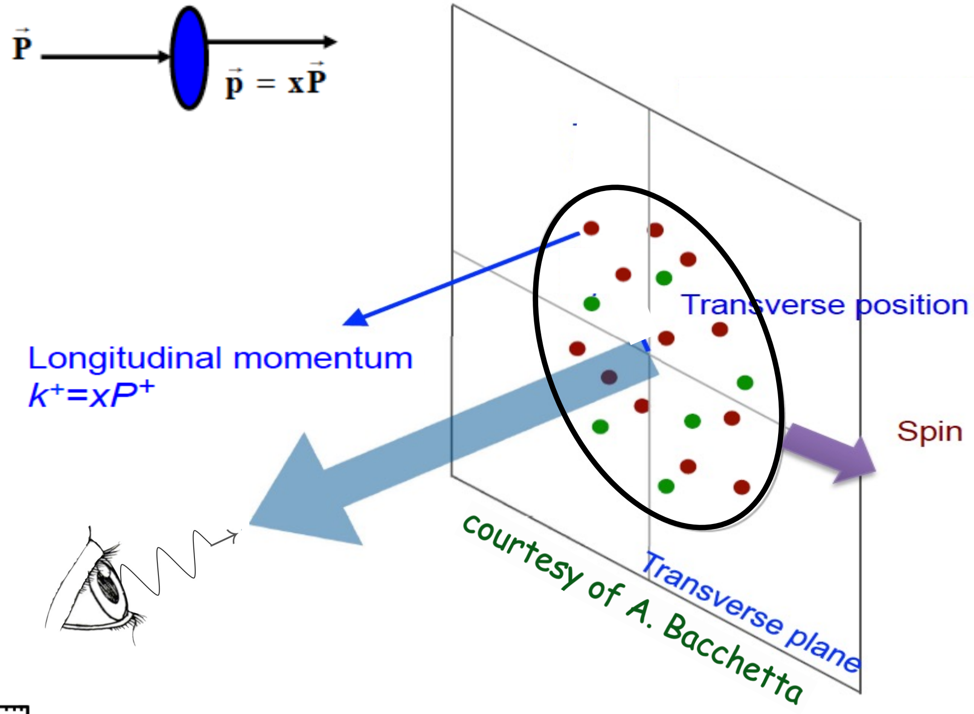

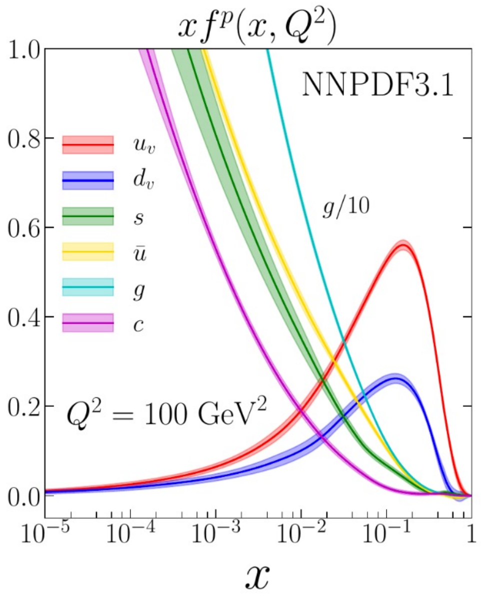

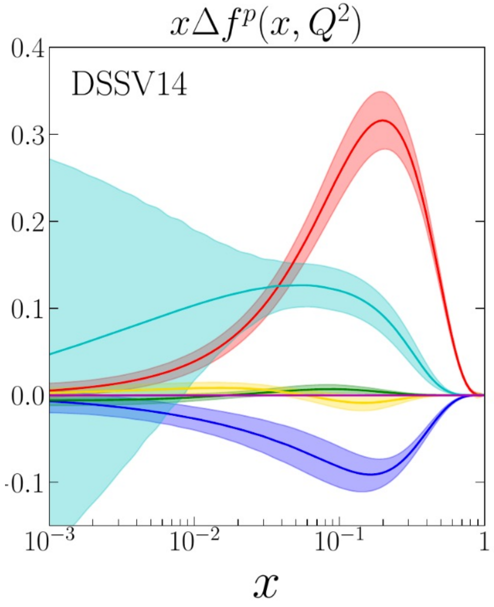

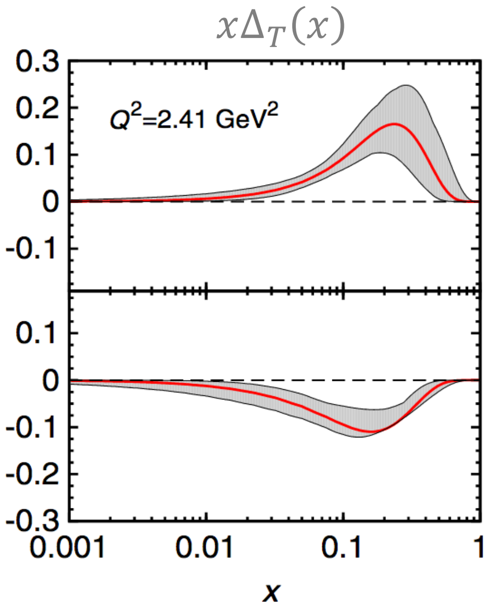

- **rather good knowledge of f_1 and g_1**
- **some knowledge of h_1 from SIDIS**

The proton collinear structure

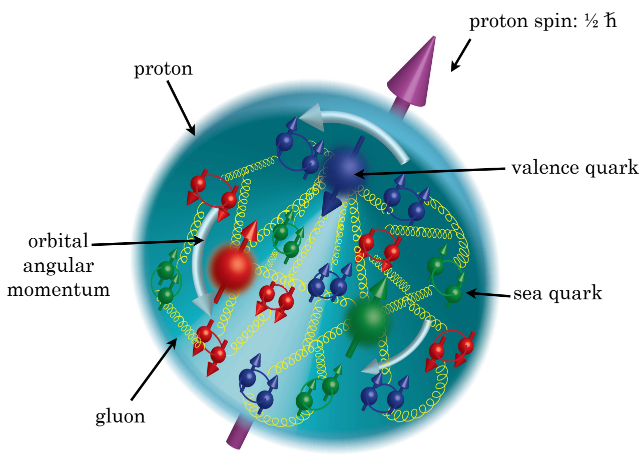

Figure courtesy of: “Electron Ion Collider: The Next QCD Frontier. Understanding the glue that binds us all”. arXiv:1212.1701

N \ Q	U	L	T
U	f_1 number density		
L		g_1 helicity	
T			h_1 transversity

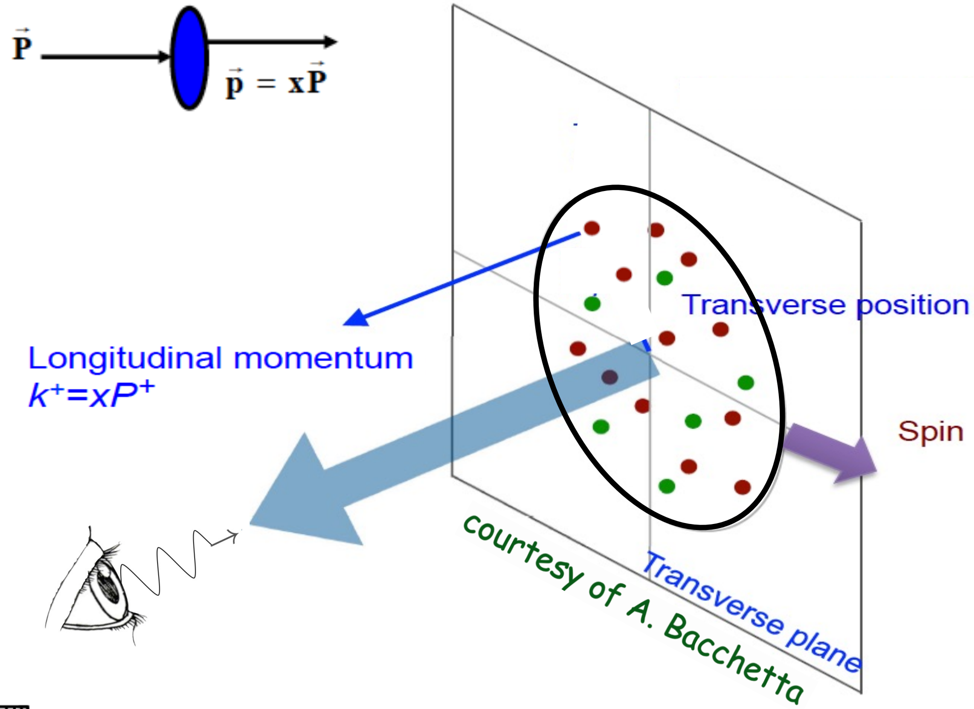

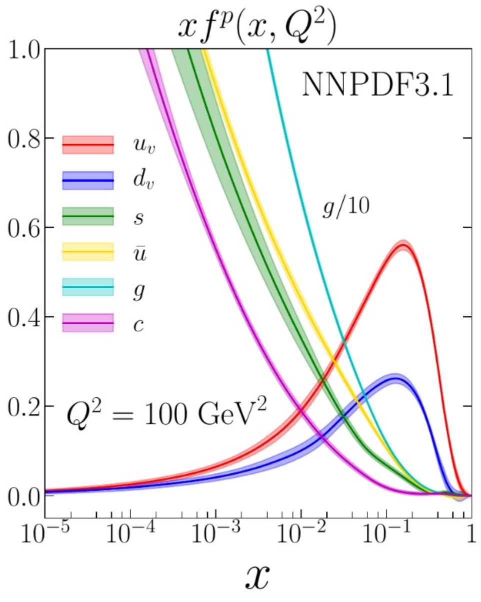

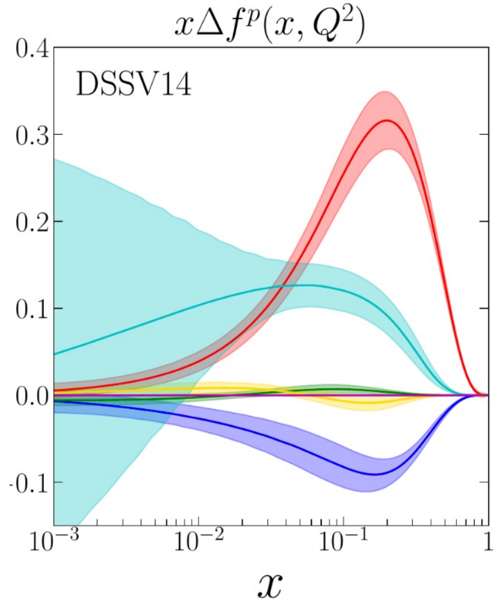

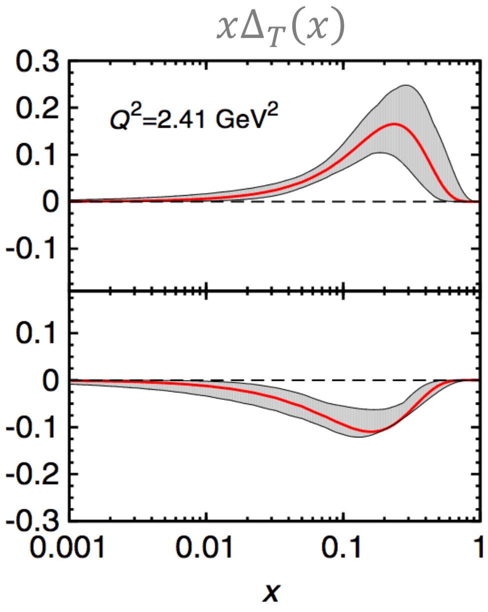

- **rather good knowledge of f_1 and g_1**
- **some knowledge of h_1 from SIDIS**
- **But collinear PDFs provide only a 1D description of the nucleon structure!**
- **A more detailed and multi-dimensional picture of the nucleon requires a new paradigm!**

A new frontier awaits us beyond the collinear approximation!

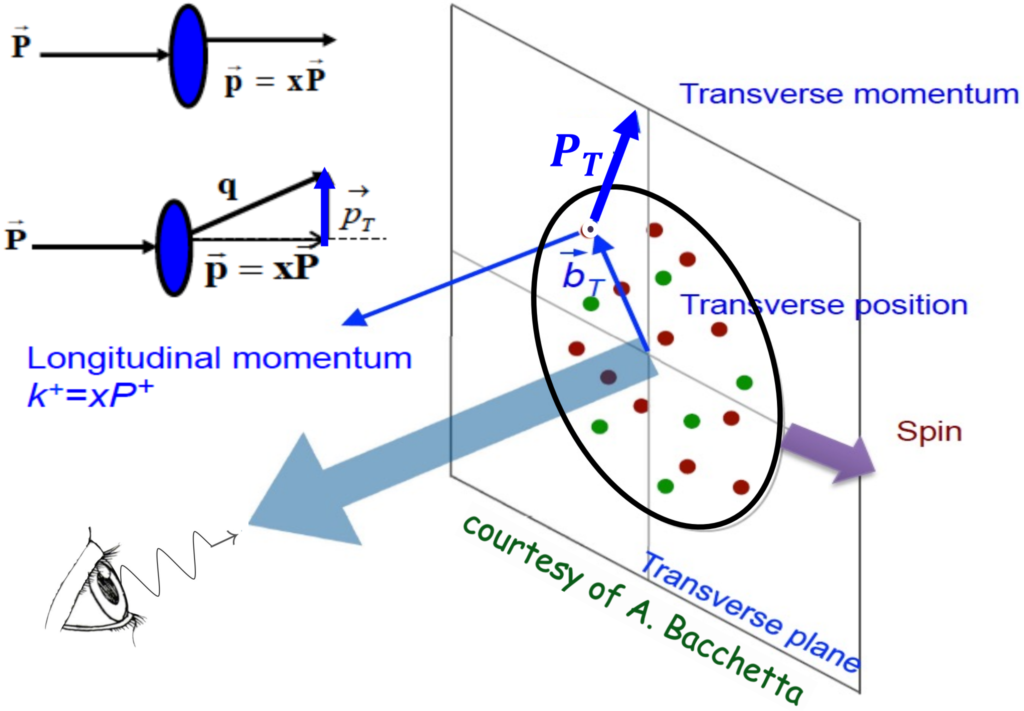

- Exploring this new territories requires taking into account the **transverse d.o.f** (momentum, position, spin) of both parton and nucleon and their correlations

A new frontier awaits us beyond the collinear approximation!

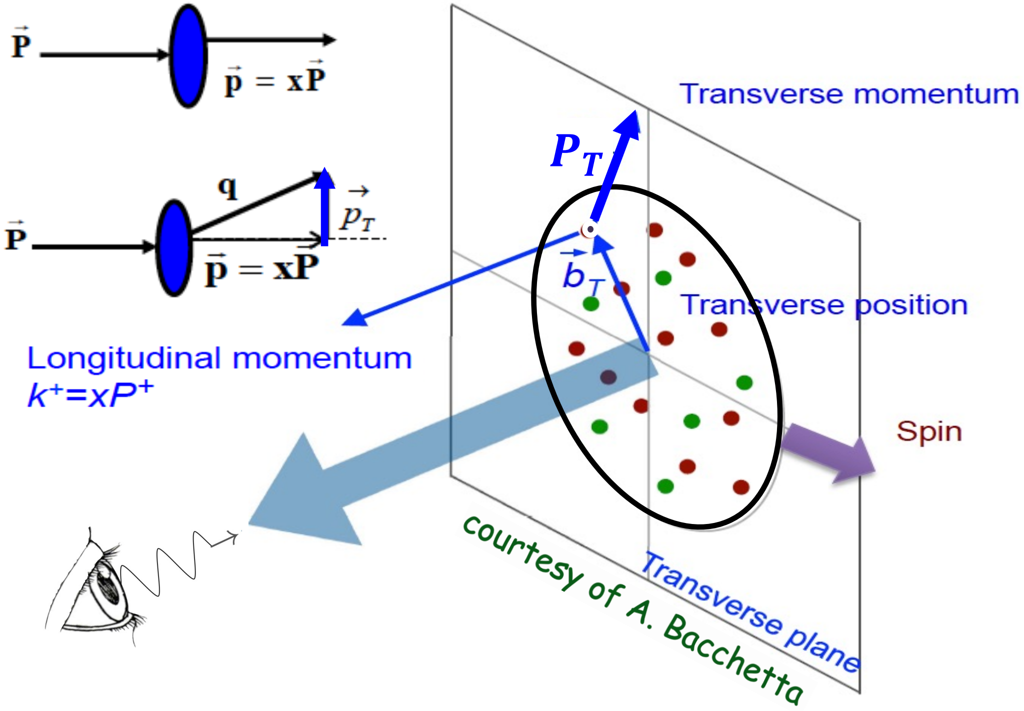

- Exploring this new territories requires taking into account the **transverse d.o.f** (momentum, position, spin) of both parton and nucleon and their correlations
- **Final goal:** **5-D Wigner function** $W(x, k_\perp, r_\perp)$ ➔ full phase-space knowledge of parton distributions …but not directly accessible experimentally!
- One can access the **3D structure of the nucleon**: there are two complementary ways!

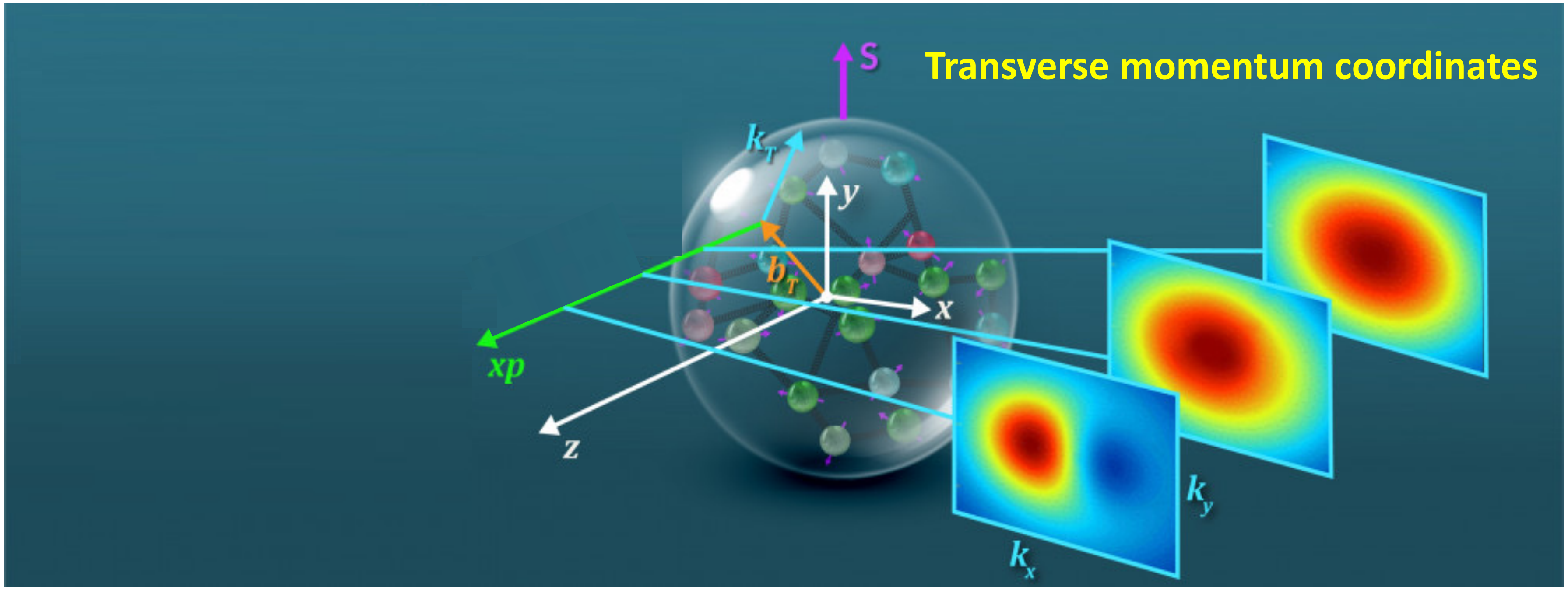

Courtesy *QuantOm Collaboration*

nucleon tomography in mom. space

$W(x, k_\perp, r_\perp)$

$\int d^2 r_\perp$

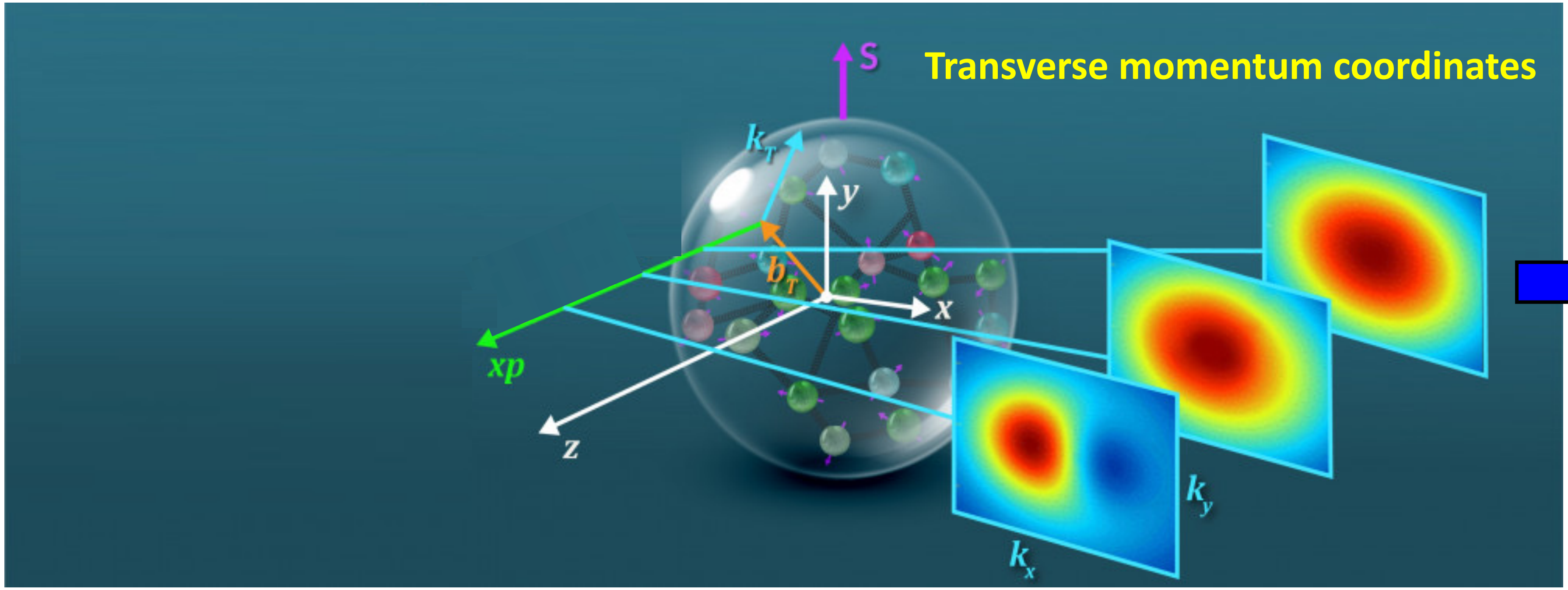

Courtesy *QuantOm Collaboration*

nucleon tomography in mom. space

TMDs

$f(x, k_\perp)$

$W(x, k_\perp, r_\perp)$

$\int d^2 r_\perp$

nucleon tomography in coord. space

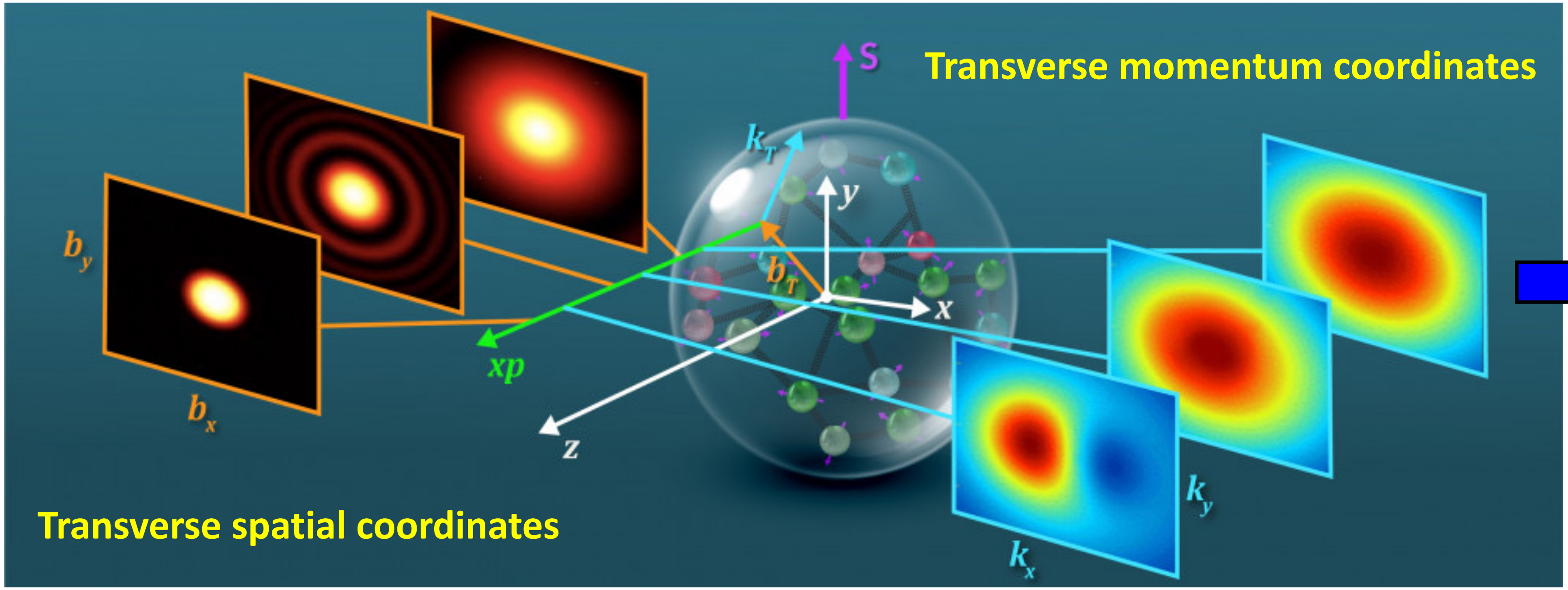

Courtesy *QuantOm Collaboration*

nucleon tomography in mom. space

TMDs

$f(x, k_\perp)$

$W(x, k_\perp, r_\perp)$

$\int d^2k_\perp$

$\int d^2r_\perp$

nucleon tomography in coord. space

$f(x, r_\perp)$

FT

GPDs

$H(x, \xi, t)$

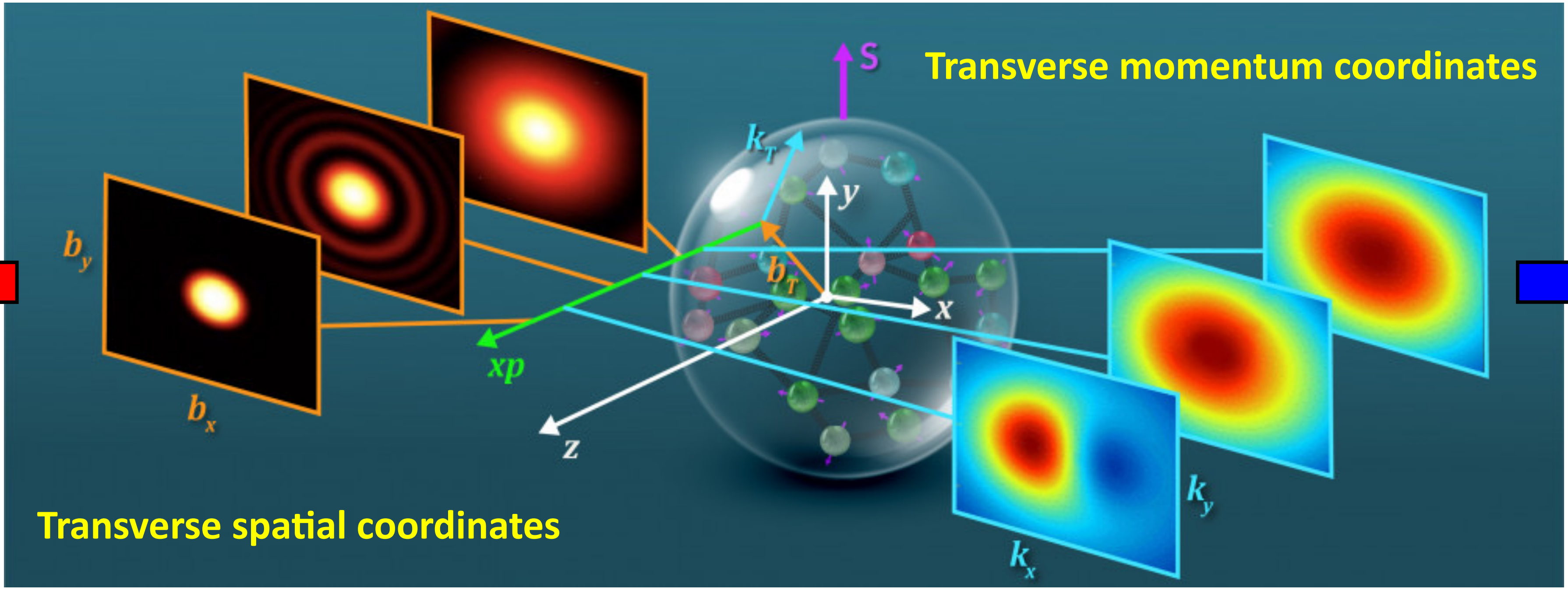

Courtesy *QuantOm Collaboration*

nucleon tomography in mom. space

TMDs

$f(x, k_\perp)$

$W(x, k_\perp, r_\perp)$

$\int d^2k_\perp$ $\int d^2r_\perp$

nucleon tomography in coord. space

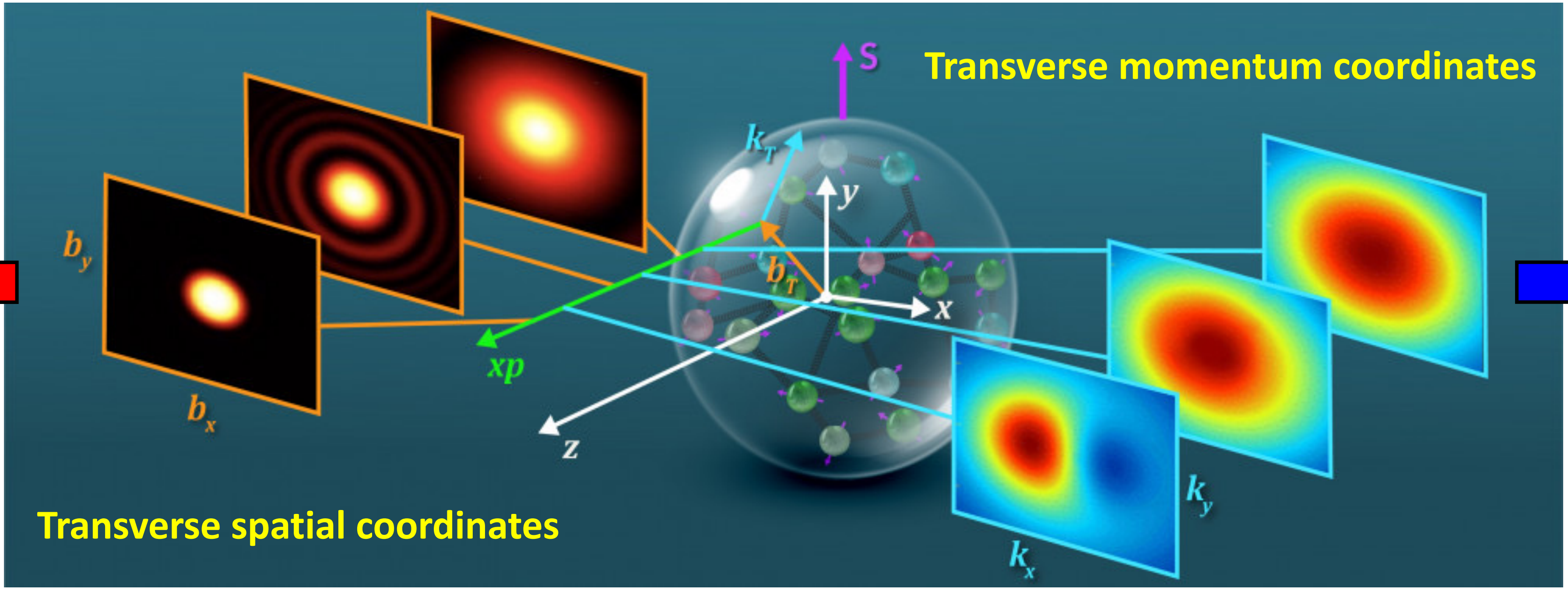

nucleon tomography in mom. space

$f(x, r_\perp)$

FT

GPDs

$H(x, \xi, t)$

$\xi = 0$ $\int dx$

FFs: $f(Q^2)$

TMDs

$f(x, k_\perp)$

$\int d^2k_\perp$

PDFs: $f(x)$

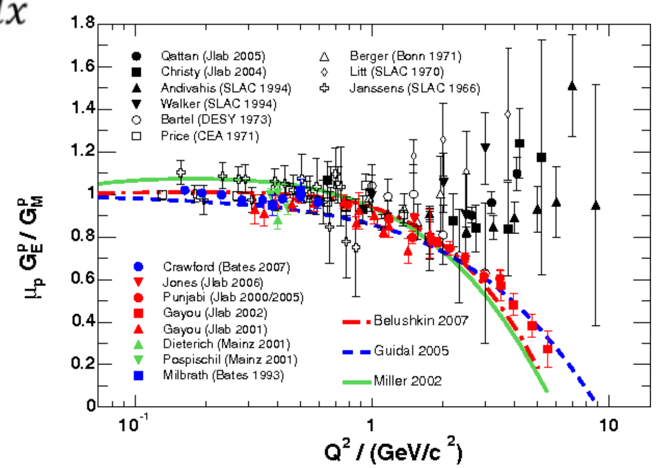

Courtesy *QuantOm Collaboration*

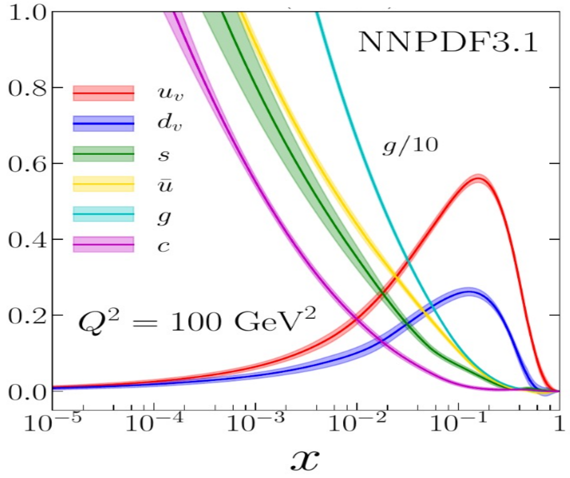

The main ingredients from experiments

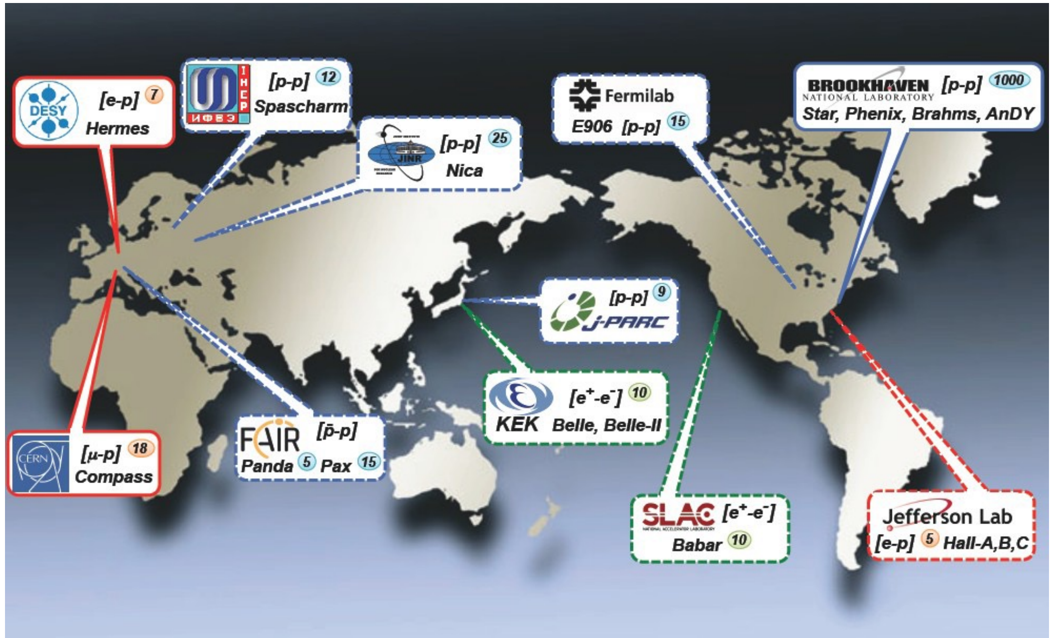

- **Multi-dimensional analysis** → high statistical precision → **High luminosity**
- **Wide kinematic coverage, access both CFR and TFR** → **Large and uniform acceptance detectors**
- **Sensitivity to intrinsic $k_\perp$** → precision measurement of $P_{h\perp}$ → **Excellent tracking**
- **Quark flavour tagging** → **Excellent hadron PID**
- **Large asymmetries** → **High beam and target polarization, small target dilution**
- **Systematics well under control** → **Reliable MC**

The main contributors (with lepton probes)

HERMES (DESY)

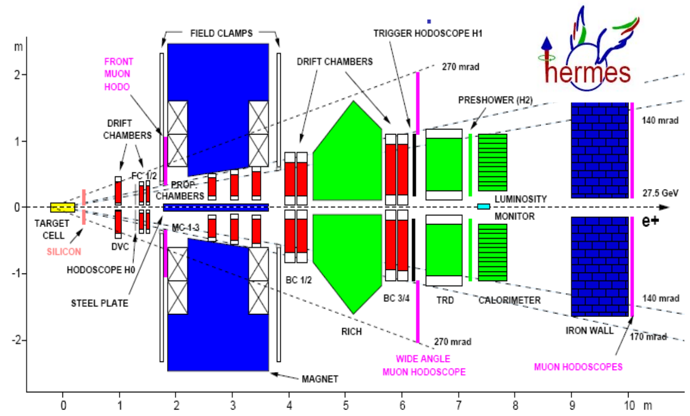

COMPASS/AMBER (CERN)

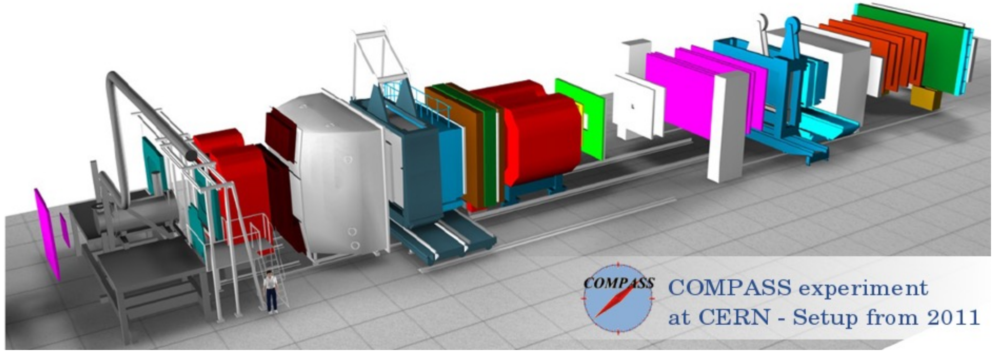

EIC (BNL)

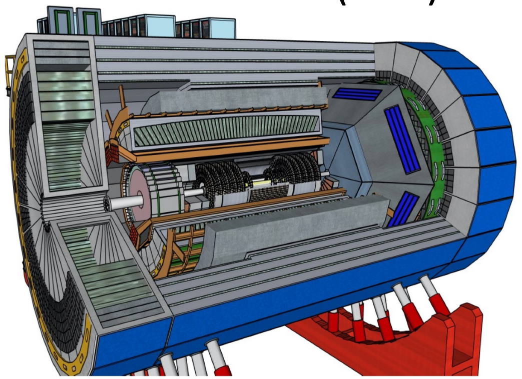

JLab Hall-A

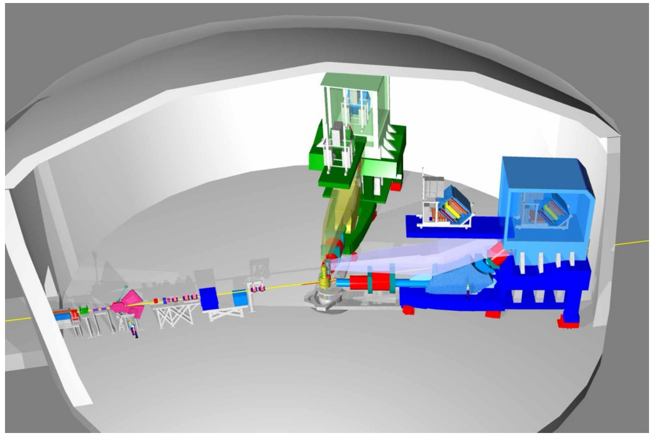

JLab Hall-B

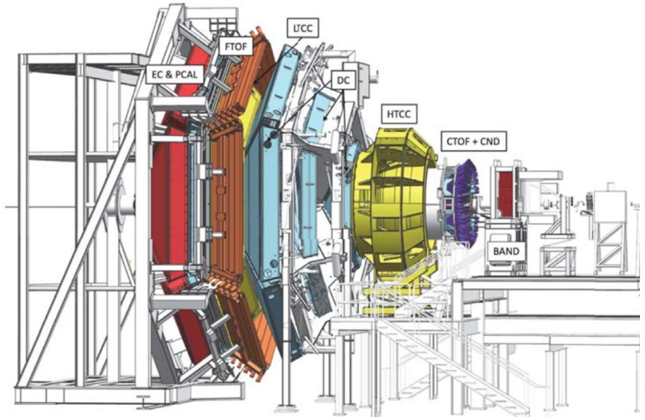

JLab Hall-C

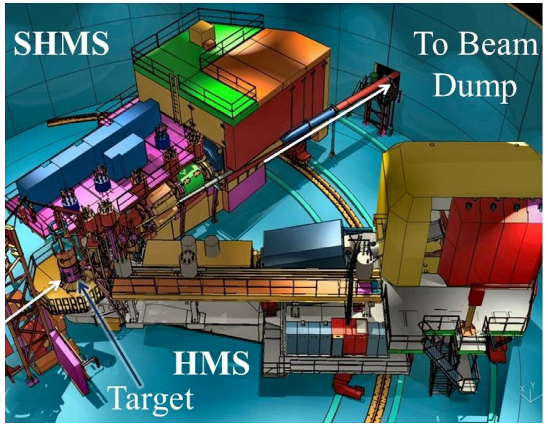

But also: BaBar, Belle, RHIC, LHC,…

The main contributors (with lepton probes)

HERMES (DESY)

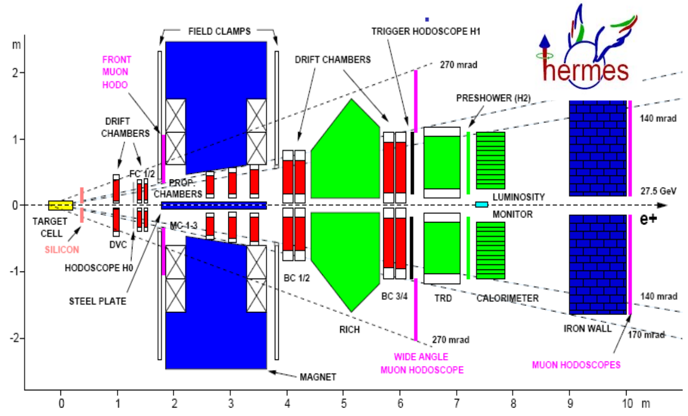

COMPASS/AMBER (CERN)

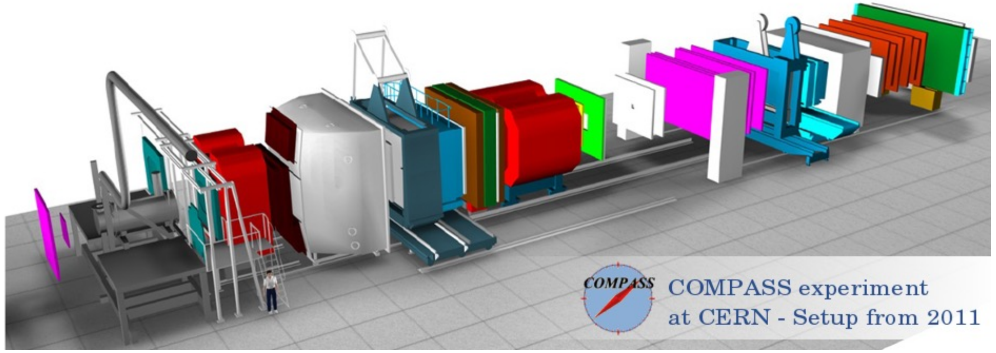

EIC (BNL)

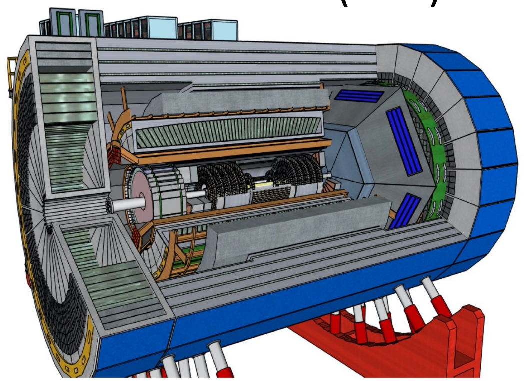

JLab Hall-A

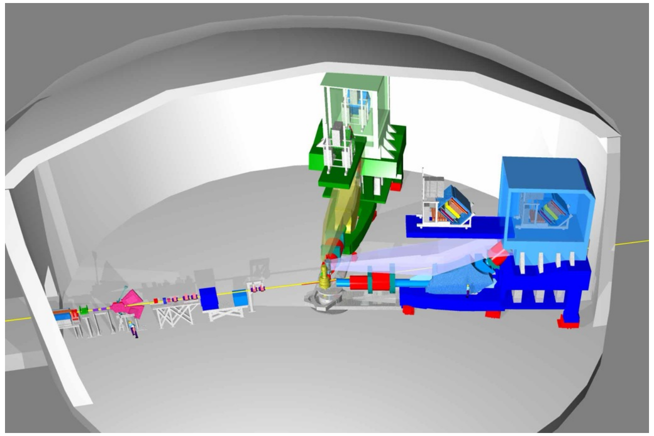

JLab Hall-B

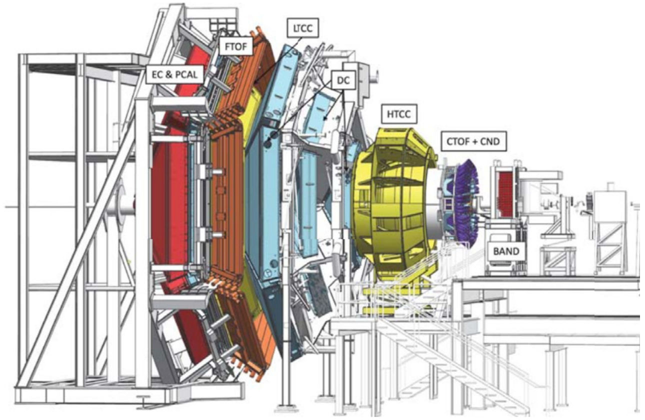

JLab Hall-C

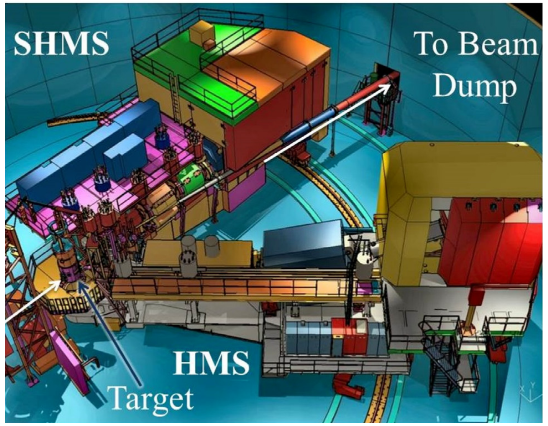

Complementarity is the key!

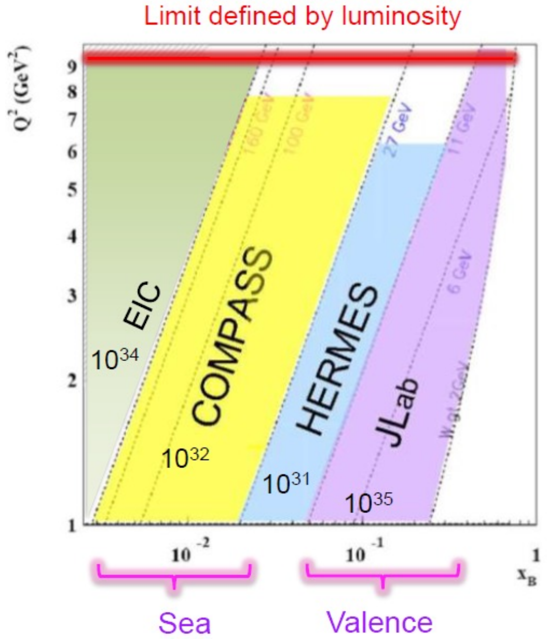

But also: BaBar, Belle, RHIC, LHC,…

GPDs

GPDs → nucleon tomography in coordinate space

- Describe correlations between the partons transverse position (impact parameter $b_\perp$) and longit. momentum (x)
- **Provide nucleon tomography in x-$b_\perp$ space**

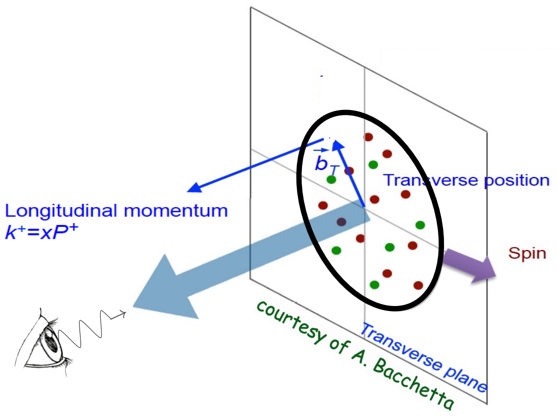

Lattice QCD prediction for transv. GPDs

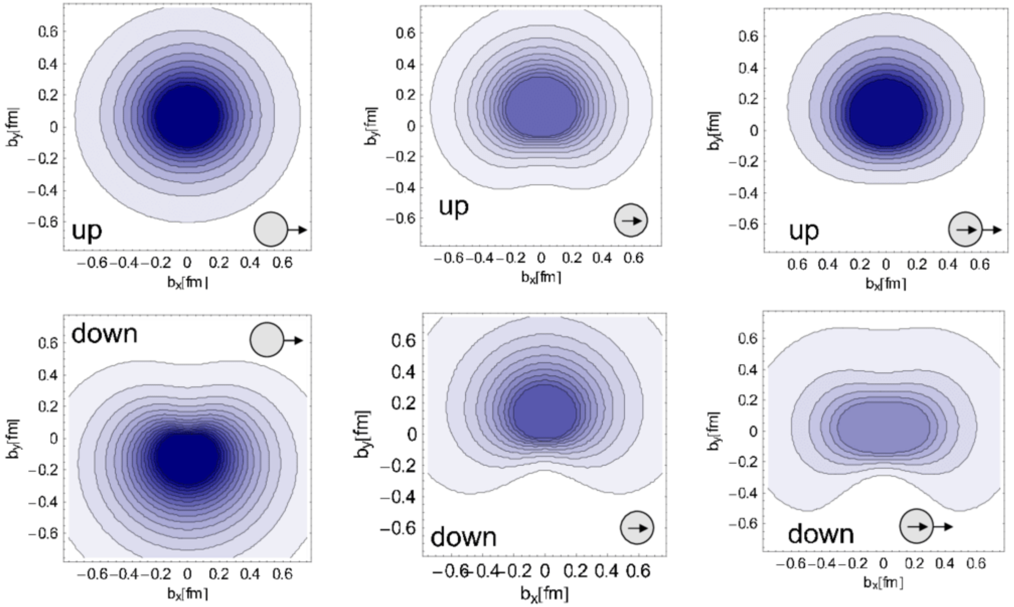

Phys.Rev.Lett.98:222001,2007

GPDs → nucleon tomography in coordinate space

- Describe correlations between the partons transverse position (impact parameter $b_\perp$) and longit. momentum (x)
- **Provide nucleon tomography in x-$b_\perp$ space**

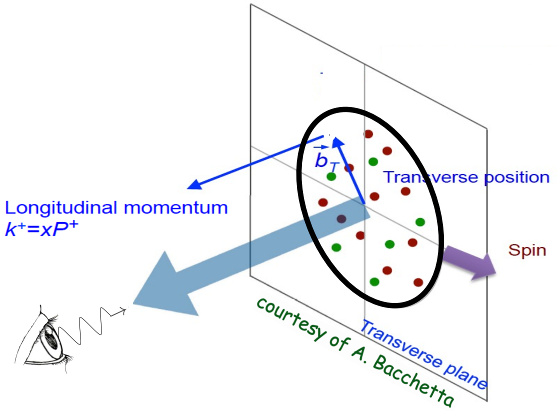

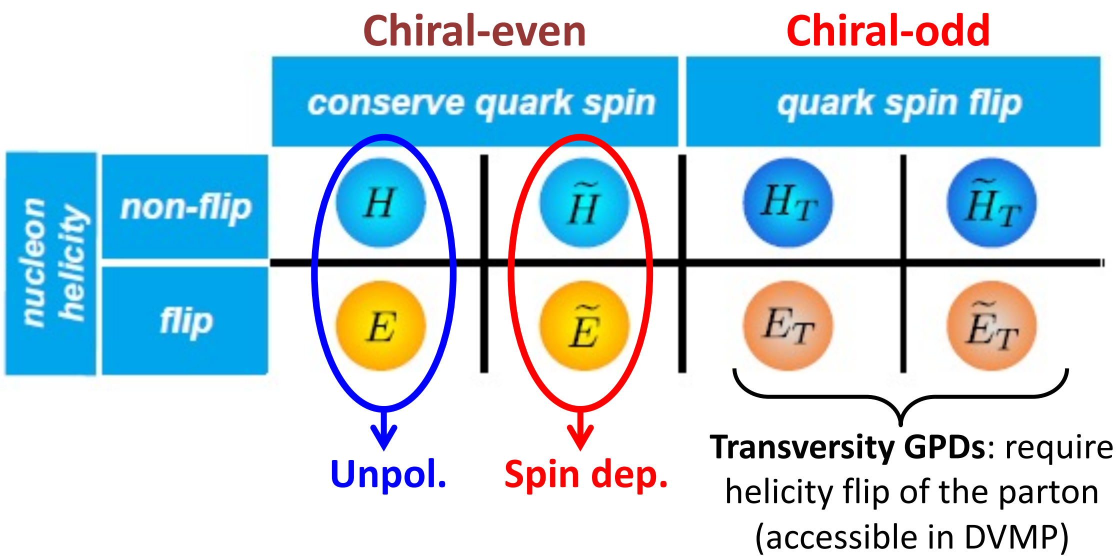

Lattice QCD prediction for transv. GPDs

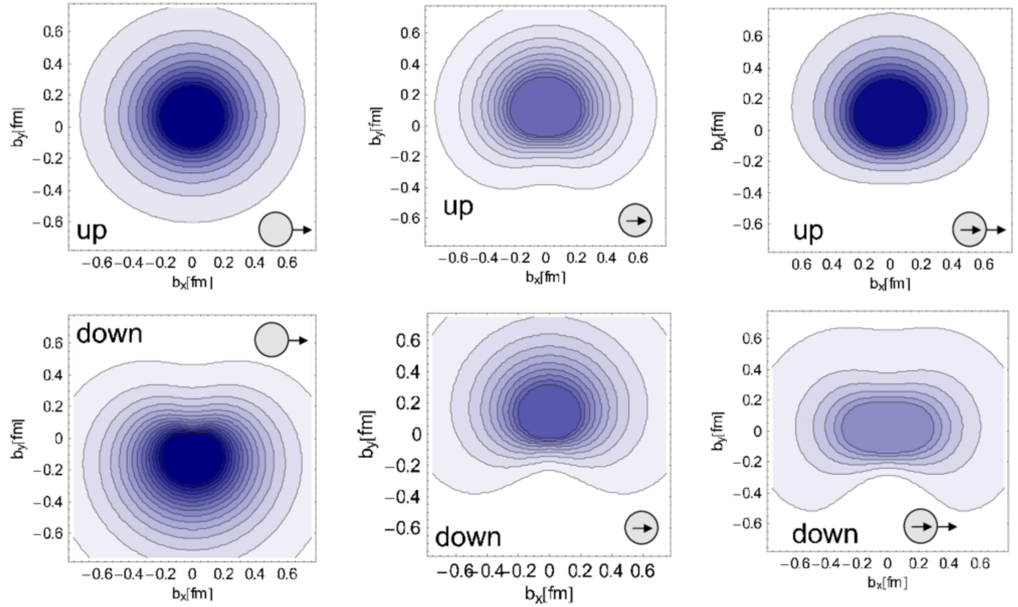

Phys.Rev.Lett.98:222001,2007

GPDs → nucleon tomography in coordinate space

- Describe correlations between the partons transverse position (impact parameter $b_\perp$) and longit. momentum (x)
- **Provide nucleon tomography in x-$b_\perp$ space**

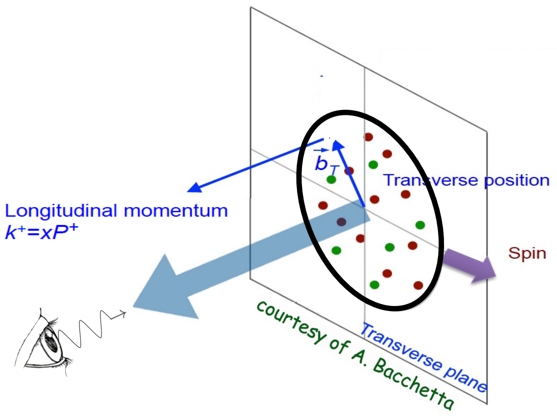

[J. High Energ. Phys. **2022**, 215 (2022)]

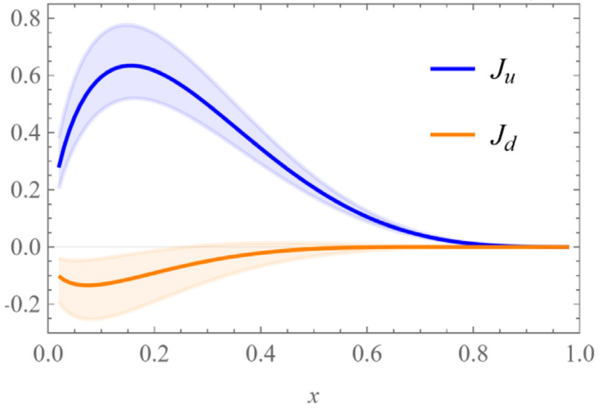

Lattice QCD prediction for transv. GPDs

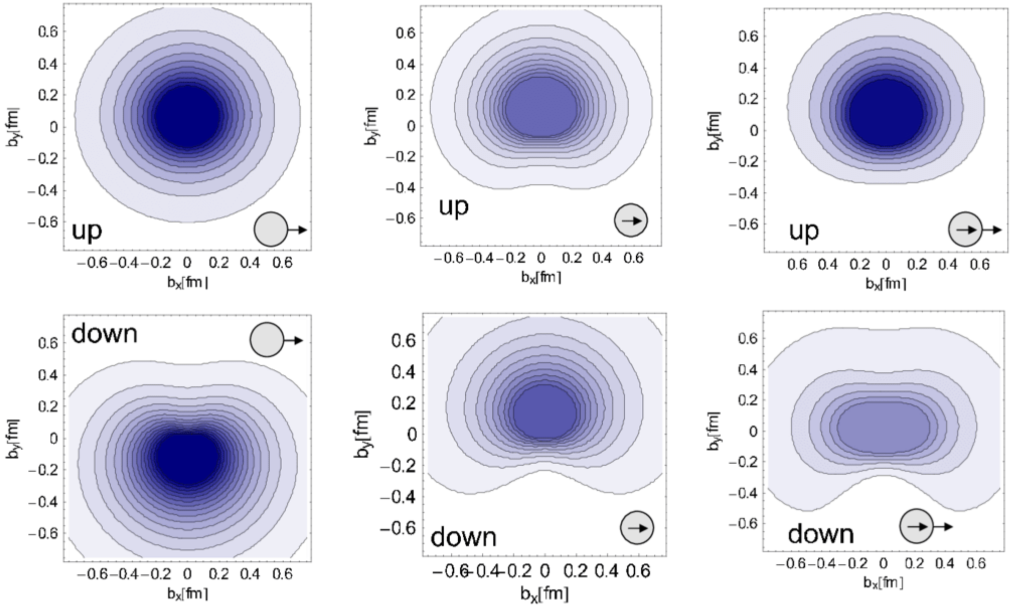

Phys.Rev.Lett.98:222001,2007

Chiral-even

Chiral-odd

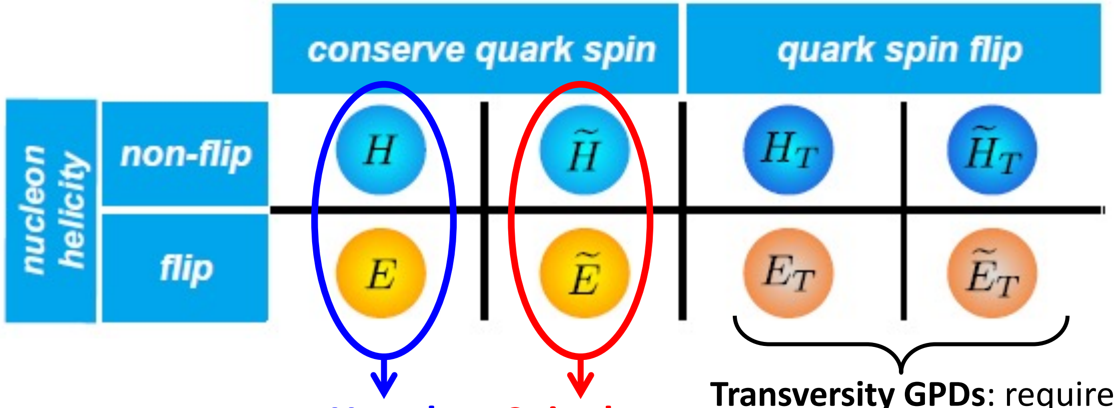

Unpol. **Spin dep.**

Transversity GPDs: require helicity flip of the parton (accessible in DVMP)

$$\lim_{t\to 0}\int_0^1 dx\, x\,(H_q(x,\xi,t)+E_q(x,\xi,t)) = J_q$$

Ji sum rule

$\xi \approx \frac{x_B}{2-x_B}$ (skewness)

$t = (P' - P)^2$

Accessing GPDs via hard exclusive processes

DVCS

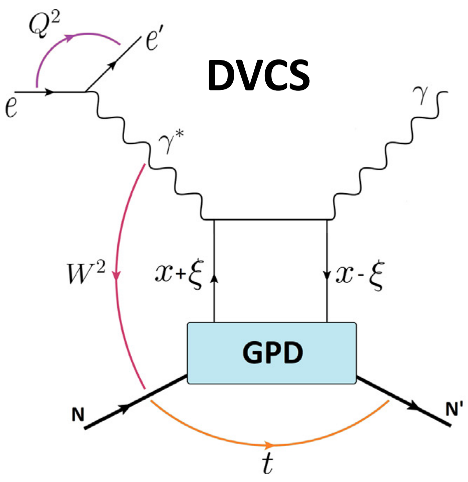

DVMP

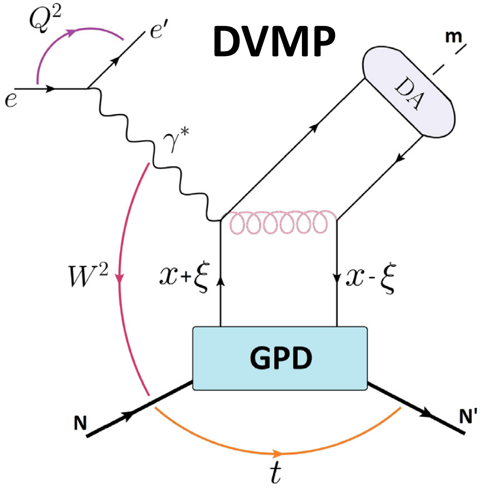

Double DVCS

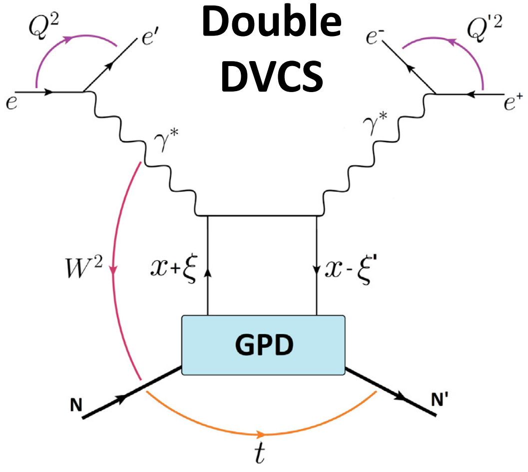

Time-like Compton Scatt. (TCS)

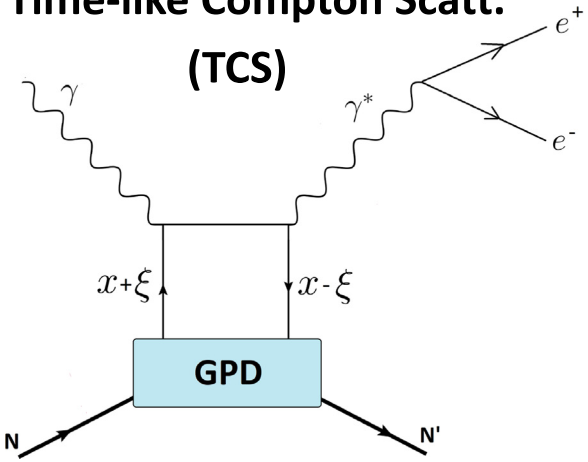

Exclusive di-photon prod.

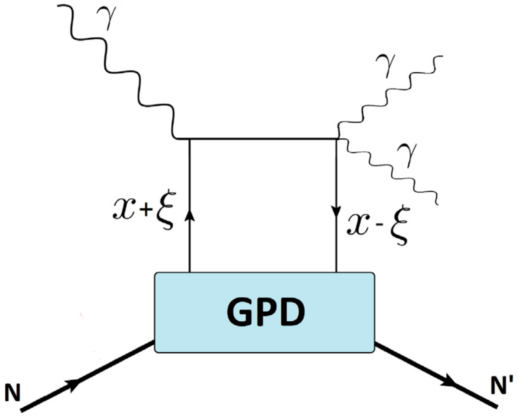

lepton-pair prod. in hard exclusive hadron scattering

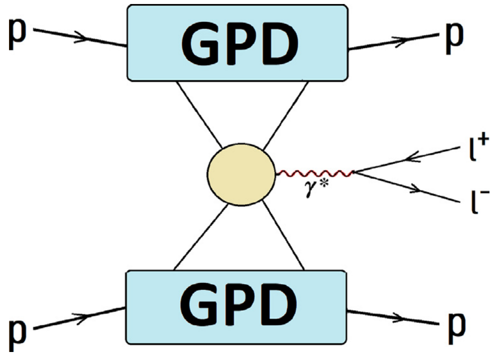

Exclusive DY

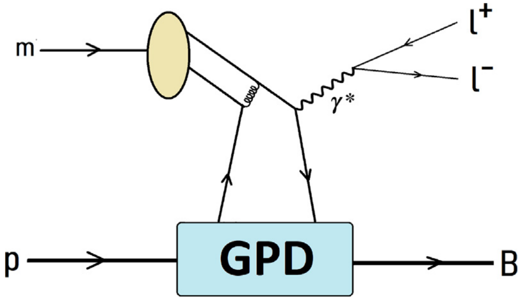

Exclusive heavy meson prod. in hh UPC

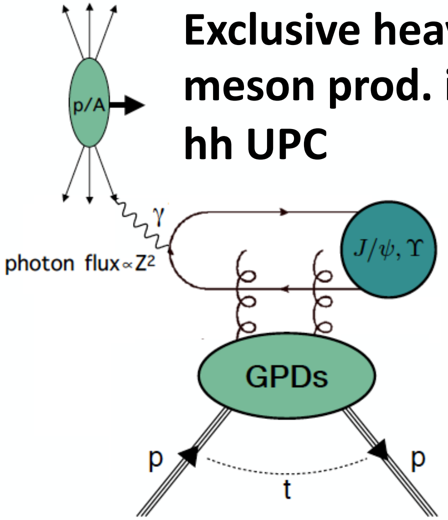

Courtesy S. Diehl [Prog. In Part. And Nucl. Phys 113 (2023) 104069]

Accessing GPDs via hard exclusive processes

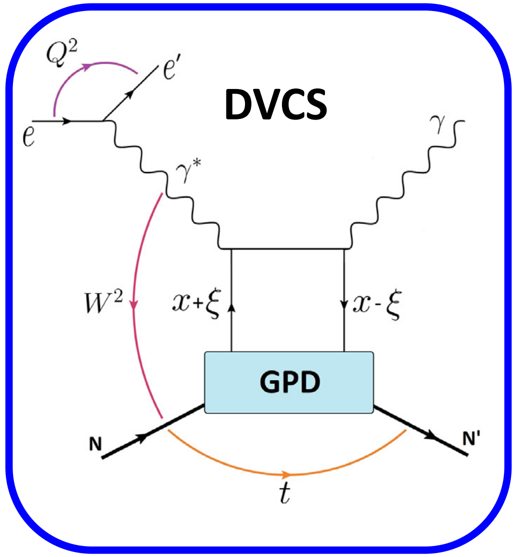

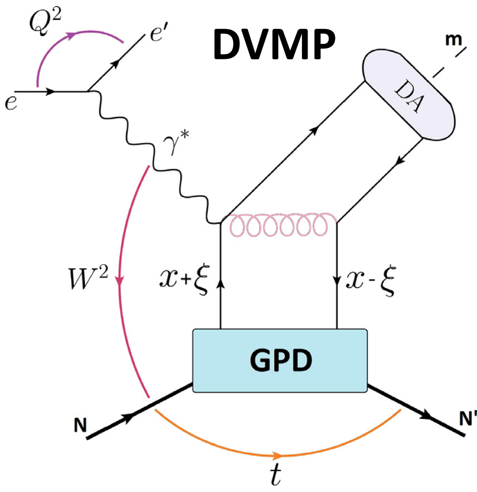

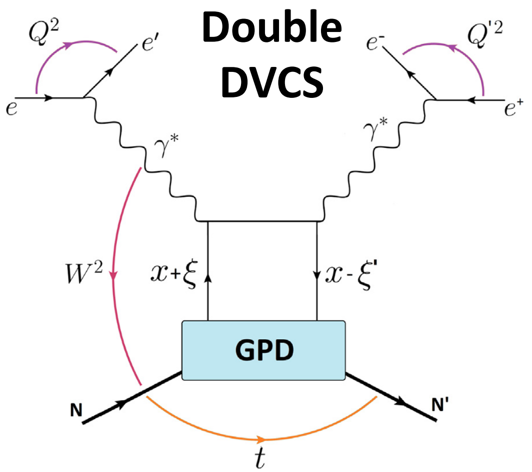

Time-like Compton Scatt. (TCS)

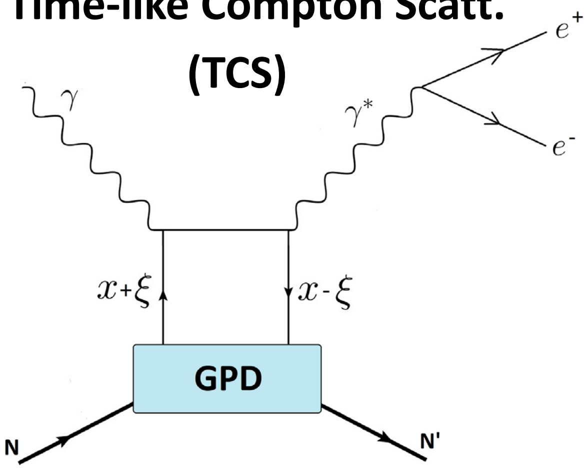

Exclusive di-photon prod.

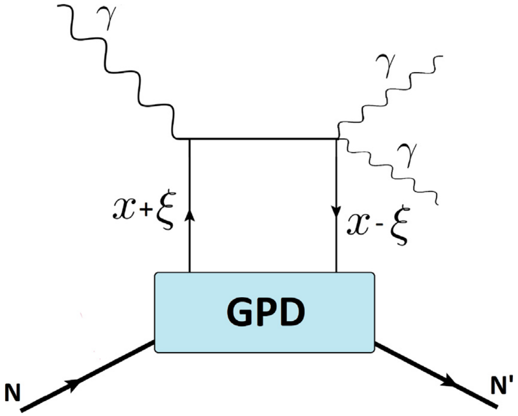

lepton-pair prod. in hard exclusive hadron scattering

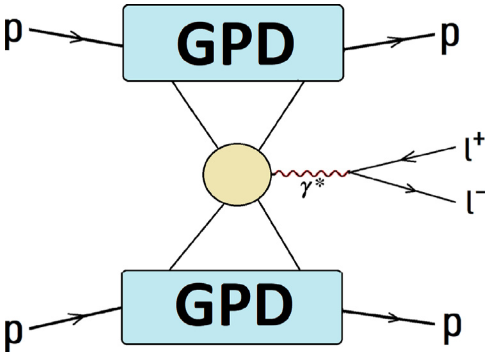

Exclusive DY

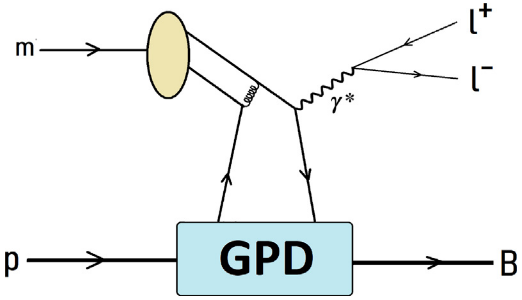

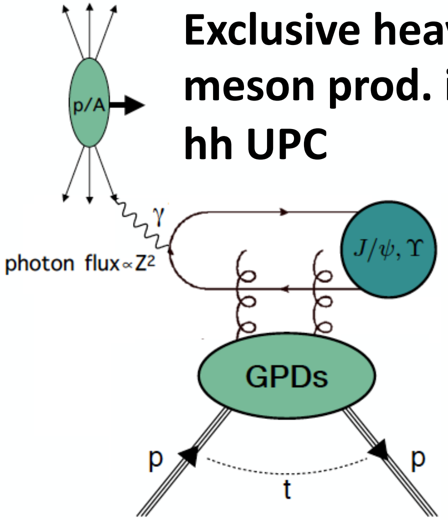

Exclusive heavy meson prod. in hh UPC

Courtesy S. Diehl Prog. In Part. And Nucl. Phys 113 (2023) 104069

Deeply Virtual Compton Scattering (DVCS)

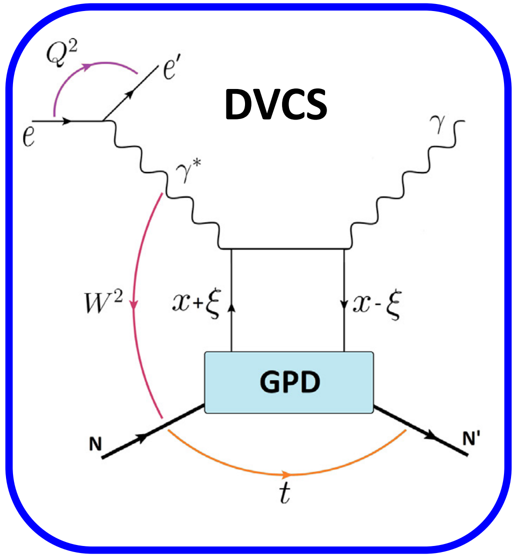

- **DVCS is the cleanest probe of GPDs** (theoretical accuracy at NNLO)
- In the limit $-t/Q^2 \ll 1$ the process factorises into a hard subprocess ($\gamma^* q \rightarrow q\gamma$) + a soft non-perturbative part parametrized in terms of GPDs
- At leading-twist provides access to all chiral-even GPDS: H E $\tilde{H}$ $\tilde{E}$
- The amplitudes of the process can be parametrized in terms of **Compton FF** (CFF), related to integrals of GPDs, e.g.:

$$\mathcal{H}(\xi, t) = \sum_q e_q^2 \left\{ \mathcal{P} \int_{-1}^{1} dx (H^q(x, \xi, t) - H^q(-x, \xi, t)) \left[\frac{1}{\xi - x} + \frac{1}{\xi + x} \right] + i\pi [H^q(\xi, \xi, t) - H^q(-\xi, \xi, t)] \right\}$$

Deeply Virtual Compton Scattering (DVCS)

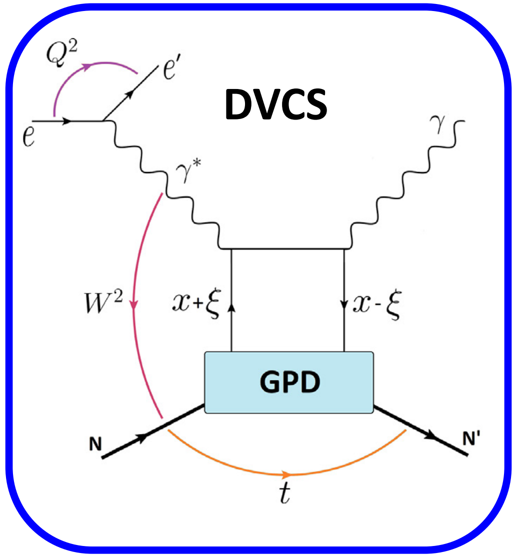

- **DVCS is the cleanest probe of GPDs** (theoretical accuracy at NNLO)
- In the limit $-t/Q^2 \ll 1$ the process factorises into a hard subprocess ($\gamma^* q \rightarrow q\gamma$) + a soft non-perturbative part parametrized in terms of GPDs
- At leading-twist provides access to all chiral-even GPDS: H E $\tilde{H}$ $\tilde{E}$
- The amplitudes of the process can be parametrized in terms of **Compton FF** (CFF), related to integrals of GPDs, e.g.:

$$\mathcal{H}(\xi,t) = \sum_q e_q^2 \left\{ \mathcal{P} \int_{-1}^{1} dx (H^q(x,\xi,t) - H^q(-x,\xi,t)) \left[\frac{1}{\xi - x} + \frac{1}{\xi + x} \right] + i\pi [H^q(\xi,\xi,t) - H^q(-\xi,\xi,t)] \right\}$$

Bethe-Heitler

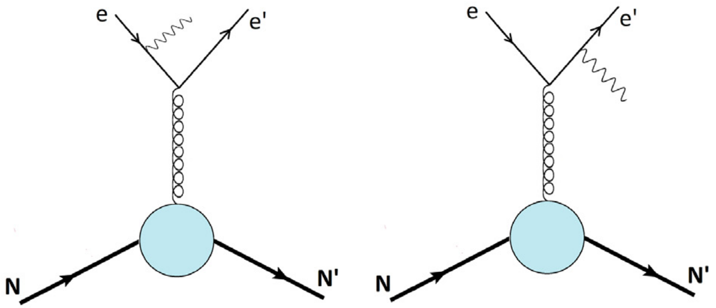

- The **Bethe-Heiltler** processes result in the same final state (e, N, γ)
  ➔ **experimentally undistinguishable**

$$\frac{d\sigma}{dx_B dQ^2 d|t| d\phi} \propto |\mathcal{T}_{BH}|^2 + |\mathcal{T}_{DVCS}|^2 + \underbrace{\mathcal{T}_{DVCS}\mathcal{T}_{BH}^* + \mathcal{T}_{BH}\mathcal{T}_{DVCS}^*}_{I}$$

Deeply Virtual Compton Scattering (DVCS)

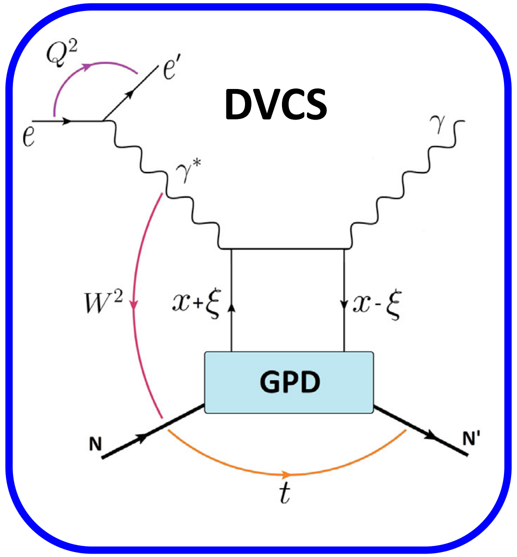

- **DVCS is the cleanest probe of GPDs** (theoretical accuracy at NNLO)
- In the limit $-t/Q^2 \ll 1$ the process factorises into a hard subprocess ($\gamma^* q \to q\gamma$) + a soft non-perturbative part parametrized in terms of GPDs
- At leading-twist provides access to all chiral-even GPDS: H E $\tilde{H}$ $\tilde{E}$
- The amplitudes of the process can be parametrized in terms of **Compton FF** (CFF), related to integrals of GPDs, e.g.:

$$\mathcal{H}(\xi,t) = \sum_q e_q^2 \left\{ \mathcal{P} \int_{-1}^{1} dx (H^q(x,\xi,t) - H^q(-x,\xi,t)) \left[\frac{1}{\xi - x} + \frac{1}{\xi + x} \right] + i\pi [H^q(\xi,\xi,t) - H^q(-\xi,\xi,t)] \right\}$$

Bethe-Heitler

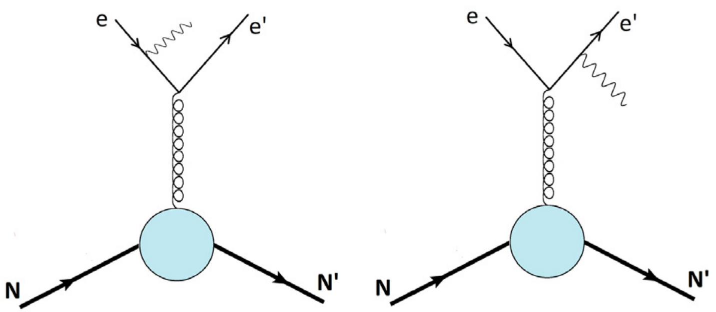

- The **Bethe-Heiltler** processes result in the same final state (e, N, γ)
  ➔ **experimentally undistinguishable**

$$\frac{d\sigma}{dx_B dQ^2 d|t| d\phi} \propto |\mathcal{T}_{BH}|^2 + |\mathcal{T}_{DVCS}|^2 + \underbrace{\mathcal{T}_{DVCS}\mathcal{T}_{BH}^* + \mathcal{T}_{BH}\mathcal{T}_{DVCS}^*}_{I}$$

- In the accessible kinematic regions the BH process is dominant over DVCS (can be precisely calculated)
- **But GPDs can be accessed also through the interference!**

Accessing GPDs

Each term of the cross section can be expressed in terms of harmonics in the azimuthal angle ϕ

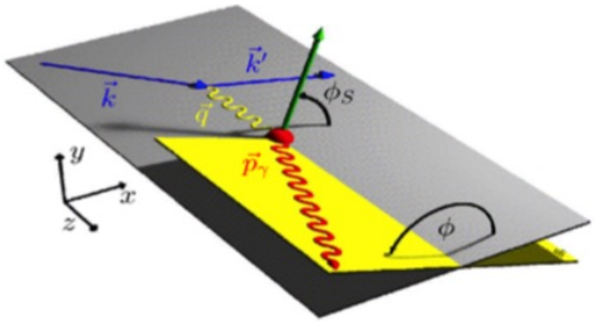

$$
\begin{aligned}
d\sigma_{BH} &\propto c_0^{BH} + c_1^{BH}\cos\phi + c_2^{BH}\cos 2\phi,\\
d\sigma_{DVCS}^{unpol} &\propto c_0^{DVCS} + c_1^{DVCS}\cos\phi + c_2^{DVCS}\cos 2\phi,\\
d\sigma_{DVCS}^{pol} &\propto s_1^{DVCS}\sin\phi,\\
\mathfrak{I}^{Re} &\propto c_0^I + c_1^I\cos\phi + c_2^I\cos 2\phi + c_3^I\cos 3\phi,\\
\mathfrak{I}^{Im} &\propto s_1^I\sin\phi + s_2^I\sin 2\phi.
\end{aligned}
$$

- the coefficients of the pure DVCS terms $\propto$ bilinear combinations CFFs
- The coefficients of the int. term $\propto$ combinations of CFF and Dirac (F_1) and Pauli (F_2) FF

Accessing GPDs

Each term of the cross section can be expressed in terms of harmonics in the azimuthal angle ϕ

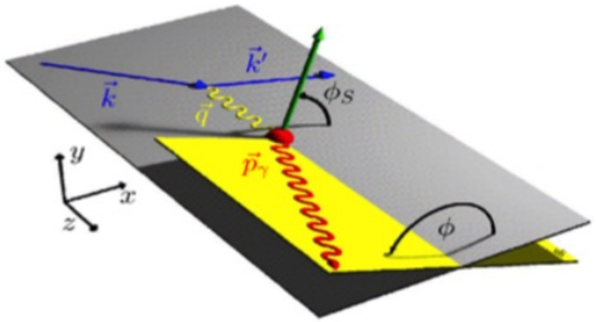

$$
\begin{aligned}
d\sigma_{BH} &\propto c_0^{BH} + c_1^{BH}\cos\phi + c_2^{BH}\cos 2\phi,\\
d\sigma_{DVCS}^{unpol} &\propto c_0^{DVCS} + c_1^{DVCS}\cos\phi + c_2^{DVCS}\cos 2\phi,\\
d\sigma_{DVCS}^{pol} &\propto s_1^{DVCS}\sin\phi,\\
\mathfrak{I}^{Re} &\propto c_0^I + c_1^I\cos\phi + c_2^I\cos 2\phi + c_3^I\cos 3\phi,\\
\mathfrak{I}^{Im} &\propto s_1^I\sin\phi + s_2^I\sin 2\phi.
\end{aligned}
$$

- the coefficients of the pure DVCS terms $\propto$ bilinear combinations CFFs
- The coefficients of the int. term $\propto$ combinations of CFF and Dirac (F_1) and Pauli (F_2) FF

Can build-up **plenty of experimental observables**, each with a specific azimuthal modulation and a specific sensitivity to the various CFF (➔ GPDs):

- Beam-Charge asymmetry
  $\sigma(e^+,\phi) - \sigma(e^-,\phi) \propto Re[F_1\mathcal{H}]$
- Beam-Spin Asymmetry
  $\sigma(\overrightarrow{e},\phi) - \sigma(\overleftarrow{e},\phi) \propto Im[F_1\mathcal{H}]$
- Longitudinal Target-Spin Asymmetry
  $\sigma(\overset{\Rightarrow}{P},\phi) - \sigma(\overset{\Leftarrow}{P},\phi) \propto Im[F_1\widetilde{\mathcal{H}}]$
- Longitudinal Double-Spin Asymmetry
  $\sigma(\overset{\Rightarrow}{P},\overrightarrow{e},\phi) - \sigma(\overset{\Rightarrow}{P},\overleftarrow{e},\phi) \propto Re[F_1\widetilde{\mathcal{H}}]$
- Transverse Target-Spin Asymmetry
  $\sigma(\phi,\phi_S) - \sigma(\phi,\phi_S+\pi) \propto Im[F_2\mathcal{H} - F_1\mathcal{E}]$
- Transverse Double-Spin Asymmetry
  $\sigma(\overrightarrow{e},\phi,\phi_S) - \sigma(\overleftarrow{e},\phi,\phi_S+\pi) \propto Re[F_2\mathcal{H} - F_1\mathcal{E}]$

Selected results

[Phys. Rev. Lett. 128, 252002 (2022)]

Highly polarized e beam on unpolarized liquid H target

Polarization averaged cross section (includes BH)

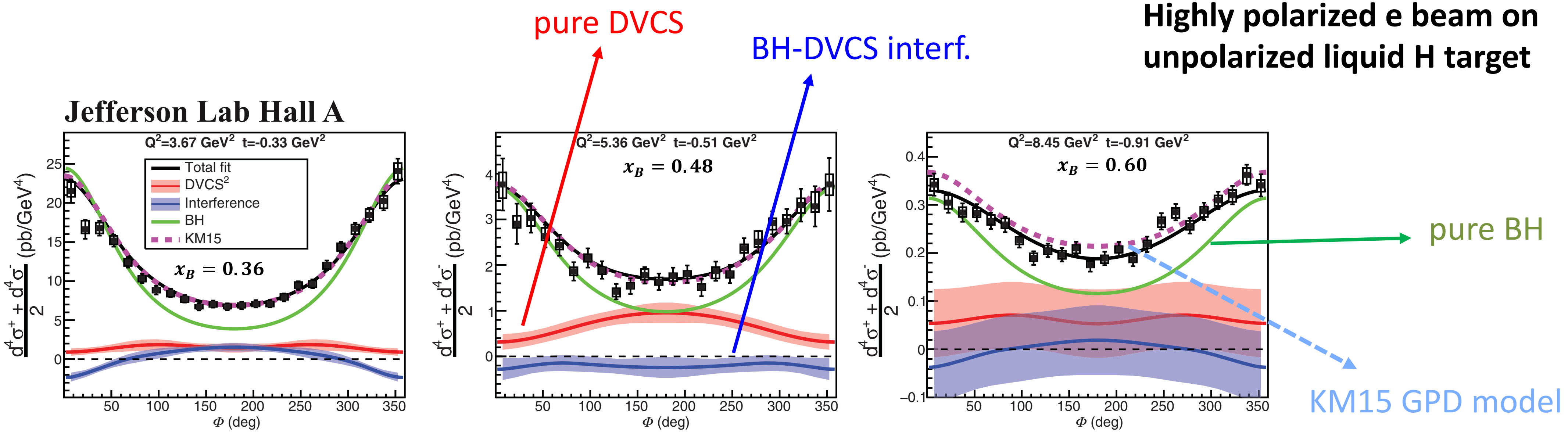

Selected results

Phys. Rev. Lett. 128, 252002 (2022)

Highly polarized e beam on unpolarized liquid H target

Polarization averaged cross section (includes BH)

Beam polarized cross section difference (free from BH)

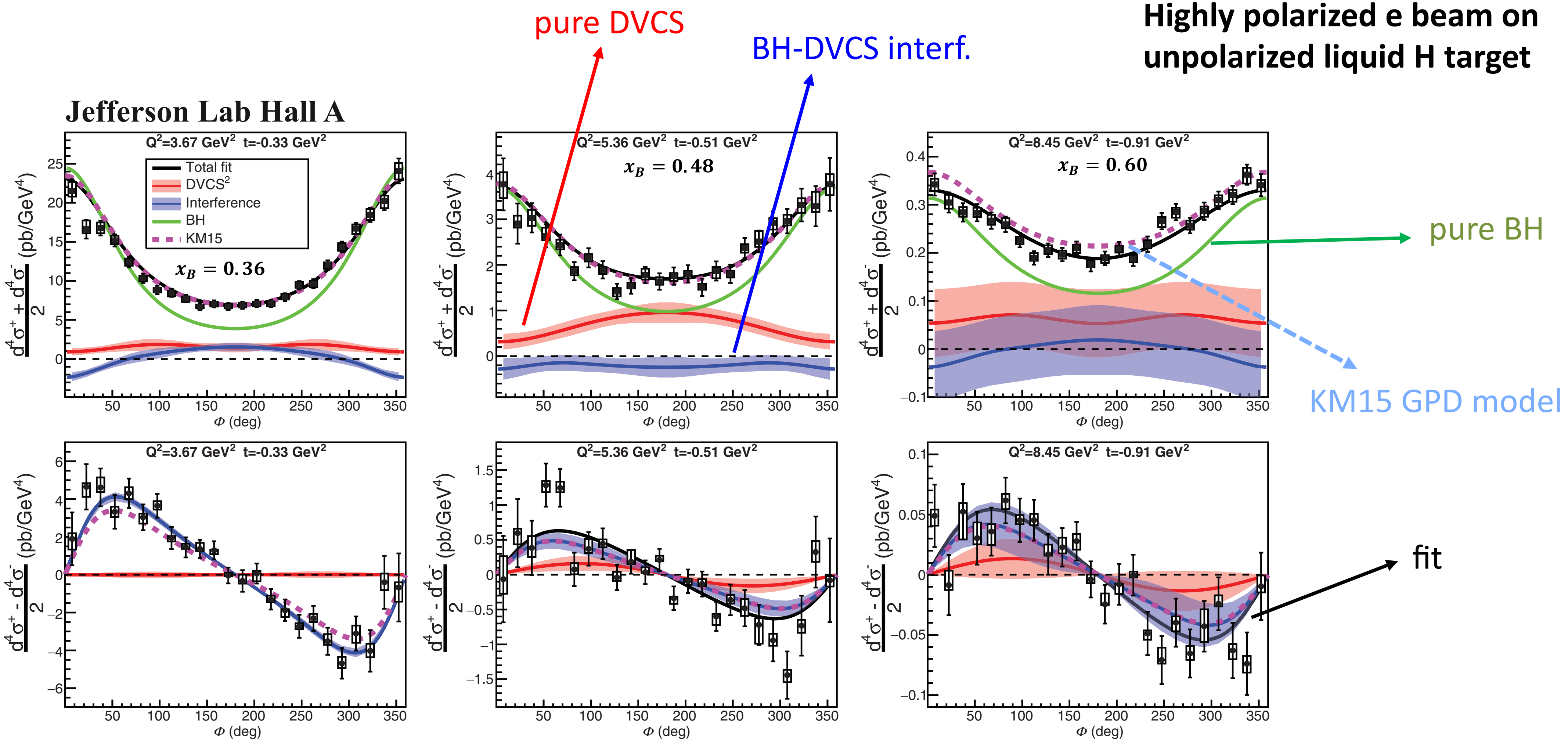

By fitting the data with a suitable parametrization in terms of the underlying CFFs one obtains the real and imaginary part of all four helicity-conserving CFFs!

Selected results

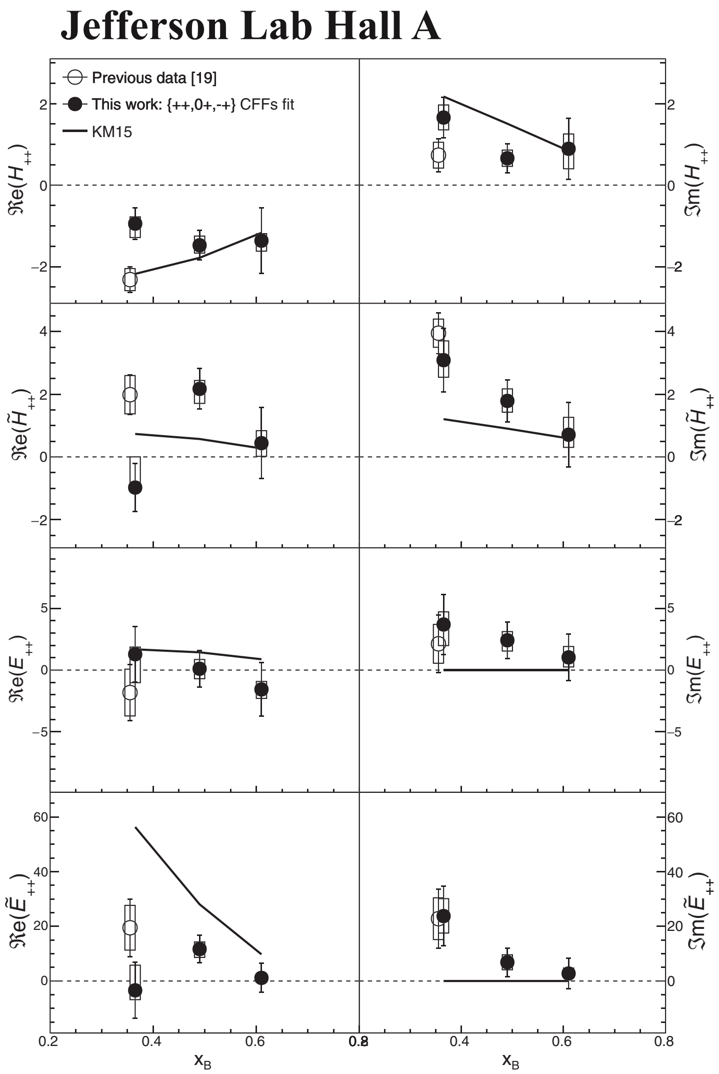

Phys. Rev. Lett. 128, 252002 (2022)

First complete extraction of all chiral-even CFFs appearing in the DVCS cross section, including $\mathcal{E}_{++}$ and $\widetilde{\mathcal{E}}_{++}$, sensitive to the poorly known E and $\tilde{E}$ GPDs.

Selected results

Jefferson Lab Hall A

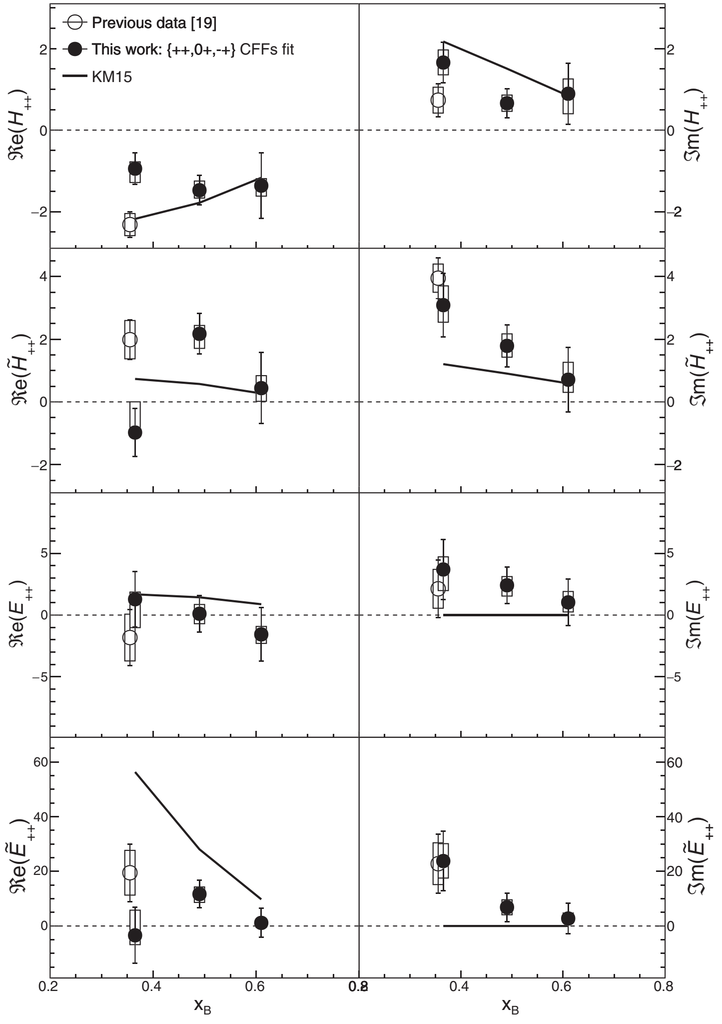

Phys. Rev. Lett. 128, 252002 (2022)

First complete extraction of all chiral-even CFFs appearing in the DVCS cross section, including $\mathcal{E}_{++}$ and $\widetilde{\mathcal{E}}_{++}$, sensitive to the poorly known E and $\tilde{E}$ GPDs.

Phys. Rev. D 95, 011501(R) (2017)

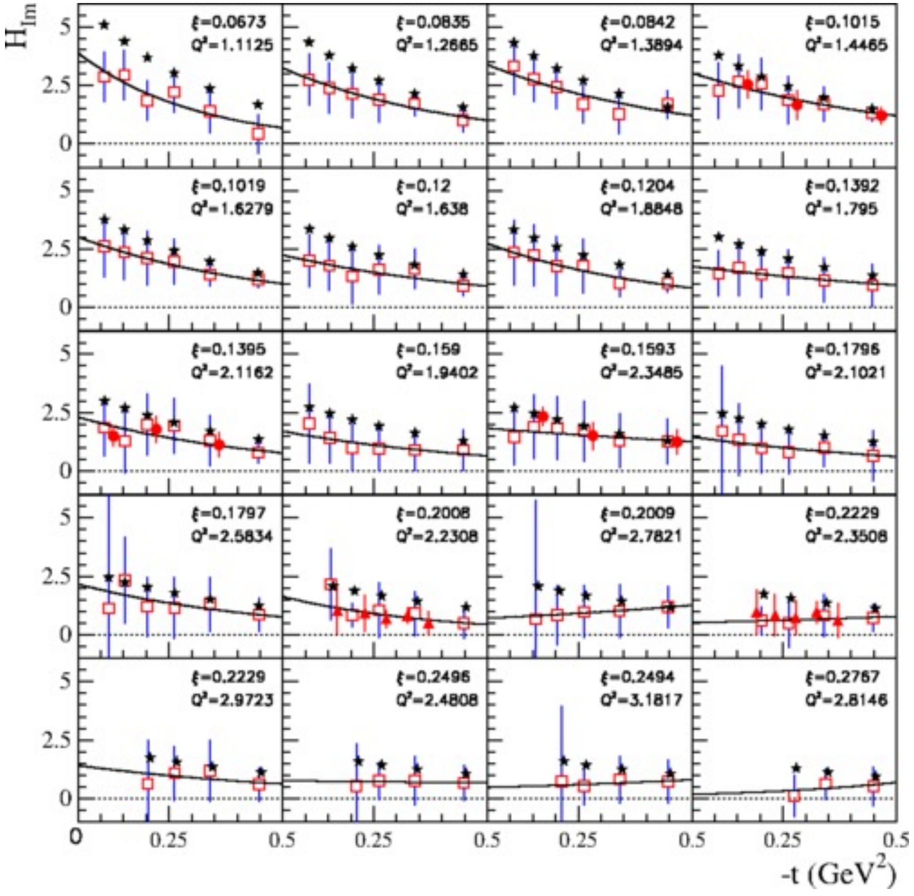

t-dependence of $Im(\mathcal{H})$ extracted in a **global fit** of measurements of σ and Δσ from **CLAS** (open squares) and **Hall-A** (solid triangles) as well as on measurements of A_{UL} and A_{LL} asymmetries from CLAS (solid circles) in 20 Q^2 bins!

Selected results

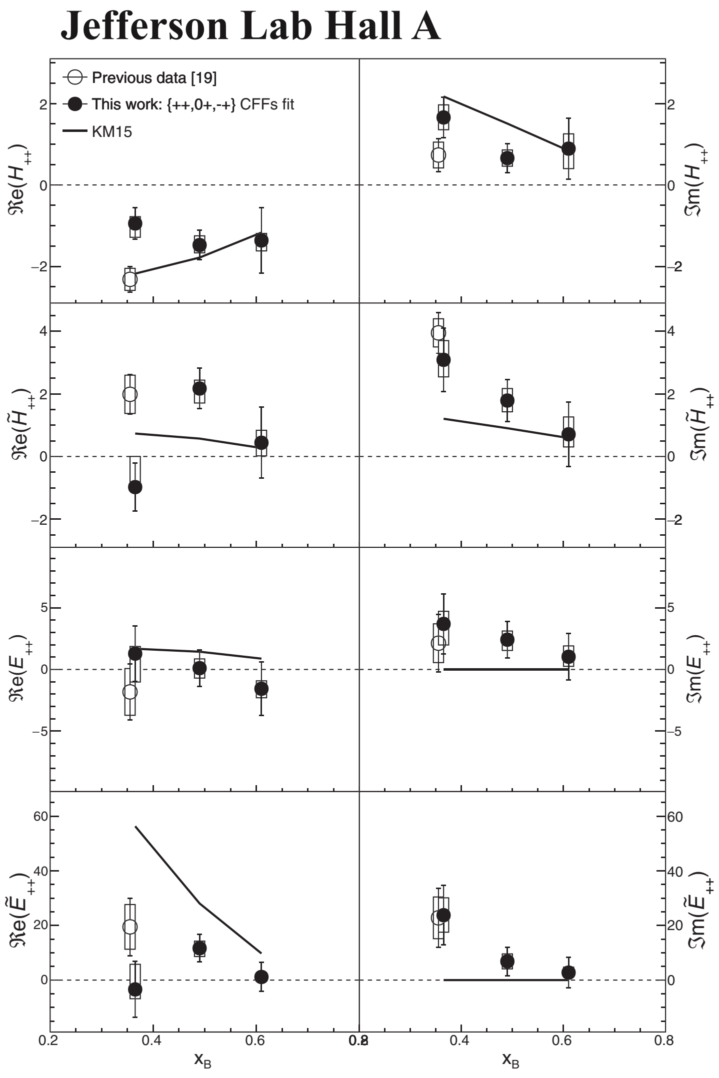

Phys. Rev. Lett. 128, 252002 (2022)

First complete extraction of all chiral-even CFFs appearing in the DVCS cross section, including $\mathcal{E}_{++}$ and $\widetilde{\mathcal{E}}_{++}$, sensitive to the poorly known E and $\tilde{E}$ GPDs.

Phys. Rev. D 95, 011501(R) (2017)

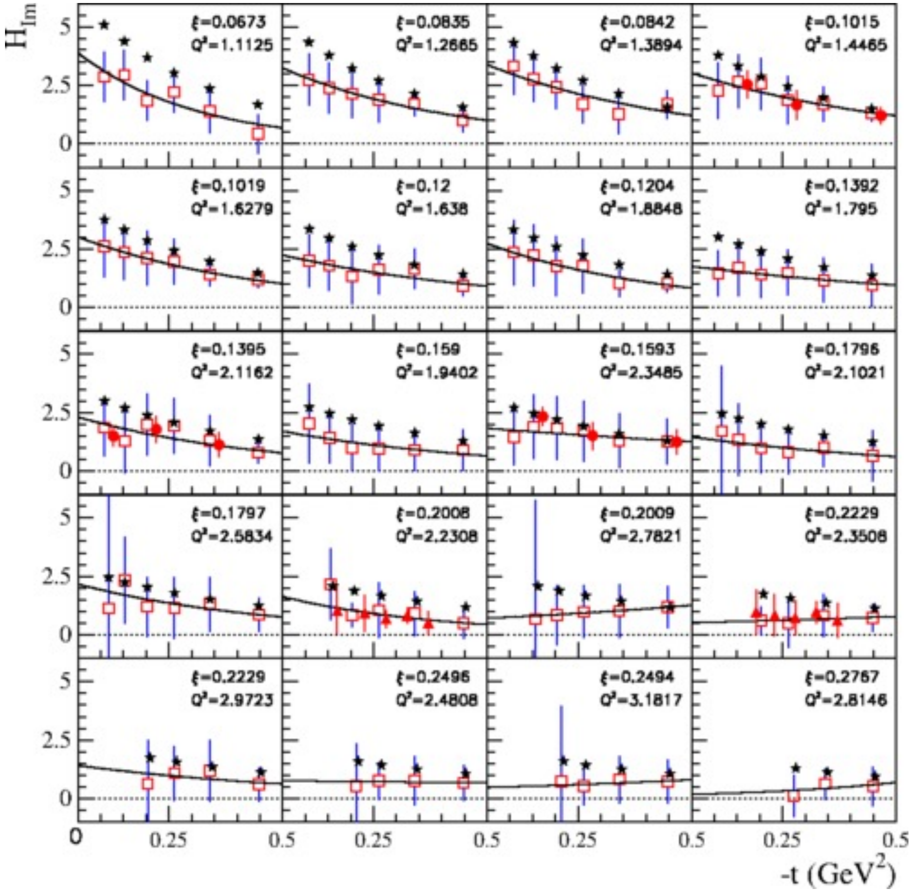

t-dependence of $Im(\mathcal{H})$ extracted in a **global fit** of measurements of σ and Δσ from **CLAS** (open squares) and **Hall-A** (solid triangles) as well as on measurements of A_{UL} and A_{LL} asymmetries from CLAS (solid circles) in 20 Q^2 bins!

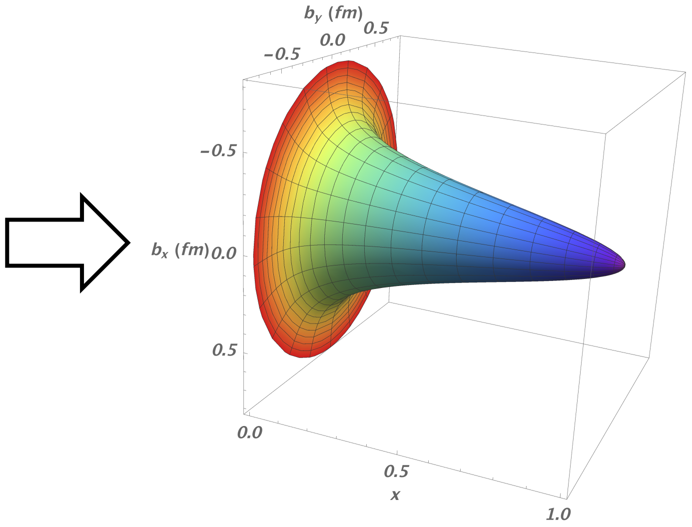

Great expectations from JLab12, AMBER and EIC!

Phys. Rev. Lett. 130, 211902 (2023) **Beam helicity 86%, unpol H target, 64 bins in Q^2, x_B, t, sensitive to $Im(\mathcal{H})$**

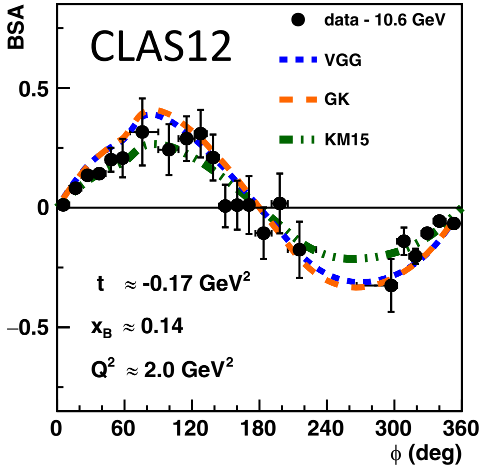

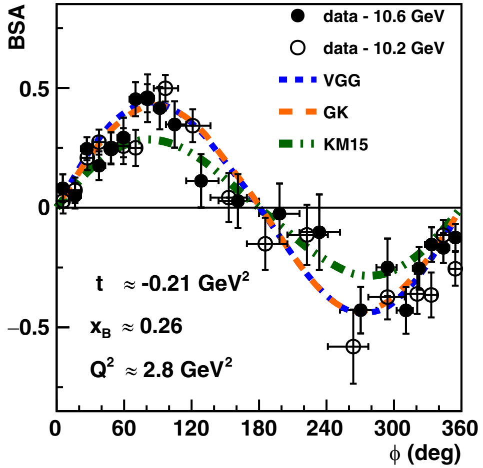

Many new high-precision DVCS results are expected from JLab12 experiments:

- cross section measurements
- neutron DVCS (D target)
- long. and transverse TSA
- BCA (positron beam ?)
- ...

Great expectations from JLab12, AMBER and EIC!

Phys. Rev. Lett. 130, 211902 (2023) **Beam helicity 86%, unpol H target, 64 bins in Q^2, x_B, t, sensitive to $Im(\mathcal{H})$**

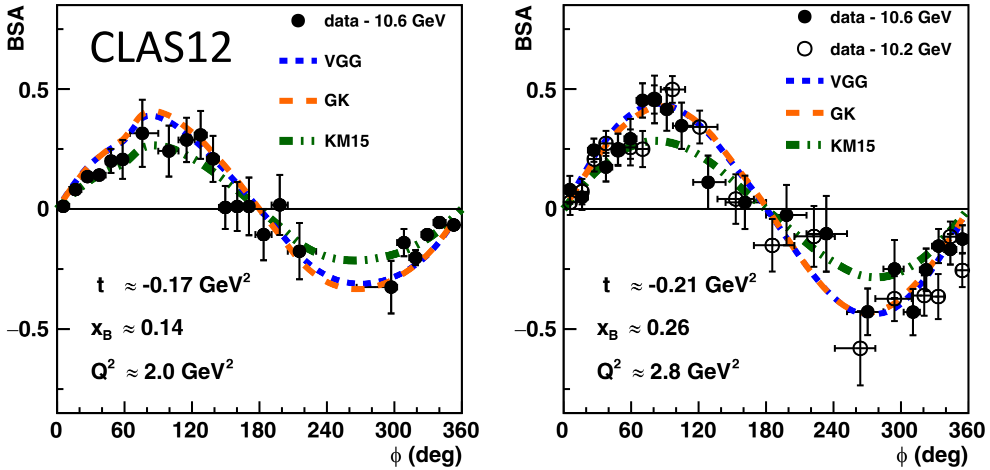

Many new high-precision DVCS results are expected from JLab12 experiments:
- cross section measurements
- neutron DVCS (D target)
- long. and transverse TSA
- BCA (positron beam ?)
- ...

arXiv:1808.00848 (2018)

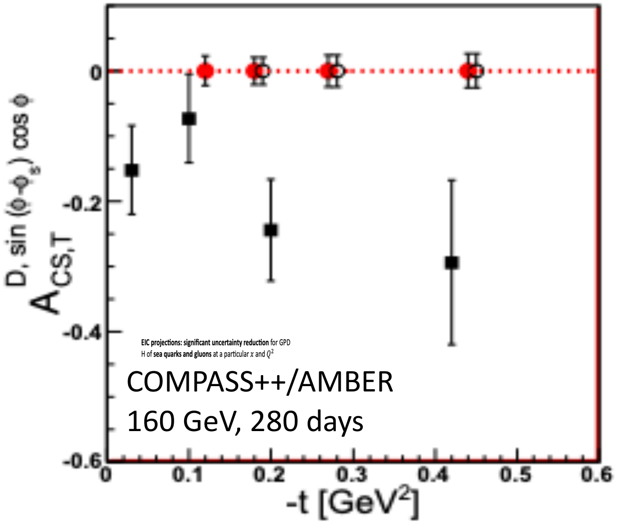

Great expectations from JLab12, AMBER and EIC!

Phys. Rev. Lett. 130, 211902 (2023) **Beam helicity 86%, unpol H target, 64 bins in Q^2, x_B, t, sensitive to $Im(\mathcal{H})$**

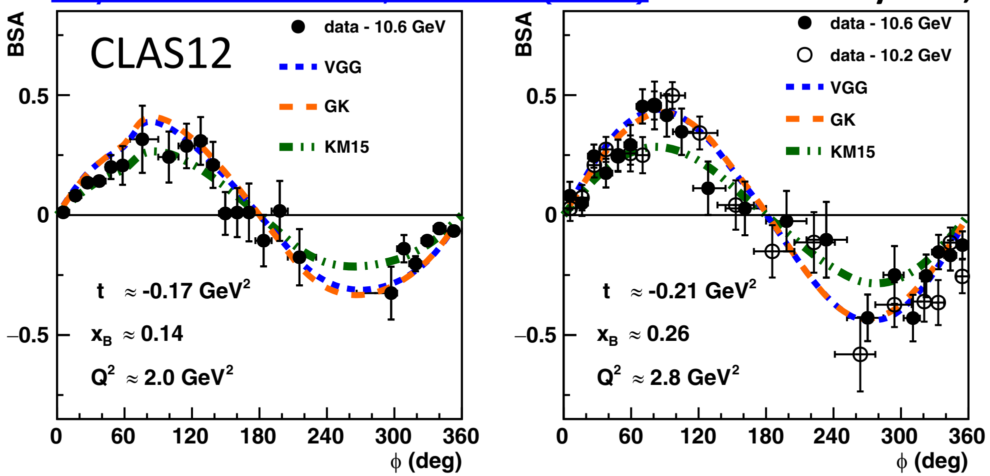

Many new high-precision DVCS results are expected from JLab12 experiments:

- cross section measurements
- neutron DVCS (D target)
- long. and transverse TSA
- BCA (positron beam ?)
- ...

arXiv:1808.00848 (2018)

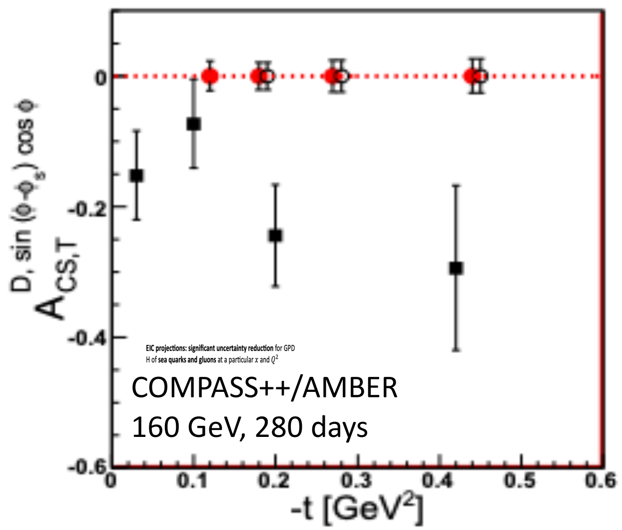

Nucl. Phys. A 1026 (2022) 122447

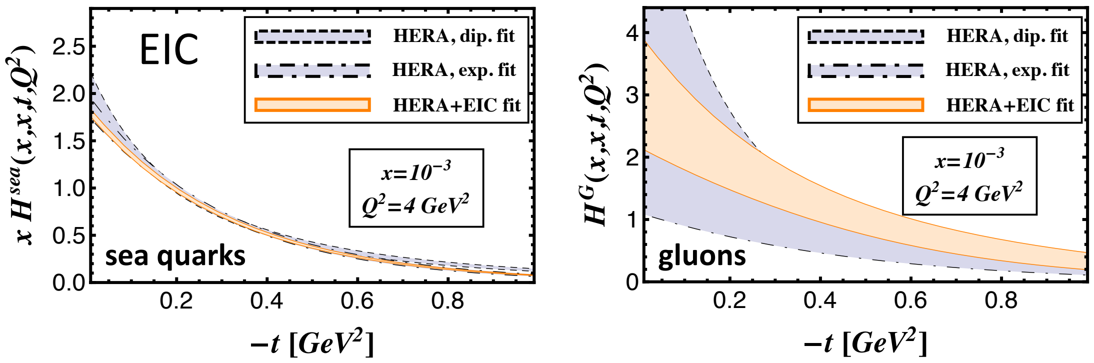

EIC projections: significant uncertainty reduction for GPD H of **sea quarks and gluons** at a particular x and Q^2

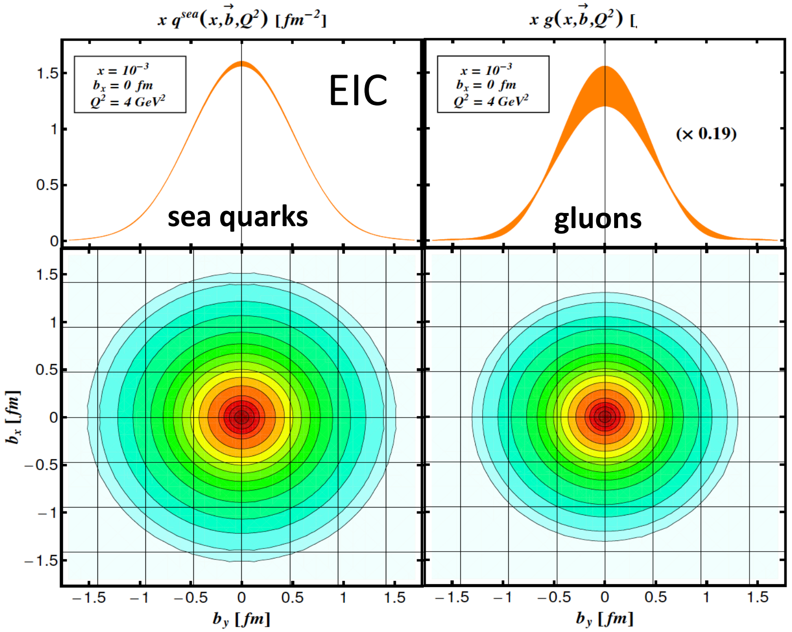

EIC projections: impact parameter distributions for **unpolarized sea quarks and gluons** in an unpol. proton

GPDs and Gravitational Form Factors

The GPD H can also be related to the **gravitational form factors** (GFFs): $\int dx \;\; x\, H(x, \xi, t) = M_2(t) + \frac{4}{5}\xi^2 d_1(t)$

$M_2(t)$ GFF: related to mass/energy distribution within the nucleon

$d_1(t)$ GFF: related to the shear forces and the pressure distribution within the nucleon

GPDs and Gravitational Form Factors

The GPD H can also be related to the **gravitational form factors** (GFFs): $\int dx\ x\,H(x,\xi,t) = M_2(t) + \frac{4}{5}\xi^2 d_1(t)$

$M_2(t)$ GFF: related to mass/energy distribution within the nucleon

$d_1(t)$ GFF: related to the shear forces and the pressure distribution within the nucleon

The **pressure distribution** within the proton has been extracted for the first time using DVCS BSAs and cross section measurements from **CLAS data at 6 GeV**.

Strong repulsive pressure near the center of the nucleon and a confining pressure for r > 0.6 fm.

A more precise determination of the CFF H and the related GPD H based on the new CLAS12 data will help to reduce the uncertainties significantly.

Nature **557**, 396–399 (2018)

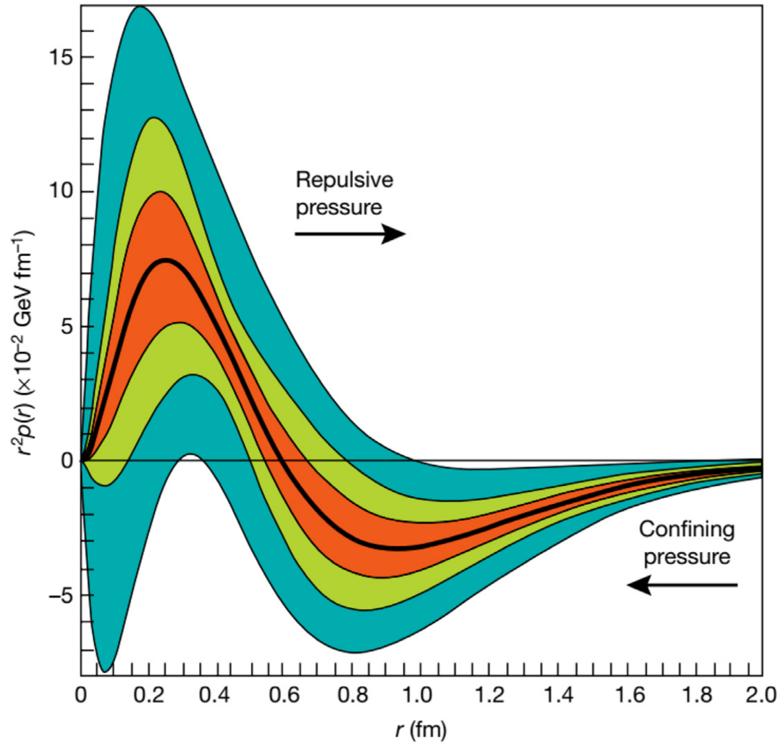

TMDs

TMDs → nucleon tomography in momentum space

TMDs surviving integration over k_T. "Collinear analysis"

naive time-reversal odd TMDs

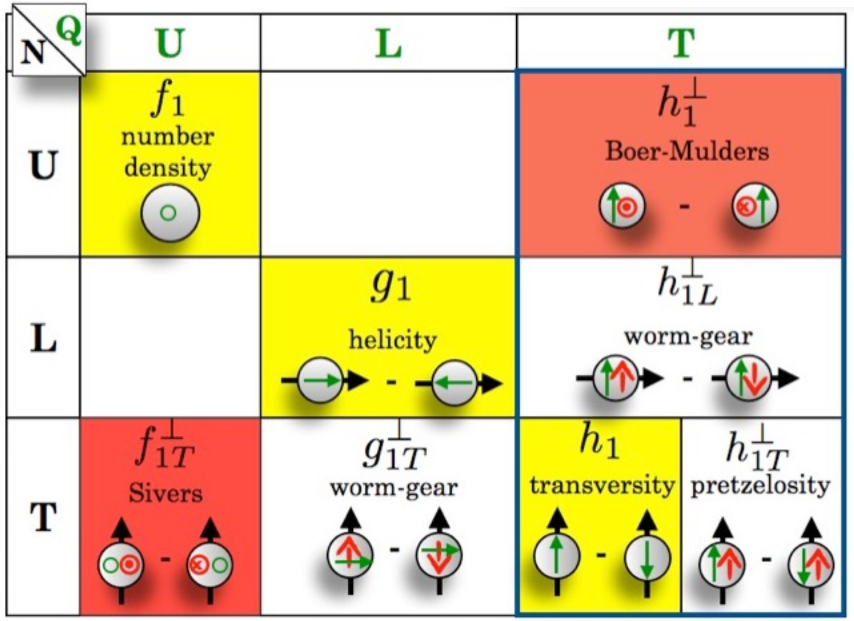

Courtesy C. Riedl

- **8 independent TMDs at LT**
- depend on x and p_T

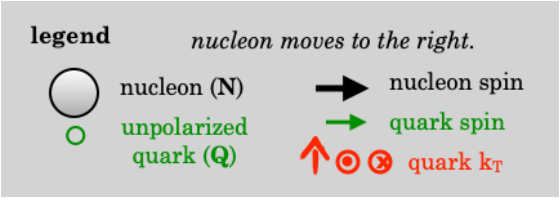

chiral odd TMDs

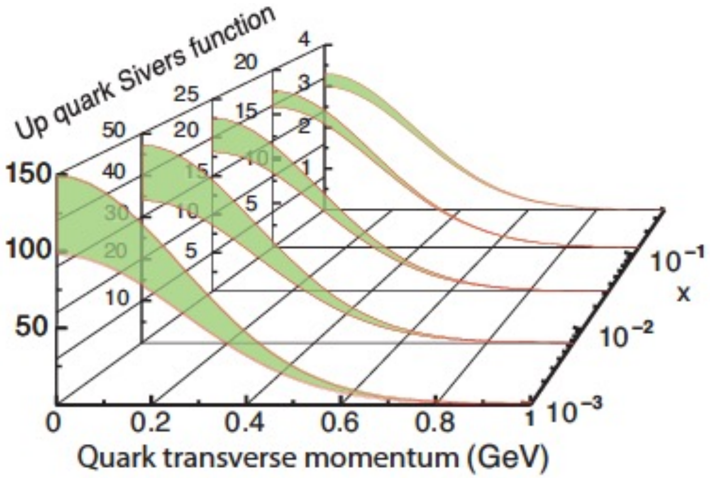

TMDs → nucleon tomography in momentum space

TMDs surviving integration over k_T. "Collinear analysis"

naive time-reversal odd TMDs

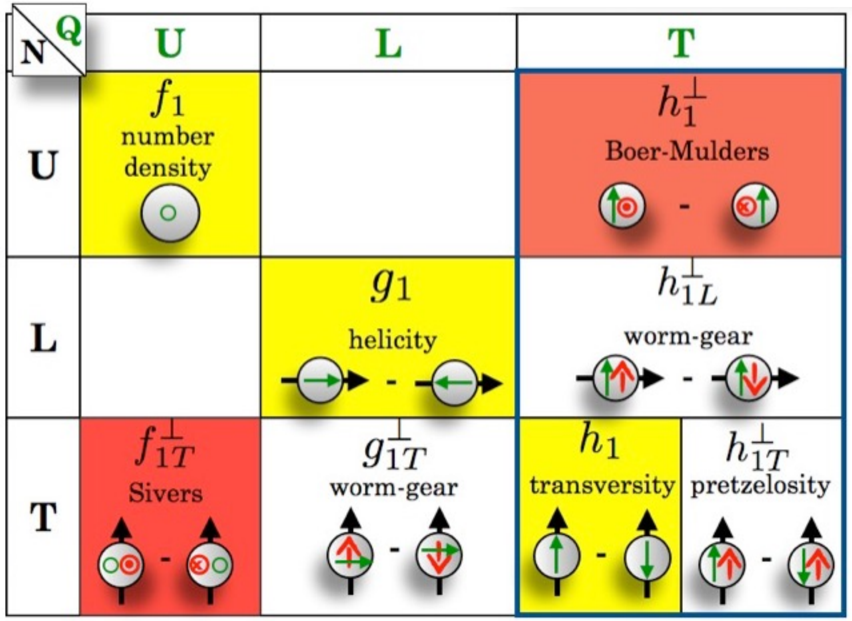

Courtesy C. Riedl

- **8 independent TMDs at LT**
- depend on x and p_T

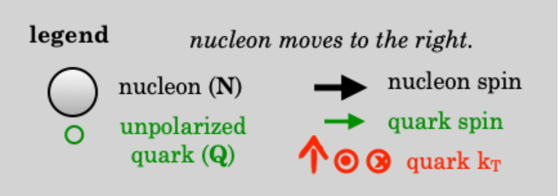

chiral odd TMDs

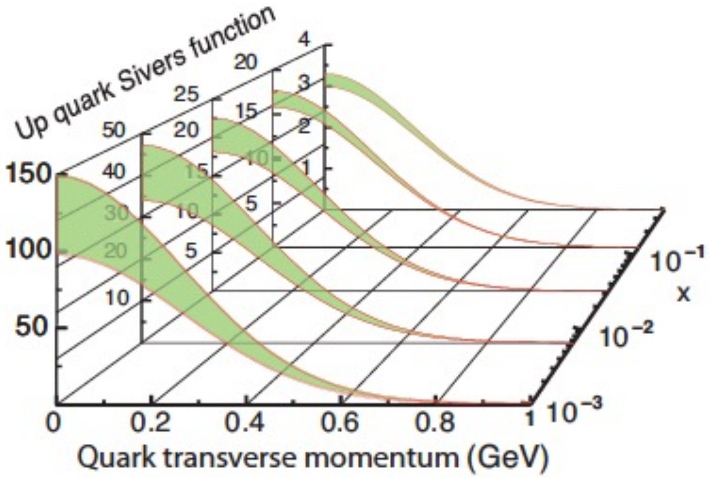

$x\, f_1(x, k_T, S_T)$

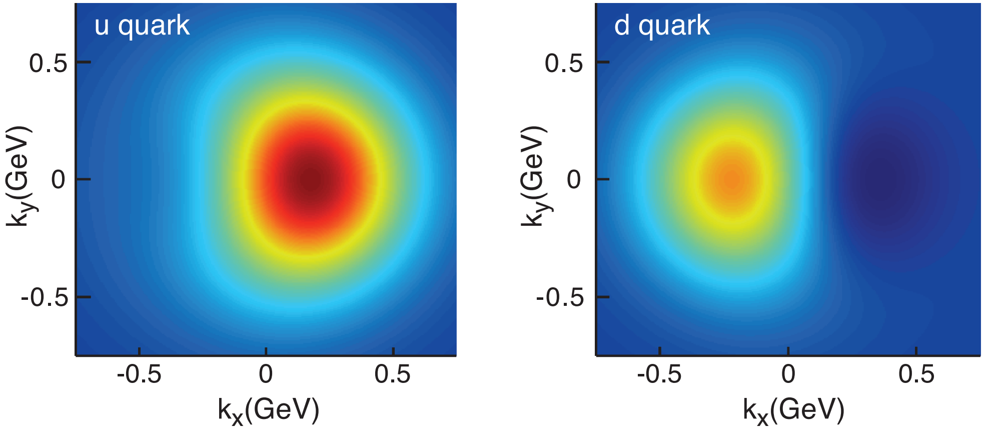

Sivers effect: unpolarized quarks in a transversely polarized nucleon

Describe **spin-orbit correlations of the form** $\vec{S} \cdot (\vec{p}_1 \times \vec{p}_2)$:

- generate flavour-dependent distortions of the parton densities in transverse momentum plane (e.g. **Sivers effect**)
- can provide **sensitivity to unknown parton OAM!**

Accessing TMDs

The golden processes to measure TMDs are **Drell-Yan** and **Semi-Inclusive DIS (SIDIS)**

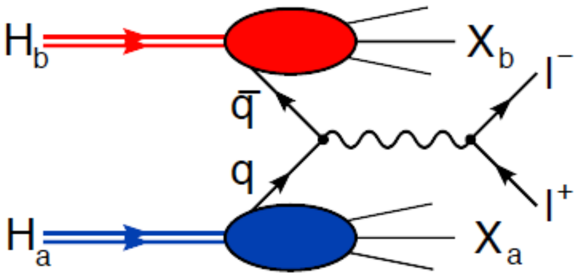

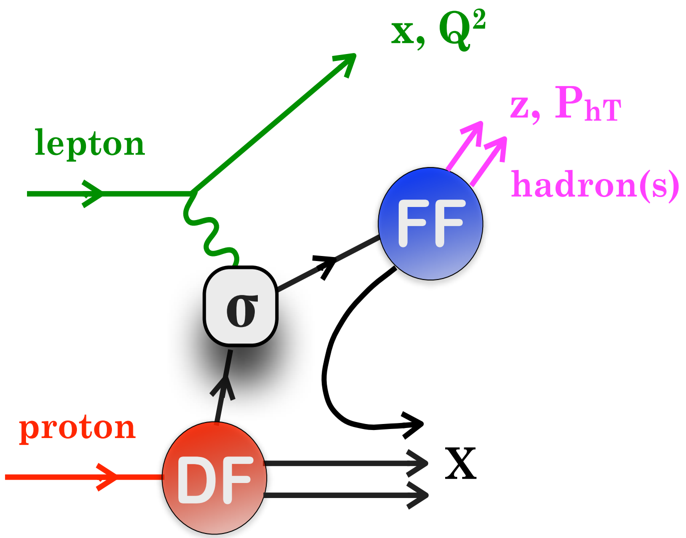

Accessing TMDs

The golden processes to measure TMDs are **Drell-Yan** and **Semi-Inclusive DIS (SIDIS)**

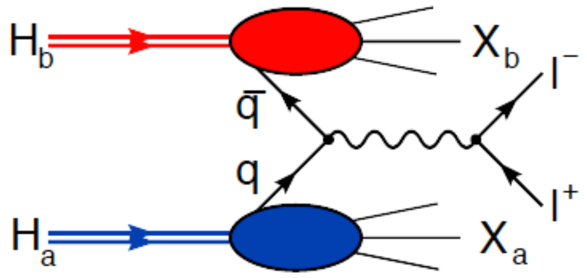

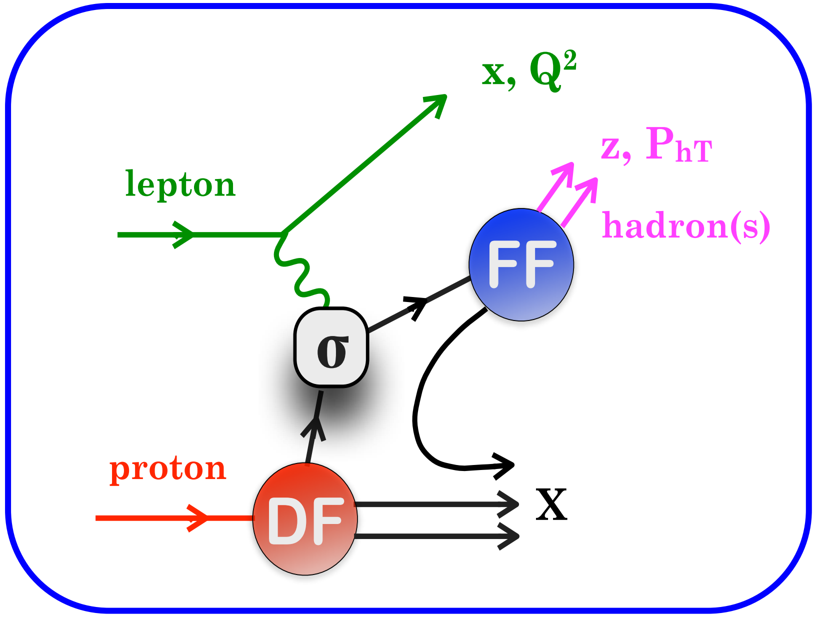

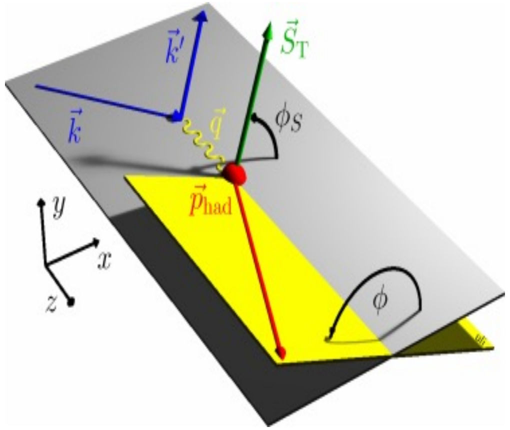

Accessing TMDs

The golden processes to measure TMDs are **Drell-Yan** and **Semi-Inclusive DIS (SIDIS)**

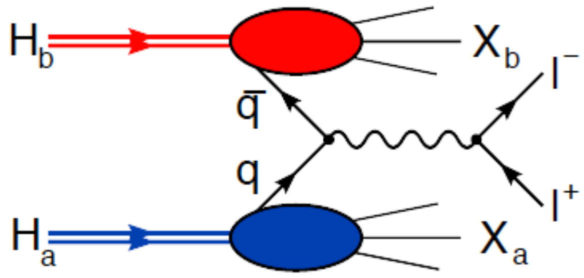

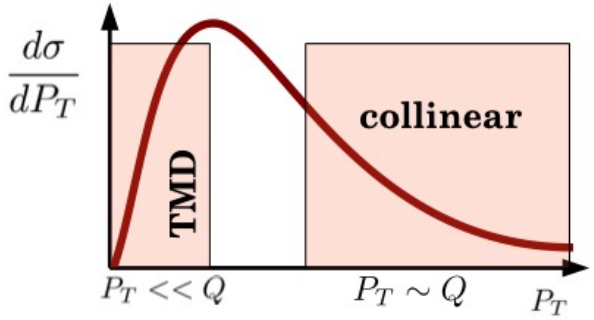

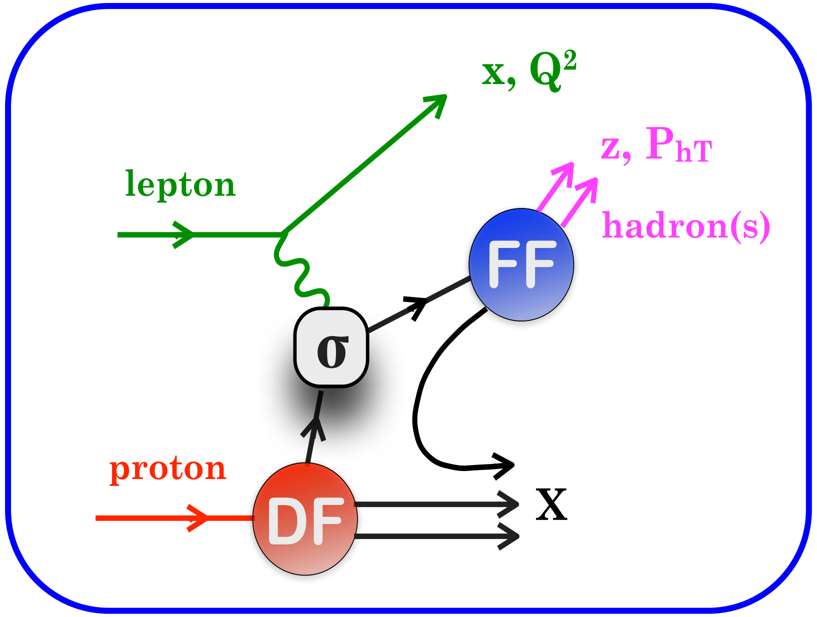

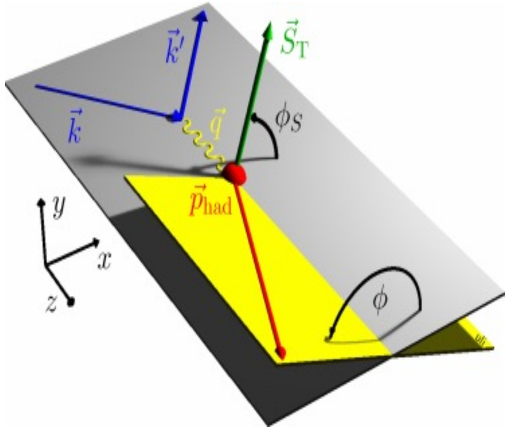

Fragmentation Functions (FF)

		quark U	quark L	quark T
h	U	D_1		$H_1^\perp$

TMD factorization:

$$\sigma^{ep\to ehX} = \sum_q DF \otimes \sigma^{eq\to eq} \otimes FF$$

Parton Distributions Functions (DF)

		quark U	quark L	quark T
nucleon	U	f_1		$h_1^\perp$
nucleon	L		g_1	$h_{1L}^\perp$
nucleon	T	$f_{1T}^\perp$	$g_{1T}^\perp$	h_1, $h_{1T}^\perp$

The SIDIS cross section

$$\frac{d\sigma^h}{dx\,dy\,d\phi_S\,dz\,d\phi\,d\mathbf{P}_{h\perp}^2} = \frac{\alpha^2}{xyQ^2}\frac{y^2}{2(1-\epsilon)}\left(1+\frac{\gamma^2}{2x}\right)$$

$$\Big\{ \Big[F_{UU,T} + \epsilon F_{UU,L} + \sqrt{2\epsilon(1+\epsilon)}\cos(\phi)F_{UU}^{\cos(\phi)} + \epsilon\cos(2\phi)F_{UU}^{\cos(2\phi)}\Big]$$

$$+ \lambda_l \Big[\sqrt{2\epsilon(1-\epsilon)}\sin(\phi)F_{LU}^{\sin(\phi)}\Big]$$

$$+ S_L \Big[\sqrt{2\epsilon(1+\epsilon)}\sin(\phi)F_{UL}^{\sin(\phi)} + \epsilon\sin(2\phi)F_{UL}^{\sin(2\phi)}\Big]$$

$$+ S_L\,\lambda_l \Big[\sqrt{1-\epsilon^2}F_{LL} + \sqrt{2\epsilon(1-\epsilon)}\cos(\phi)F_{LL}^{\cos(\phi)}\Big]$$

$$+ S_T \Big[\sin(\phi-\phi_S)\left(F_{UT,T}^{\sin(\phi-\phi_S)} + \epsilon F_{UT,L}^{\sin(\phi-\phi_S)}\right) + \epsilon\sin(\phi+\phi_S)F_{UT}^{\sin(\phi+\phi_S)} + \epsilon\sin(3\phi-\phi_S)F_{UT}^{\sin(3\phi-\phi_S)} + \sqrt{2\epsilon(1+\epsilon)}\sin(\phi_S)F_{UT}^{\sin(\phi_S)} + \sqrt{2\epsilon(1+\epsilon)}\sin(2\phi-\phi_S)F_{UT}^{\sin(2\phi-\phi_S)}\Big]$$

$$+ S_T\,\lambda_l \Big[\sqrt{1-\epsilon^2}\cos(\phi-\phi_S)F_{LT}^{\cos(\phi-\phi_S)} + \sqrt{2\epsilon(1-\epsilon)}\cos(\phi_S)F_{LT}^{\cos(\phi_S)} + \sqrt{2\epsilon(1-\epsilon)}\cos(2\phi-\phi_S)F_{LT}^{\cos(2\phi-\phi_S)}\Big]$$

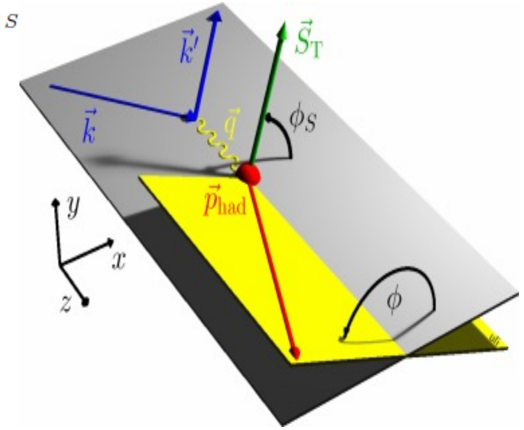

Bacchetta et al., JHEP 02, 093 (2007)

The SIDIS cross section

$$
\frac{d\sigma^h}{dx\,dy\,d\phi_S\,dz\,d\phi\,dP_{h\perp}^2} = \frac{\alpha^2}{xyQ^2}\frac{y^2}{2(1-\epsilon)}\left(1+\frac{\gamma^2}{2x}\right)
$$

$$
\begin{aligned}
\Big\{ \; & \Big[F_{UU,T} + \epsilon F_{UU,L} \\
& + \sqrt{2\epsilon(1+\epsilon)}\cos(\phi) F_{UU}^{\cos(\phi)} + \epsilon\cos(2\phi) F_{UU}^{\cos(2\phi)}\Big] \\
+ \; \lambda_l \; & \Big[\sqrt{2\epsilon(1-\epsilon)}\sin(\phi) F_{LU}^{\sin(\phi)}\Big] \\
+ \; S_L \; & \Big[\sqrt{2\epsilon(1+\epsilon)}\sin(\phi) F_{UL}^{\sin(\phi)} + \epsilon\sin(2\phi) F_{UL}^{\sin(2\phi)}\Big] \\
+ \; S_L\,\lambda_l \; & \Big[\sqrt{1-\epsilon^2} F_{LL} + \sqrt{2\epsilon(1-\epsilon)}\cos(\phi) F_{LL}^{\cos(\phi)}\Big] \\
+ \; S_T \; & \Big[\sin(\phi-\phi_S)\Big(F_{UT,T}^{\sin(\phi-\phi_S)} + \epsilon F_{UT,L}^{\sin(\phi-\phi_S)}\Big) \\
& + \epsilon\sin(\phi+\phi_S) F_{UT}^{\sin(\phi+\phi_S)} + \epsilon\sin(3\phi-\phi_S) F_{UT}^{\sin(3\phi-\phi_S)} \\
& + \sqrt{2\epsilon(1+\epsilon)}\sin(\phi_S) F_{UT}^{\sin(\phi_S)} \\
& + \sqrt{2\epsilon(1+\epsilon)}\sin(2\phi-\phi_S) F_{UT}^{\sin(2\phi-\phi_S)}\Big] \\
+ \; S_T\,\lambda_l \; & \Big[\sqrt{1-\epsilon^2}\cos(\phi-\phi_S) F_{LT}^{\cos(\phi-\phi_S)} \\
& + \sqrt{2\epsilon(1-\epsilon)}\cos(\phi_S) F_{LT}^{\cos(\phi_S)} \\
& + \sqrt{2\epsilon(1-\epsilon)}\cos(2\phi-\phi_S) F_{LT}^{\cos(2\phi-\phi_S)}\Big]
\end{aligned}
$$

Bacchetta et al., JHEP 02, 093 (2007)

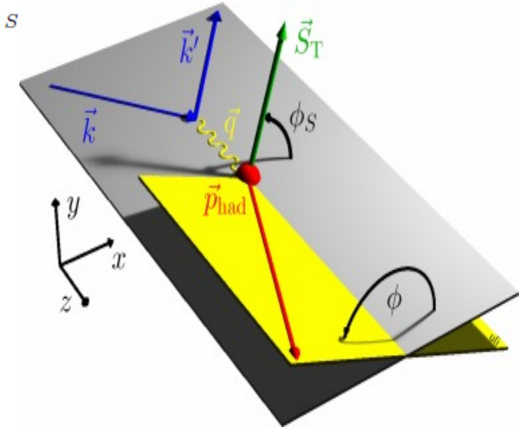

Fragmentation Functions (FF)

		quark U	quark L	quark T
h	U	D_1		$H_1^\perp$

target polarization

$F_{XY,Z} \propto$ **DF** $\otimes$ **FF**

beam polarization — virtual photon polarization

Parton Distributions Functions (DF)

		quark U	quark L	quark T
nucleon	U	f_1		$h_1^\perp$
nucleon	L		g_1	$h_{1L}^\perp$
nucleon	T	$f_{1T}^\perp$	$g_{1T}^\perp$	h_1, $h_{1T}^\perp$

TMD effects and azimuthal modulations

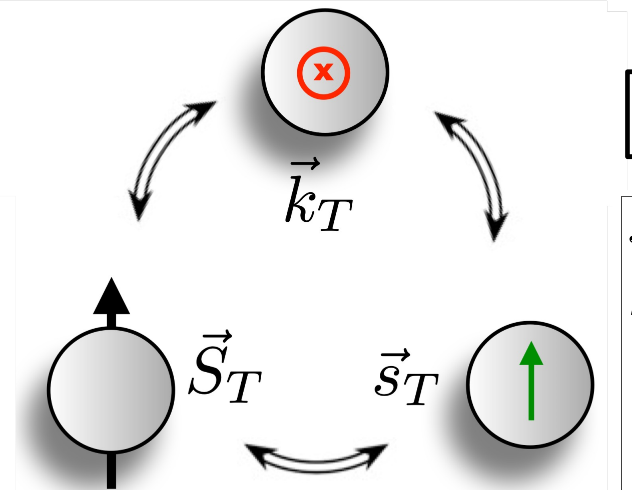

Courtesy C. Riedl

$$\vec{S}\cdot(\vec{p}_1\times\vec{p}_2)$$

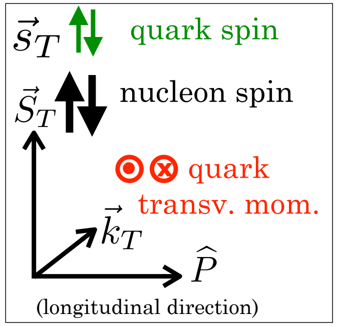

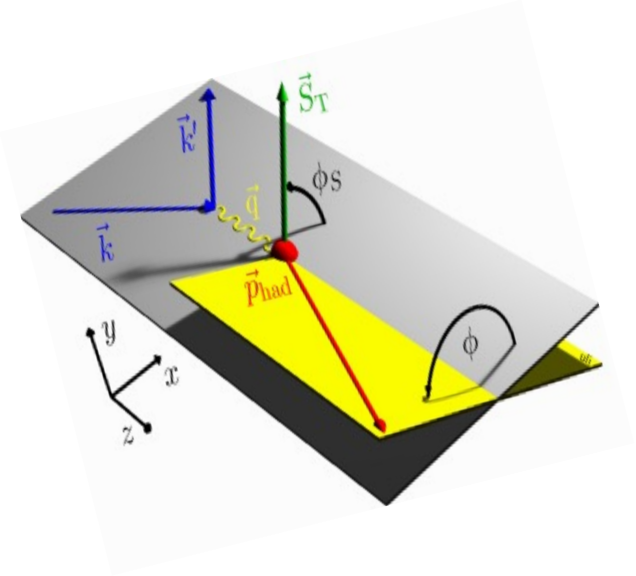

TMD effects and azimuthal modulations

Sivers function

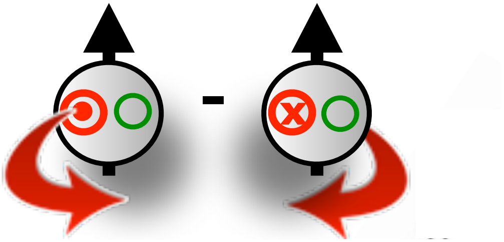

$\vec{S}_T \cdot (\hat{P} \times \vec{k}_T)$

If non-zero: indicate **orbital angular momentum (OAM)** of partons inside the nucleon.

Sivers effect ($f_{1T}^{\perp} \otimes D_1$): correlation between quark transverse momentum k_T and nucleon transverse polarization S_T generates a $\sin(\phi - \phi_S)$ modulation

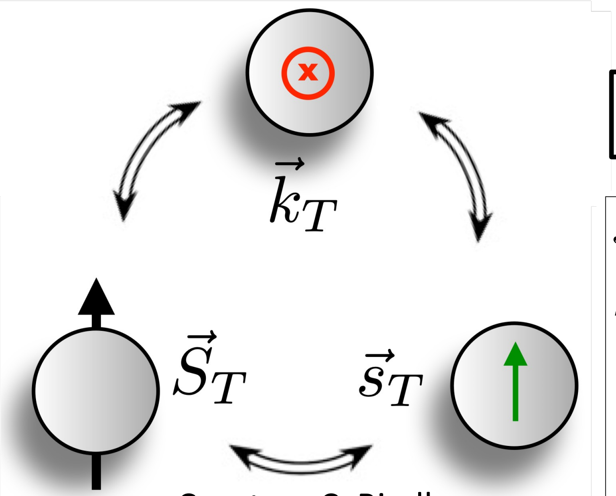

Courtesy C. Riedl

$\vec{S} \cdot (\vec{p}_1 \times \vec{p}_2)$

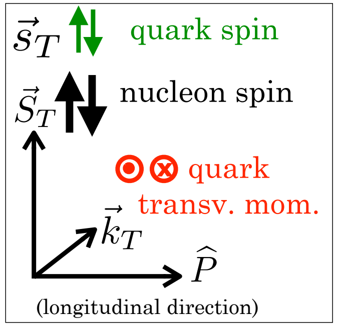

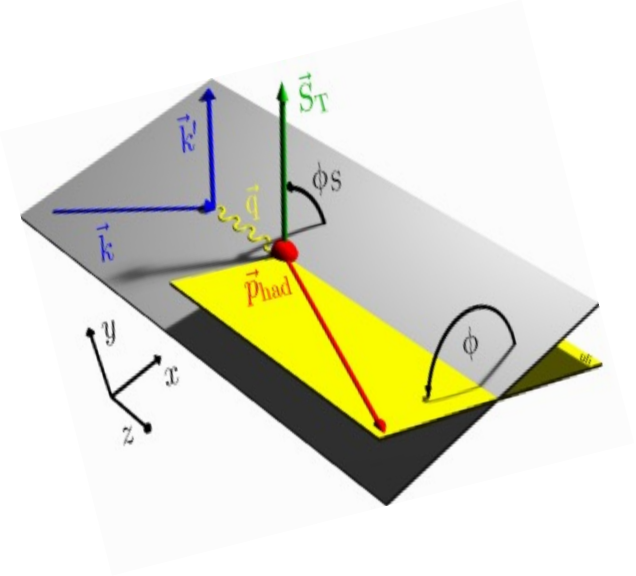

TMD effects and azimuthal modulations

Sivers function

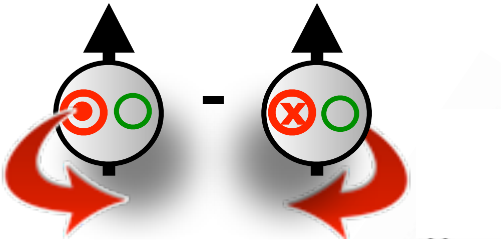

$$\vec{S}_T \cdot (\widehat{P} \times \vec{k}_T)$$

If non-zero: indicate **orbital angular momentum (OAM)** of partons inside the nucleon.

Sivers effect ($f_{1T}^{\perp} \otimes D_1$): correlation between quark transverse momentum k_T and nucleon transverse polarization S_T generates a $\sin(\phi - \phi_S)$ modulation

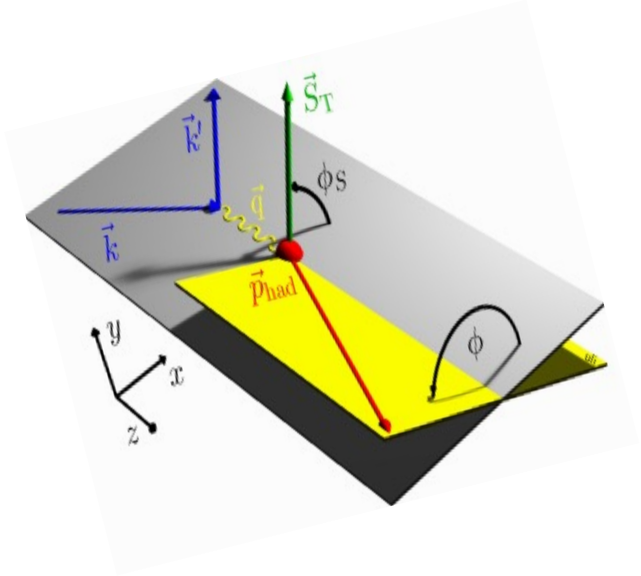

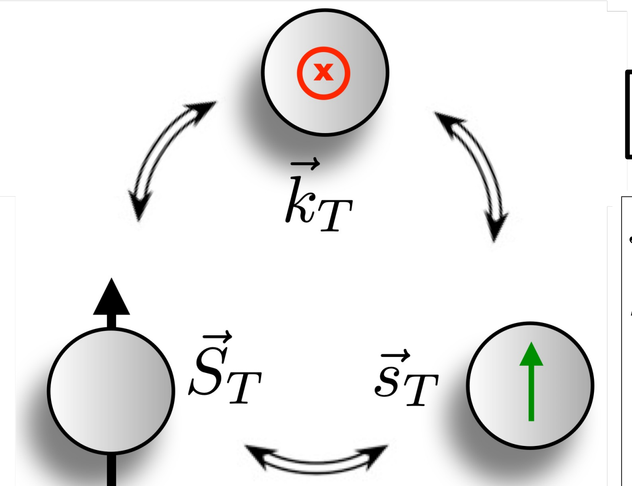

Courtesy C. Riedl

$$\vec{S} \cdot (\vec{p}_1 \times \vec{p}_2)$$

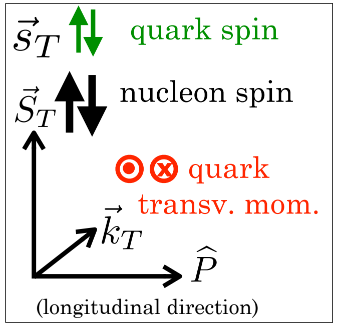

Boer-Mulders function

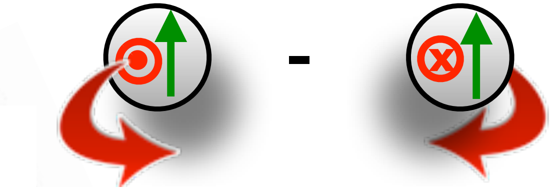

$$\vec{s}_T \cdot (\widehat{P} \times \vec{k}_T)$$

B-M effect: ($h_1^{\perp} \otimes H_1^{\perp}$): correlation between quark transverse polarization s_T and transverse momentum k_T generates a $\cos(2\phi)$ modulation

TMD effects and azimuthal modulations

Sivers function

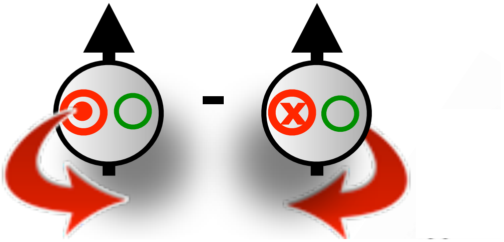

$\vec{S}_T \cdot (\hat{P} \times \vec{k}_T)$

If non-zero: indicate **orbital angular momentum (OAM)** of partons inside the nucleon.

Sivers effect ($f_{1T}^{\perp} \otimes D_1$): correlation between quark transverse momentum k_T and nucleon transverse polarization S_T generates a $\mathbf{sin}(\boldsymbol{\phi} - \boldsymbol{\phi_S})$ modulation

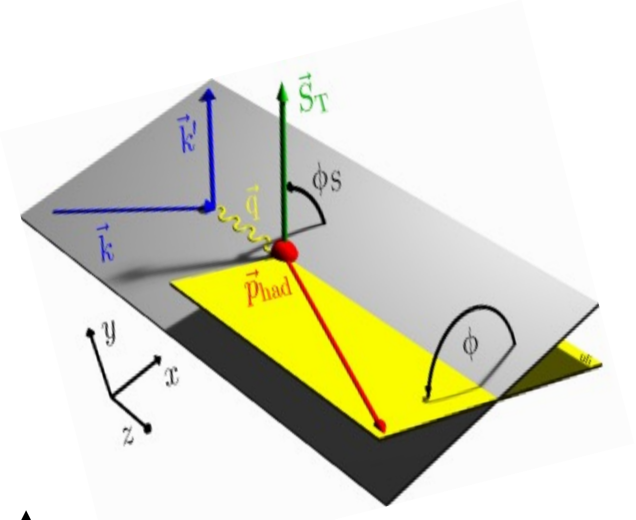

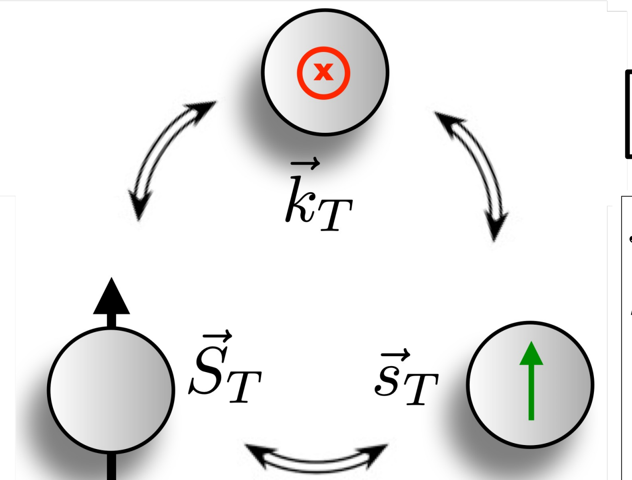

$\vec{S} \cdot (\vec{p}_1 \times \vec{p}_2)$

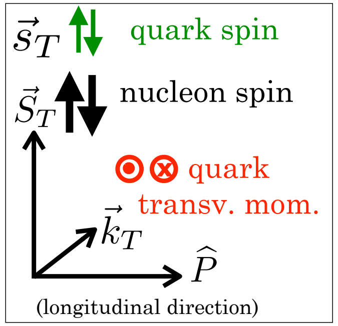

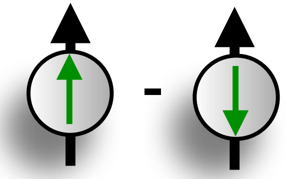

$\vec{s}_T \cdot (\hat{k} \times \vec{P}_{hT})$

Transversity $\otimes$ Collins function

chiral-odd PDF

chiral-odd FF

Collins effect ($h_1 \otimes H_1^{\perp}$): correlation between quark transverse polarization s_T and final-state hadron transverse momentum P_{hT} generates a $\mathbf{sin}(\boldsymbol{\phi} + \boldsymbol{\phi_S})$ modulation

Boer-Mulders function

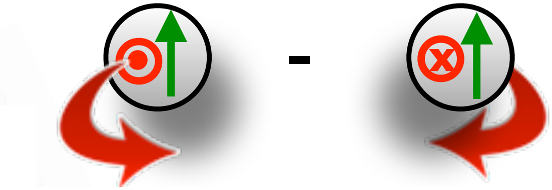

$\vec{s}_T \cdot (\hat{P} \times \vec{k}_T)$

B-M effect: ($h_1^{\perp} \otimes H_1^{\perp}$): correlation between quark transverse polarization s_T and transverse momentum k_T generates a $\mathbf{cos}(\mathbf{2}\boldsymbol{\phi})$ modulation

…and many others

The multi-D CLAS12 BSAs

- 10.6 GeV polarized electrons on unpol. H target
- beam polarization $\sim 86\%$!
- Large statistics, large acceptance
- multi-dimensional analysis (344 4-Dim bins!)

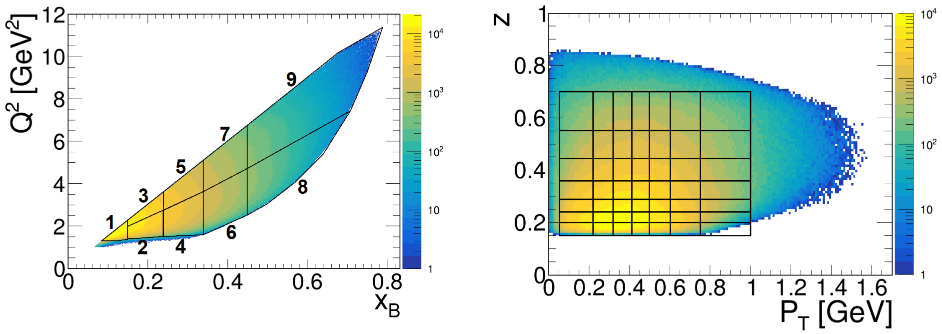

The multi-D CLAS12 BSAs

- 10.6 GeV polarized electrons on unpol. H target
- beam polarization $\sim 86\%$!
- Large statistics, large acceptance
- multi-dimensional analysis (344 4-Dim bins!)

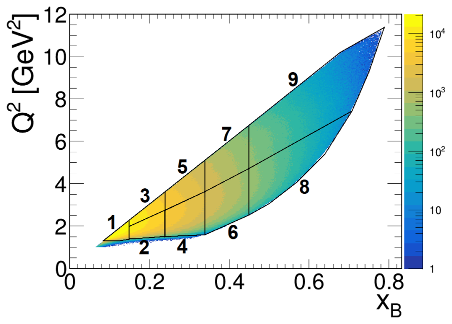

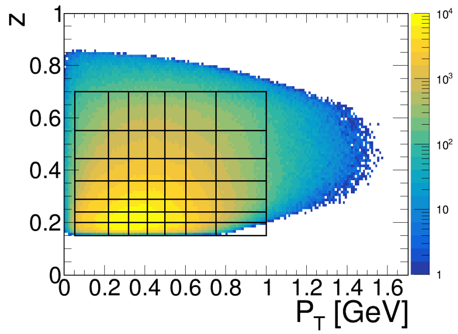

$$A_{LU}^{\sin(\phi)} \propto \frac{F_{LU}^{\sin(\phi)}}{F_{UU}} \propto \frac{M}{Q}\left[eH_1^{\perp} + f_1\tilde{G}^{\perp} + g^{\perp}D_1 + h_1^{\perp}\tilde{E}\right]$$

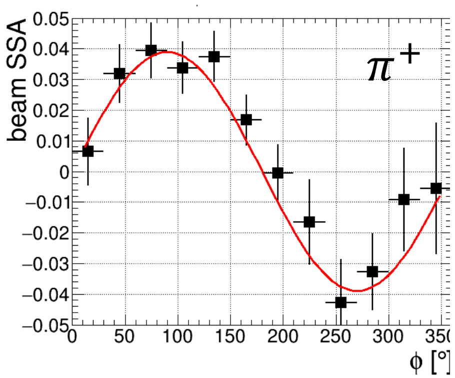

$\sin\phi$ modulation in a specific 4-dim bin

The multi-D CLAS12 BSAs

[Phys. Rev. Lett. 128 (2022) 6, 062005](#)

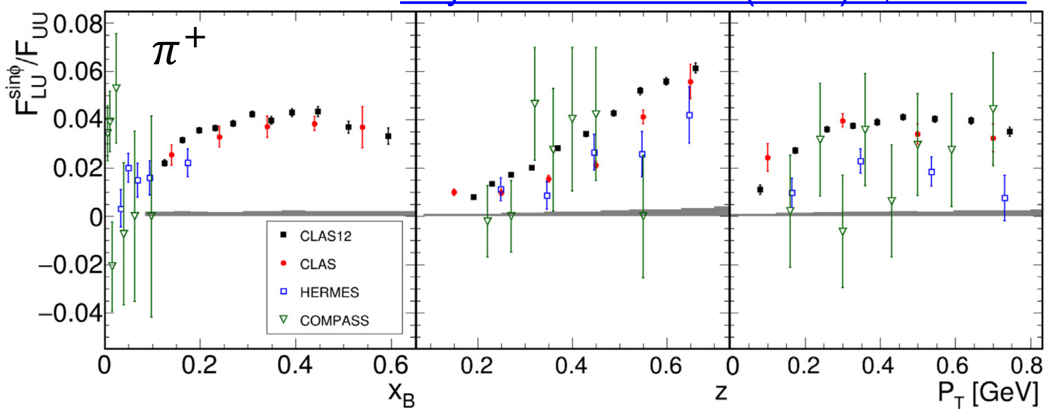

- 10.6 GeV polarized electrons on unpol. H target
- beam polarization ~86%!
- Large statistics, large acceptance
- multi-dimensional analysis (344 4-Dim bins!)

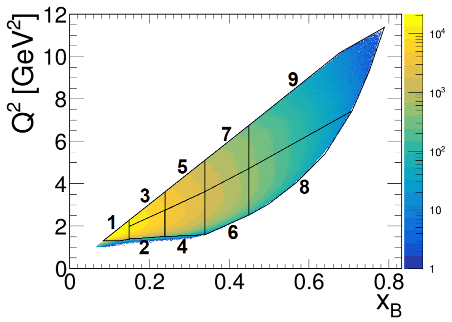

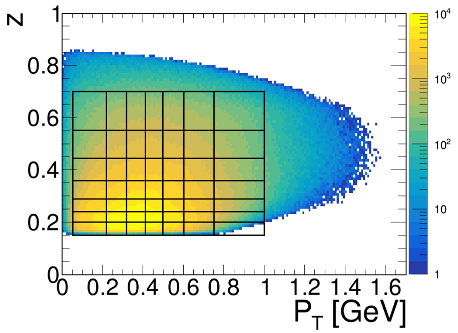

$$A_{LU}^{\sin(\phi)} \propto \frac{F_{LU}^{\sin(\phi)}}{F_{UU}} \propto \frac{M}{Q}\left[eH_1^{\perp} + f_1\tilde{G}^{\perp} + g^{\perp}D_1 + h_1^{\perp}\tilde{E}\right]$$

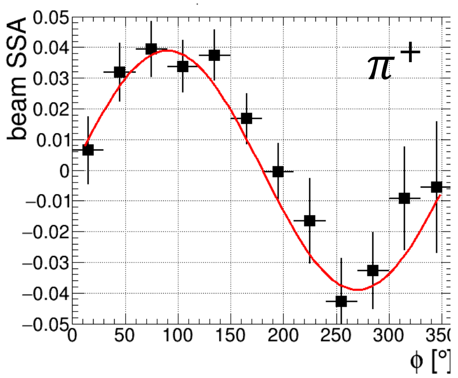

$\sin\phi$ modulation in a specific 4-dim bin

The multi-D CLAS12 BSAs

Phys. Rev. Lett. 128 (2022) 6, 062005

- 10.6 GeV polarized electrons on unpol. H target
- beam polarization ~86%!
- Large statistics, large acceptance
- multi-dimensional analysis (344 4-Dim bins!)

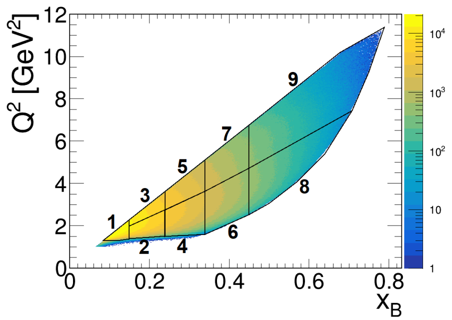

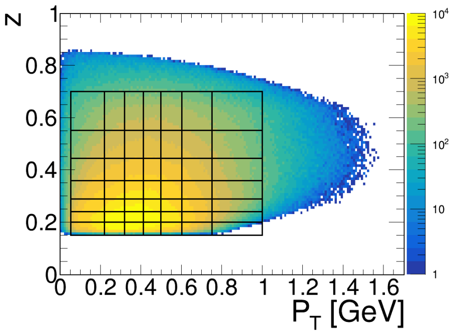

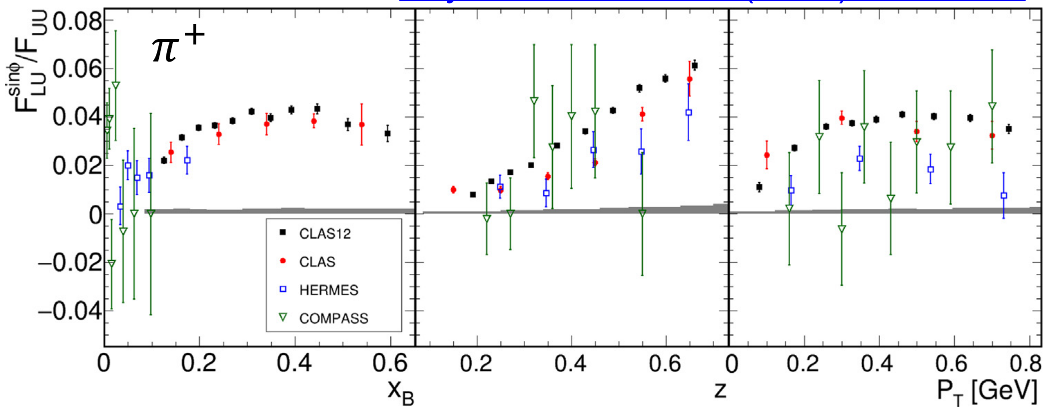

$$A_{LU}^{\sin(\phi)} \propto \frac{F_{LU}^{\sin(\phi)}}{F_{UU}} \propto \frac{M}{Q}\left[eH_1^{\perp} + f_1\widetilde{G}^{\perp} + g^{\perp}D_1 + h_1^{\perp}\widetilde{E}\right]$$

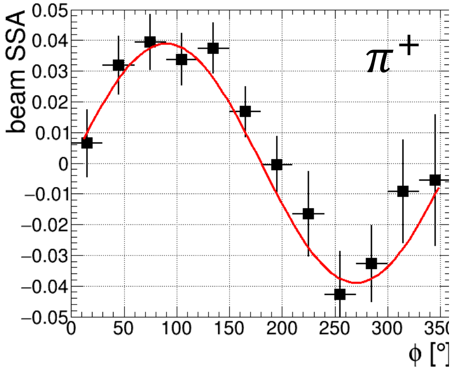

sin ϕ modulation in a specific 4-dim bin

Data compared with 3 models assuming different contributions to $F_{LU}^{\sin(\phi)}$

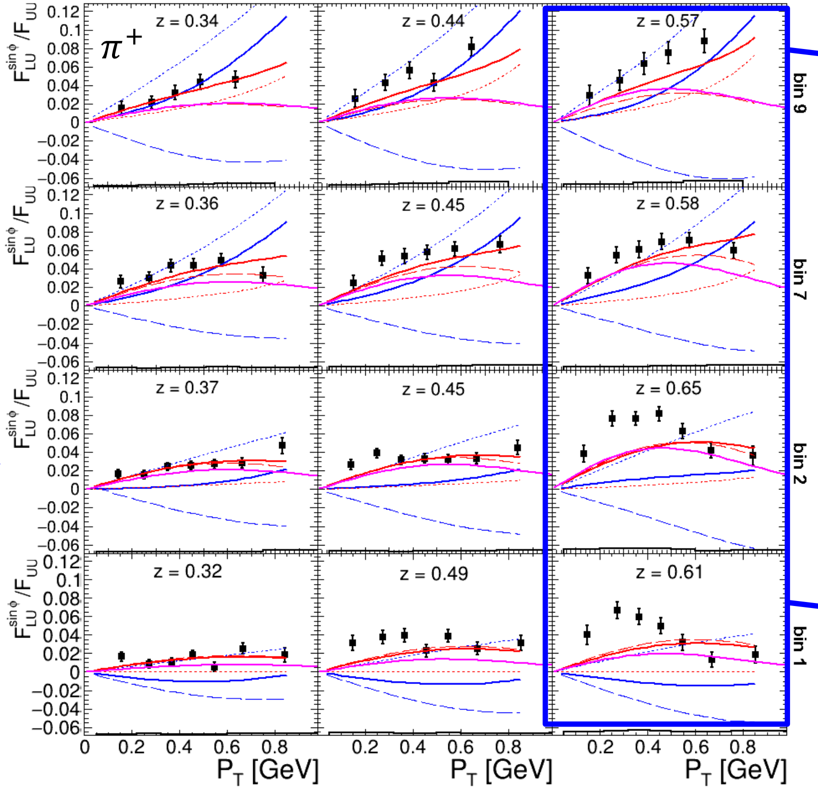

amplitudes increase with increasing z, x, Q^2

Increasing x and Q^2

peaking structure with varying mean value and width appears at large z

The COMPASS SIDIS Christmass present

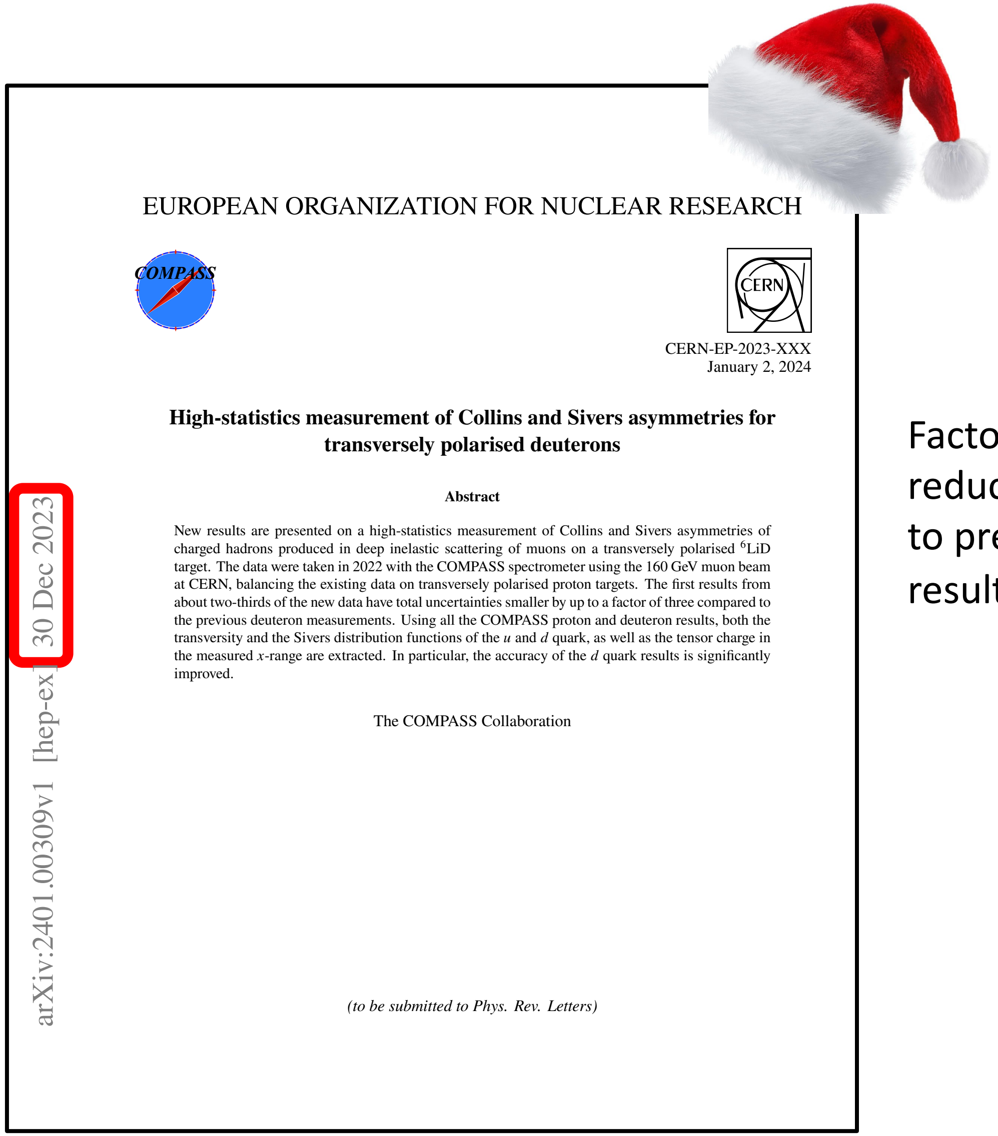

EUROPEAN ORGANIZATION FOR NUCLEAR RESEARCH

COMPASS

CERN

CERN-EP-2023-XXX
January 2, 2024

High-statistics measurement of Collins and Sivers asymmetries for transversely polarised deuterons

Abstract

New results are presented on a high-statistics measurement of Collins and Sivers asymmetries of charged hadrons produced in deep inelastic scattering of muons on a transversely polarised ^{6}LiD target. The data were taken in 2022 with the COMPASS spectrometer using the 160 GeV muon beam at CERN, balancing the existing data on transversely polarised proton targets. The first results from about two-thirds of the new data have total uncertainties smaller by up to a factor of three compared to the previous deuteron measurements. Using all the COMPASS proton and deuteron results, both the transversity and the Sivers distribution functions of the *u* and *d* quark, as well as the tensor charge in the measured *x*-range are extracted. In particular, the accuracy of the *d* quark results is significantly improved.

The COMPASS Collaboration

(to be submitted to Phys. Rev. Letters)

arXiv:2401.00309v1 [hep-ex] 30 Dec 2023

arXiv:2401.00309v1

Factor 3 uncertainty reduction compared to previous deuteron results (2002-2004)!

160 GeV μ on a ^6LiD transv. pol target

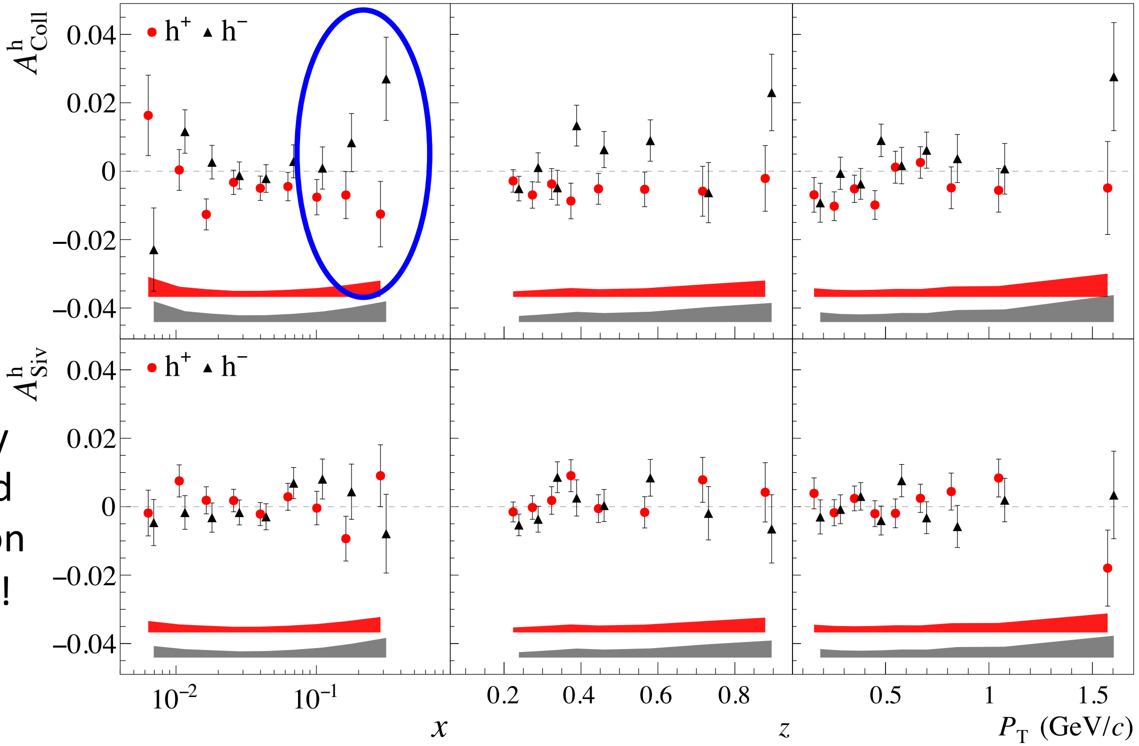

The COMPASS SIDIS Christmass present

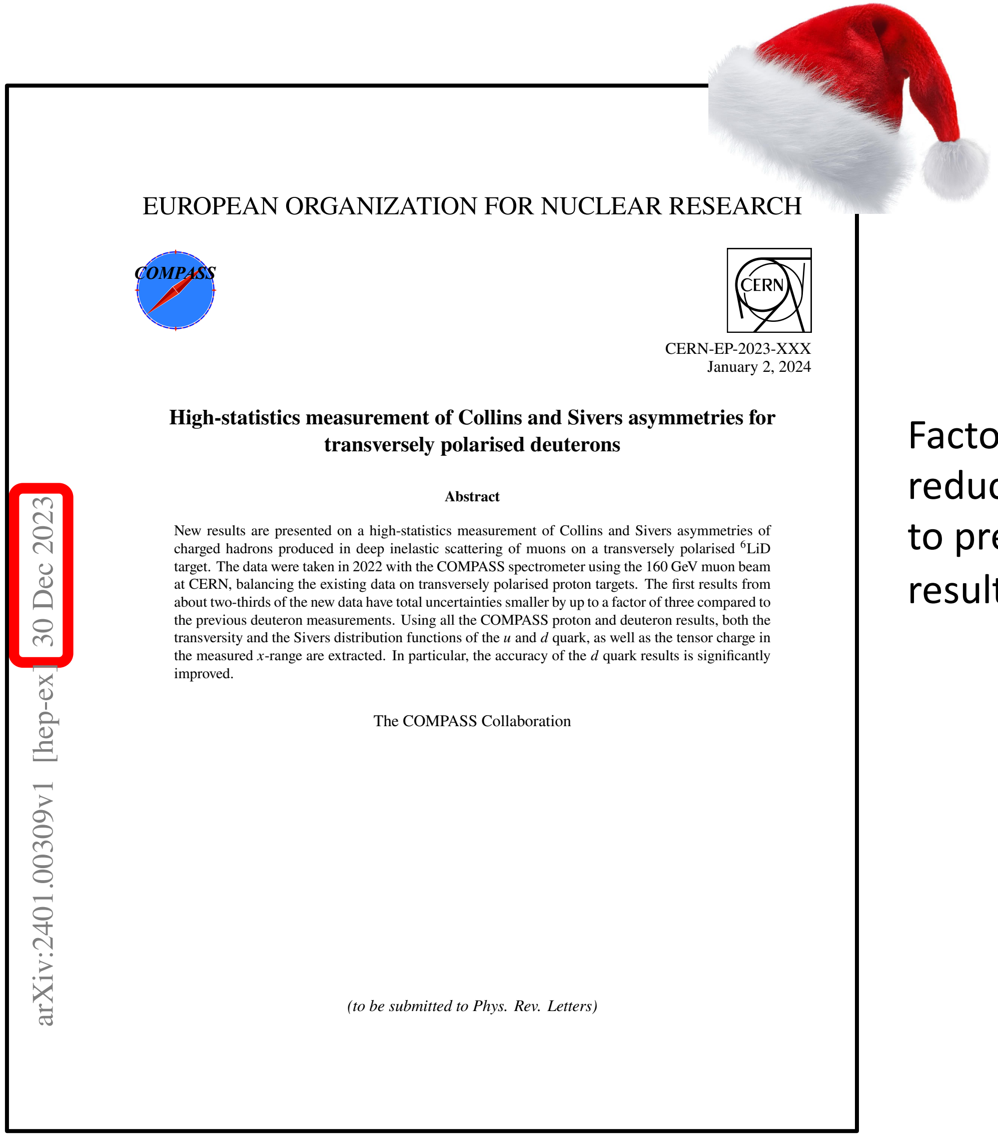
EUROPEAN ORGANIZATION FOR NUCLEAR RESEARCH

COMPASS

CERN

CERN-EP-2023-XXX
January 2, 2024

High-statistics measurement of Collins and Sivers asymmetries for transversely polarised deuterons

Abstract

New results are presented on a high-statistics measurement of Collins and Sivers asymmetries of charged hadrons produced in deep inelastic scattering of muons on a transversely polarised ^{6}LiD target. The data were taken in 2022 with the COMPASS spectrometer using the 160 GeV muon beam at CERN, balancing the existing data on transversely polarised proton targets. The first results from about two-thirds of the new data have total uncertainties smaller by up to a factor of three compared to the previous deuteron measurements. Using all the COMPASS proton and deuteron results, both the transversity and the Sivers distribution functions of the *u* and *d* quark, as well as the tensor charge in the measured *x*-range are extracted. In particular, the accuracy of the *d* quark results is significantly improved.

The COMPASS Collaboration

(to be submitted to Phys. Rev. Letters)

arXiv:2401.00309v1 [hep-ex] 30 Dec 2023

arXiv:2401.00309v1

160 GeV μ on a ^6LiD transv. pol target

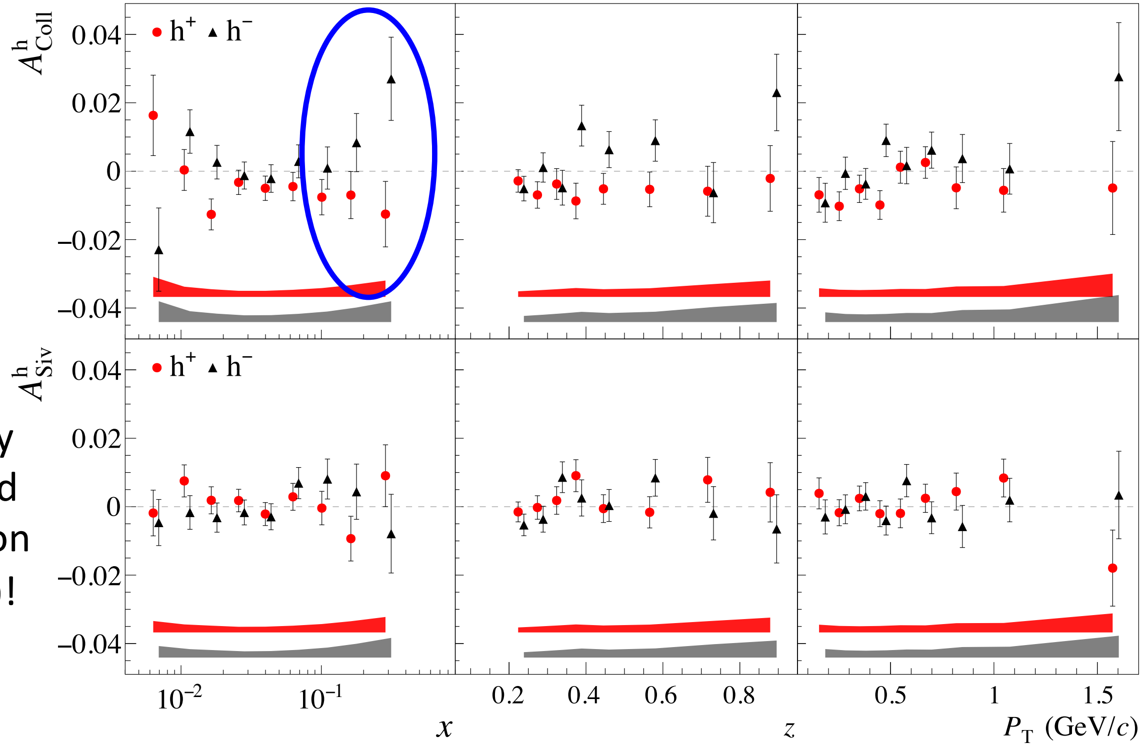

Factor 3 uncertainty reduction compared to previous deuteron results (2002-2004)!

using combined data with previously published p and d results

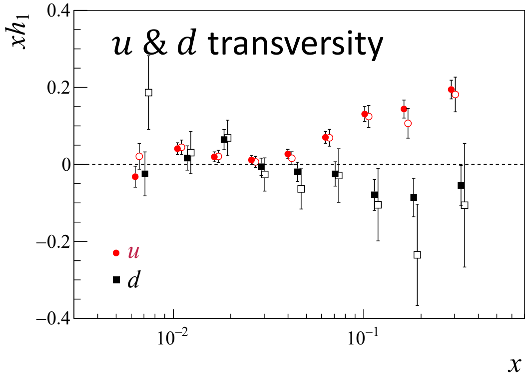

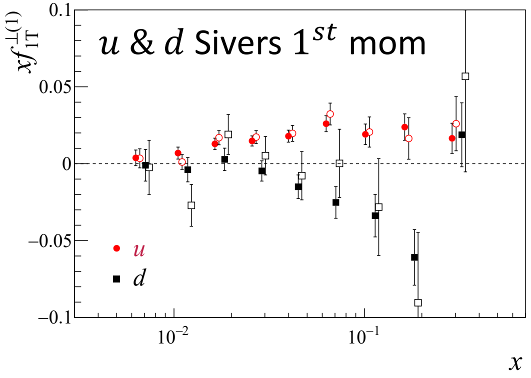

TMDs extractions from global fits

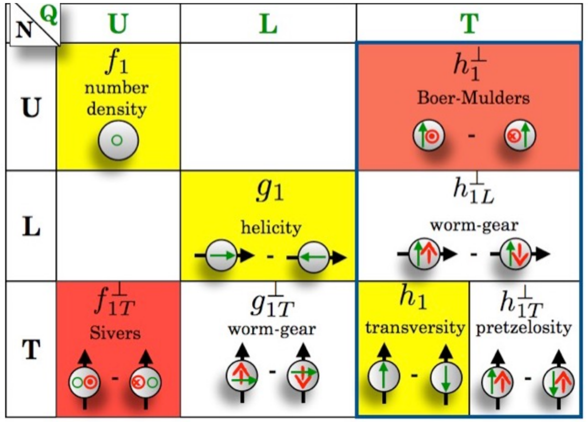

TMDs extractions from global fits

J. High Energ. Phys. 2022, 127 (2022)

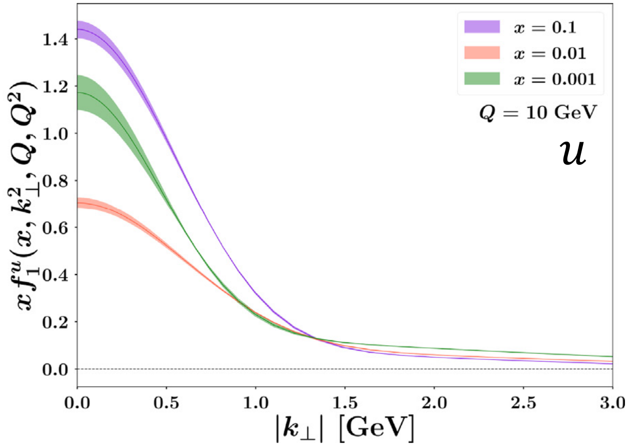

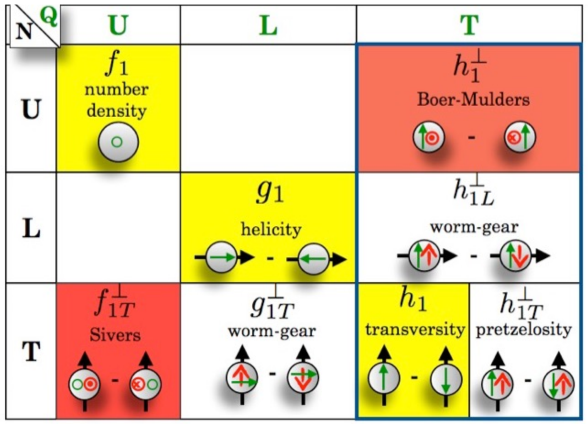

TMDs extractions from global fits

J. High Energ. Phys. 2022, 127 (2022)

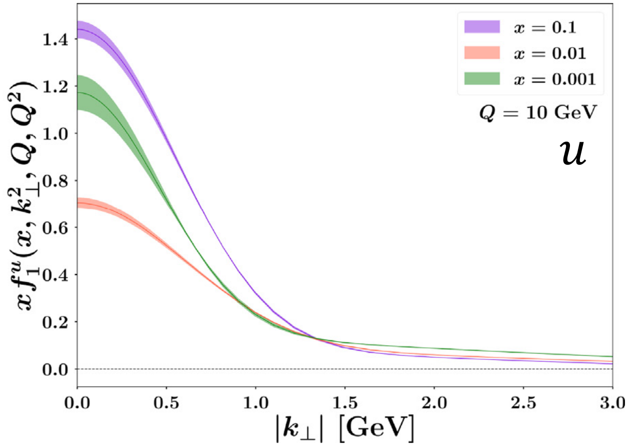

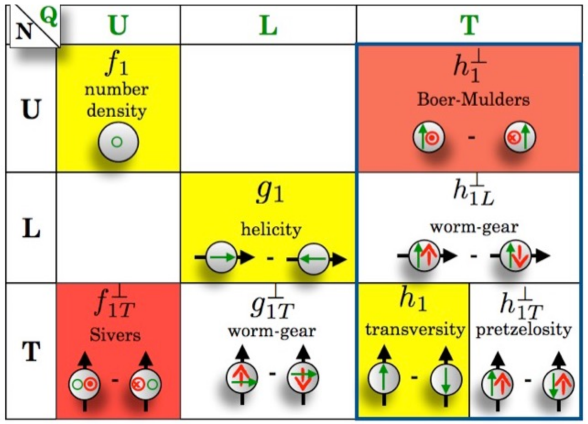

Phys. Rev. D 81, 034023 (2010)

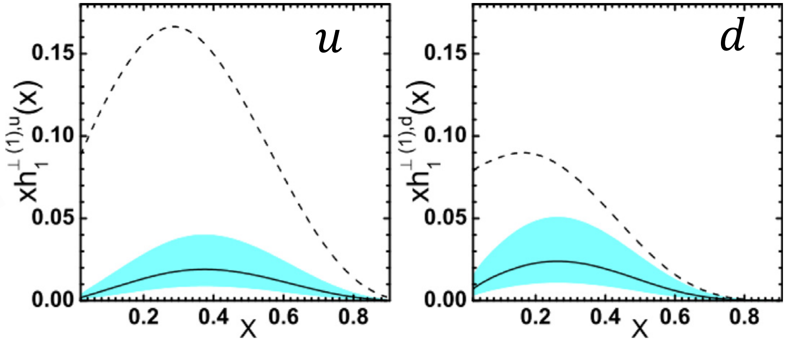

TMDs extractions from global fits

J. High Energ. Phys. 2022, 127 (2022)

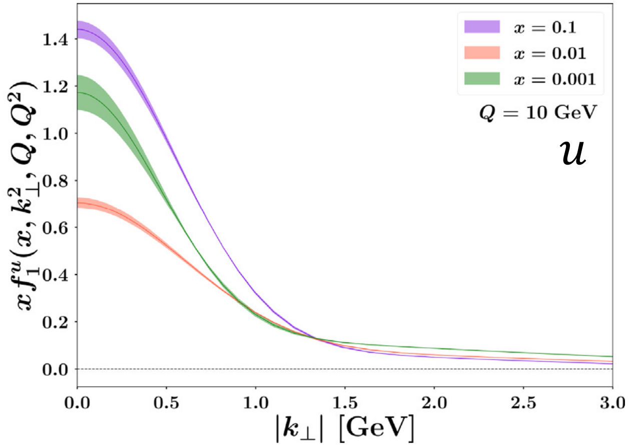

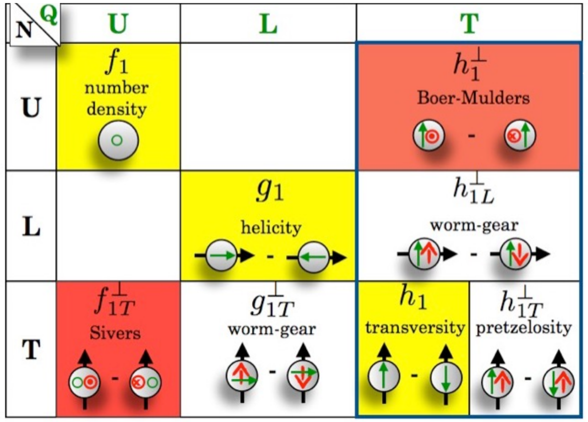

Phys. Rev. D 81, 034023 (2010)

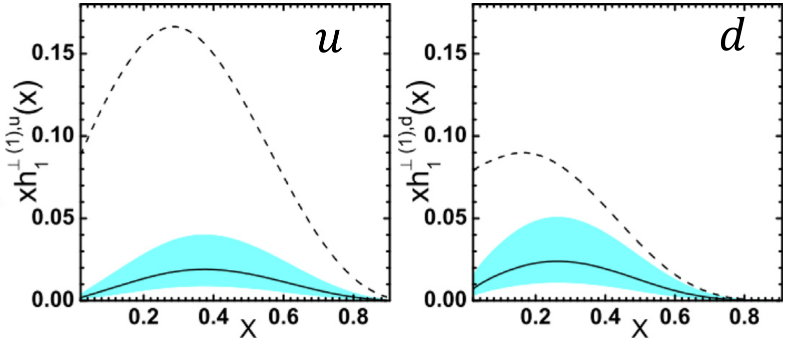

Phys. Rev. D 102, 054002 (2020)

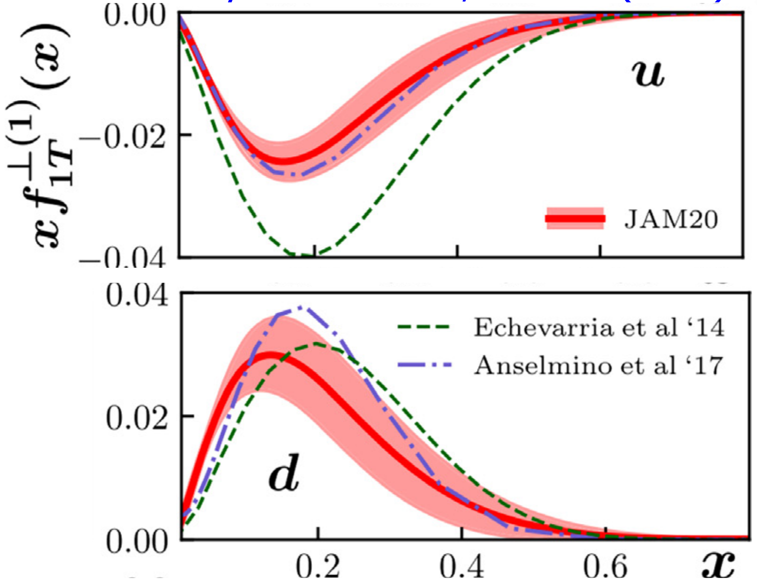

TMDs extractions from global fits

J. High Energ. Phys. 2022, 127 (2022)

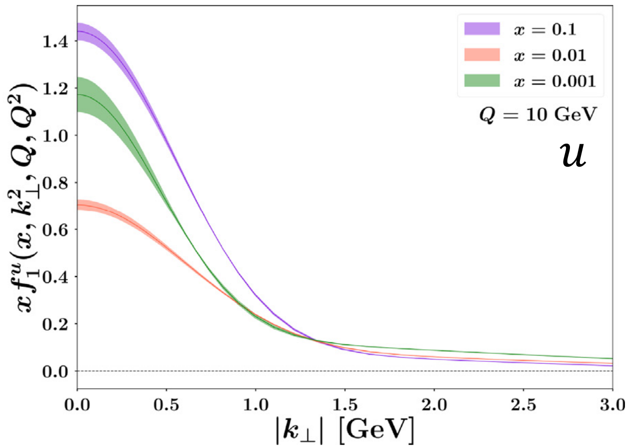

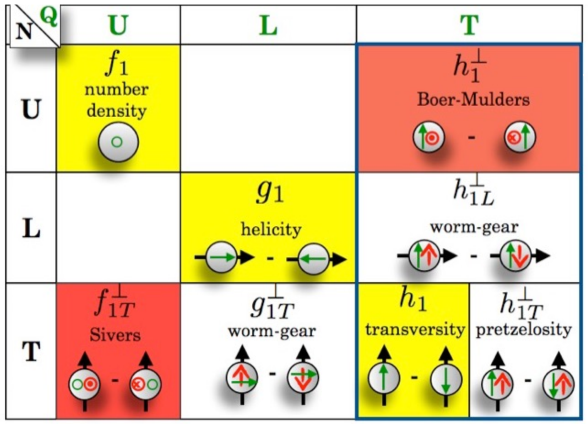

Phys. Rev. D 81, 034023 (2010)

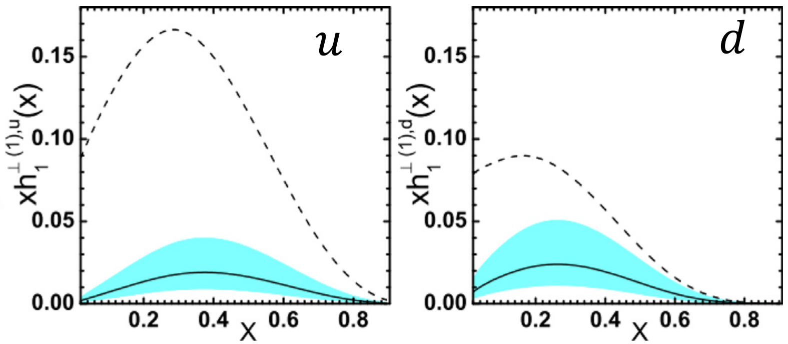

Phys. Rev. D 102, 054002 (2020)

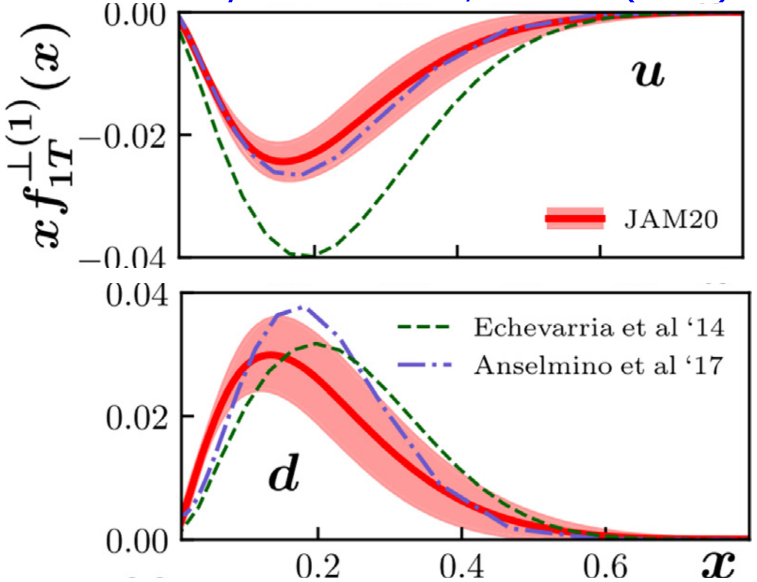

Phys. Rev. D 102, 054002 (2020)

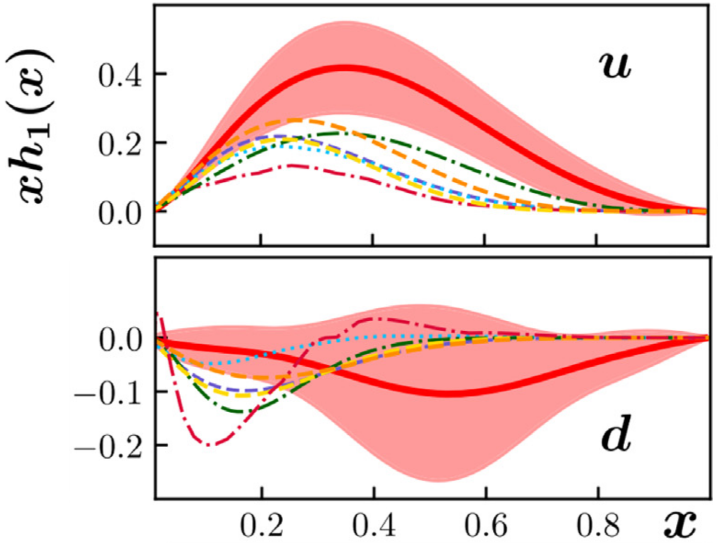

TMDs extractions from global fits

J. High Energ. Phys. 2022, 127 (2022)

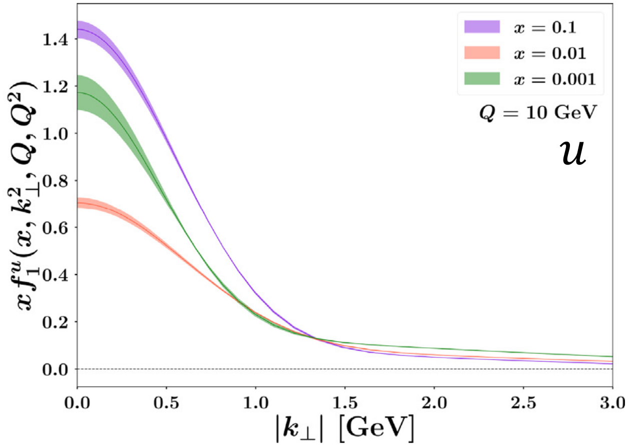

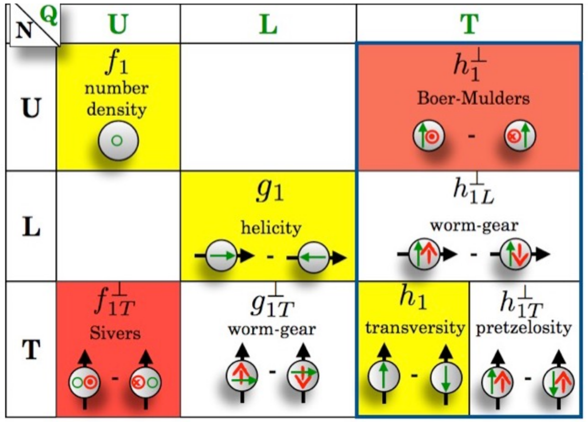

Phys. Rev. D 81, 034023 (2010)

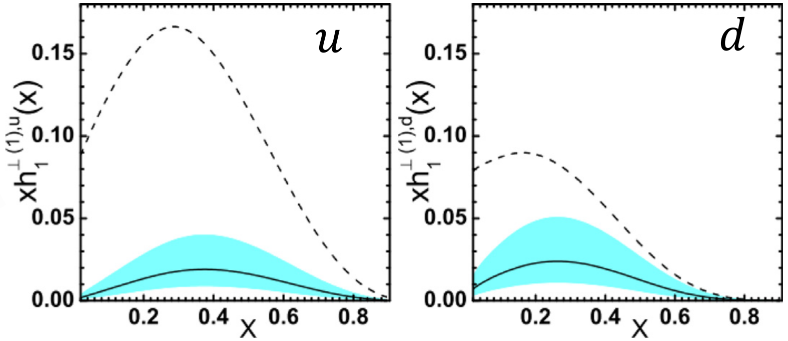

Phys. Rev. D 102, 054002 (2020)

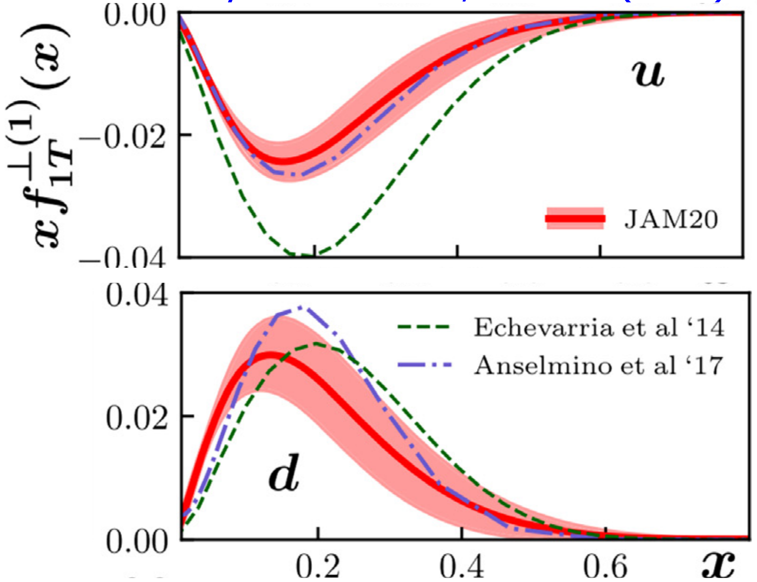

Phys. Rev. D 105, 034007 (2022)

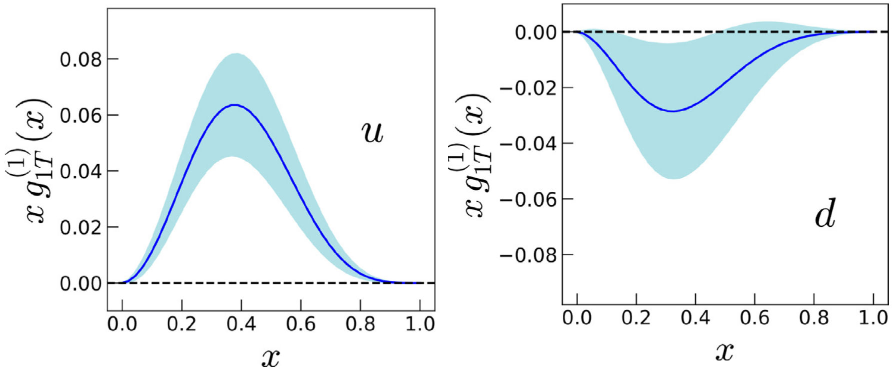

Phys. Rev. D 102, 054002 (2020)

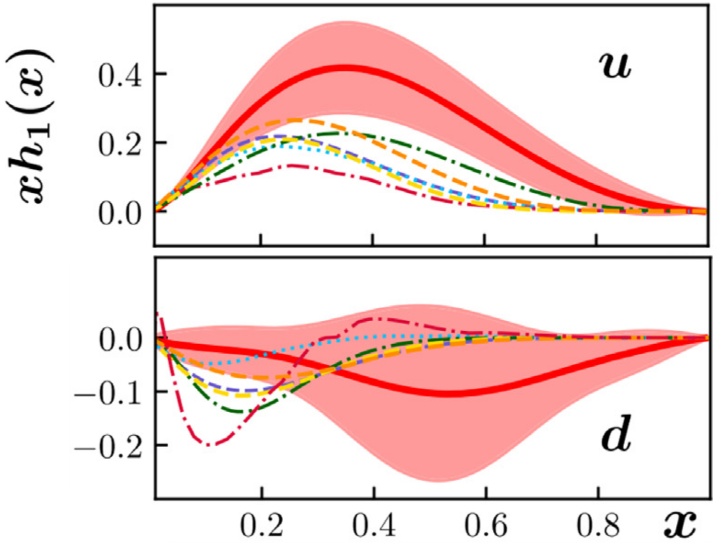

Conclusions

- After decades of collinear studies, the **3D structure of the nucleon is now being revealed** thanks to a huge International experimental and theoretical effort!

Conclusions

- After decades of collinear studies, the **3D structure of the nucleon is now being revealed** thanks to a huge International experimental and theoretical effort!
- A **rich phenomenology and surprising effects** arise when intrinsic transverse degrees of freedom (spin, momentum) are not integrated out!

Conclusions

- After decades of collinear studies, the **3D structure of the nucleon is now being revealed** thanks to a huge International experimental and theoretical effort!
- A **rich phenomenology and surprising effects** arise when intrinsic transverse degrees of freedom (spin, momentum) are not integrated out!
- Revealing the complex QCD dynamics of nucleons requires **high-precision multi-dimensional measurements**: need large acceptance detectors, high luminosity, low systematics.

Conclusions

- After decades of collinear studies, the **3D structure of the nucleon is now being revealed** thanks to a huge International experimental and theoretical effort!
- A **rich phenomenology and surprising effects** arise when intrinsic transverse degrees of freedom (spin, momentum) are not integrated out!
- Revealing the complex QCD dynamics of nucleons requires **high-precision multi-dimensional measurements**: need large acceptance detectors, high luminosity, low systematics.
- New high-precision multi-dimensional results are expected in the near future from **JLab12** and **Amber**, while in the next decade the **EIC** will complete the program with precise measurements in the poorly explored sea-quark and gluon domain at low-x and high-Q^2 region.

Conclusions

- After decades of collinear studies, the **3D structure of the nucleon is now being revealed** thanks to a huge International experimental and theoretical effort!
- A **rich phenomenology and surprising effects** arise when intrinsic transverse degrees of freedom (spin, momentum) are not integrated out!
- Revealing the complex QCD dynamics of nucleons requires **high-precision multi-dimensional measurements**: need large acceptance detectors, high luminosity, low systematics.
- New high-precision multi-dimensional results are expected in the near future from **JLab12** and **Amber**, while in the next decade the **EIC** will complete the program with precise measurements in the poorly explored sea-quark and gluon domain at low-x and high-Q^2 region.
- A solid **theoretical framework**, sophisticated phenomenological **global analyses** and reliable **theoretical models** are necessary to interpret the physics beyond the experimental observables and pin down the underlying distribution functions (TMDs, GPDs,…).

Backup

Accessing GPDs

The extraction of GPDs from DVCS observables is not trivial:

- experimental observables are only sensitive to CFFs, which contain the GPDs integrated over x
- different observables exhibit different sensitivity to a single CFF
- a precise extraction of the various CFFs is only possible through **model dependent global fits** over different observables and complementary kinematic regions

For the extraction of the underlying GPDs data are compared with different classes of **theoretical models:**

- Vanderhaeghen-Guichon-Guidal (**VGG**)
- Goloskokov-Kroll (**GK**)
- Goldstein-Liuti (**GL**)
- Kumerički-Liuti-Müller (**KM15**) [provides best agreement with data]
- …

The SIDIS cross section

$$\sigma(\phi,\phi_S) \equiv \frac{d^6\sigma}{dx\,dy\,dz\,d\phi\,d\phi_S\,dP_{hT}^2} = \frac{\alpha^2}{xyQ^2}\frac{y^2}{2(1-\epsilon)}\left(1+\frac{\gamma^2}{2x}\right)$$

$$\Big\{ F_{UU,T} + \epsilon F_{UU,L} + \sqrt{2\epsilon(1+\epsilon)}\,\cos\phi\, F_{UU}^{\cos\phi} + \epsilon\cos(2\phi)\, F_{UU}^{\cos(2\phi)} + \lambda_e\left[\sqrt{2\epsilon(1-\epsilon)}\,\sin\phi\, F_{LU}^{\sin\phi}\right] +$$

$$+ S_L\left[\sqrt{2\epsilon(1+\epsilon)}\,\sin\phi\, F_{UL}^{\sin\phi} + \epsilon\sin(2\phi)\, F_{UL}^{\sin(2\phi)}\right] + S_L\lambda_e\left[\sqrt{1-\epsilon^2}\, F_{LL} + \sqrt{2\epsilon(1-\epsilon)}\,\cos\phi\, F_{LL}^{\cos\phi}\right]$$

$$+ |S_T|\Big[\sin(\phi-\phi_S)\left(F_{UT,T}^{\sin(\phi-\phi_S)} + \epsilon F_{UT,L}^{\sin(\phi-\phi_S)}\right) + \epsilon\sin(\phi+\phi_S)\, F_{UT}^{\sin(\phi+\phi_S)} + \epsilon\sin(3\phi-\phi_S)\, F_{UT}^{\sin(3\phi-\phi_S)}$$

$$+ \sqrt{2\epsilon(1+\epsilon)}\,\sin\phi_S\, F_{UT}^{\sin\phi_S} + \sqrt{2\epsilon(1+\epsilon)}\,\sin(2\phi-\phi_S)\, F_{UT}^{\sin(2\phi-\phi_S)}\Big]$$

$$+ |S_T|\lambda_e\Big[\sqrt{1-\epsilon^2}\,\cos(\phi-\phi_S)\, F_{LT}^{\cos(\phi-\phi_S)} + \sqrt{2\epsilon(1-\epsilon)}\,\cos\phi_S\, F_{LT}^{\cos\phi_S} + \sqrt{2\epsilon(1-\epsilon)}\,\cos(2\phi-\phi_S)\, F_{LT}^{\cos(2\phi-\phi_S)}\Big]\Big\}$$

Cahn-effect + BM ⊗ Collins ($\cos\phi$ term)

Worm-gear (Kotzinian-Mulders) ⊗ Collins ($\sin(2\phi)$ term, F_{UL})

BM ⊗ Collins ($\cos(2\phi)$ term)

Sivers ⊗ D1 ($\sin(\phi-\phi_S)$ term)

Transversity ⊗ Collins ($\sin(\phi+\phi_S)$ term)

Pretzelosity ⊗ Collins ($\sin(3\phi-\phi_S)$ term)

Worm-gear ⊗ D1 ($\cos(\phi-\phi_S)$ term)

- $F_{XY[Z]}$ = structure function. X=beam, Y= target polarization, [Z= virtual-photon polarization]. X, Y ∈ {U, L, T} (Unpolarized, Longitudinally, Transversely)
- λ_e = helicity of the lepton beam
- S_L and S_T = longitudinal and transverse target polarization
- ε = ratio of longitudinal and transverse photon fluxes

Bacchetta et al., JHEP 02, 093 (2007)

The experimental observables

Spin-orbit correlations encoded in the TMDs induce observable azimuthal asymmetries in the distribution of the final-state hadrons.

E.g., for the case of SIDIS of an unpolarized lepton beam (U) on a transversely polarized nucleon (T) on can

1. construct a **Single-Spin Asymmetry** in each kinematic bin by reverting the target polarization
2. expand the asymmetry in a Fourier decomposition in terms of the relevant harmonics in ϕ and ϕ_S
3. extract the amplitude of each Fourier component (related to a specific combination of TMDs PDFs and FFs):

$$A_{UT}(\phi,\phi_S) = \frac{1}{S_T}\frac{\sigma_{UT}^{\uparrow} - \sigma_{UT}^{\uparrow}}{\sigma_{UT}^{\uparrow} + \sigma_{UT}^{\uparrow}} \propto \boldsymbol{A}_{\boldsymbol{UT}}^{\boldsymbol{\sin(\phi-\phi_S)}} \sin(\phi-\phi_S) + \boldsymbol{A}_{\boldsymbol{UT}}^{\boldsymbol{\sin(\phi+\phi_S)}} \sin(\phi+\phi_S) + \cdots .$$

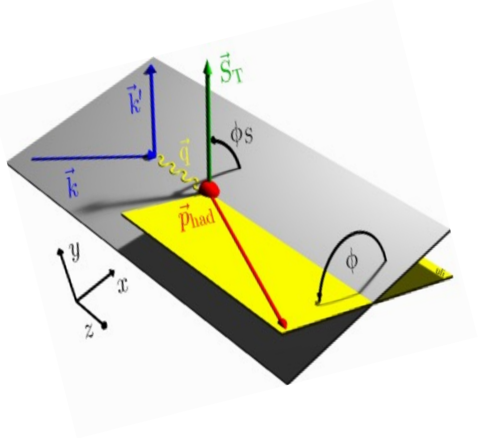

$$\boldsymbol{A}_{\boldsymbol{UT}}^{\boldsymbol{\sin(\phi-\phi_S)}} \propto \frac{F_{UT}^{\sin(\phi-\phi_S)}}{F_{UU}} \propto f_{1T}^{\perp} \otimes D_1 \; ; \qquad \boldsymbol{A}_{\boldsymbol{UT}}^{\boldsymbol{\sin(\phi+\phi_S)}} \propto \frac{F_{UT}^{\sin(\phi+\phi_S)}}{F_{UU}} \propto h_1 \otimes H_1^{\perp} \; ; \quad \ldots$$

$$\boldsymbol{A}_{\boldsymbol{LU}}^{\boldsymbol{\sin(\phi)}} \propto \frac{F_{LU}^{\sin(\phi)}}{F_{UU}} \propto \frac{M}{Q}\left[eH_1^{\perp} + f_1\widetilde{\boldsymbol{G}}^{\perp} + g^{\perp}D_1 + h_1^{\perp}\widetilde{\boldsymbol{E}}\right]$$

(sub-leading twist, related to quark-gluon-correlator)

The COMPASS DY Christmass present

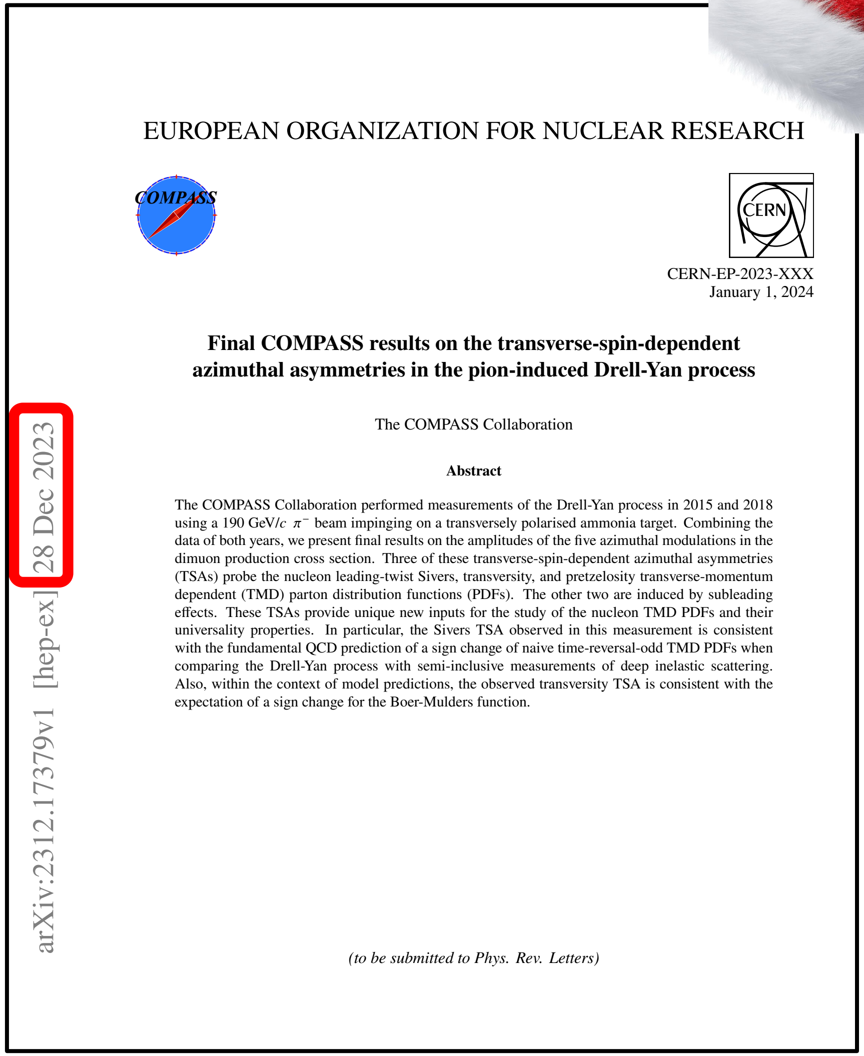

arXiv:2312.17379v1 [hep-ex] 28 Dec 2023

EUROPEAN ORGANIZATION FOR NUCLEAR RESEARCH

CERN-EP-2023-XXX
January 1, 2024

Final COMPASS results on the transverse-spin-dependent azimuthal asymmetries in the pion-induced Drell-Yan process

The COMPASS Collaboration

Abstract

The COMPASS Collaboration performed measurements of the Drell-Yan process in 2015 and 2018 using a 190 GeV/c π^- beam impinging on a transversely polarised ammonia target. Combining the data of both years, we present final results on the amplitudes of the five azimuthal modulations in the dimuon production cross section. Three of these transverse-spin-dependent azimuthal asymmetries (TSAs) probe the nucleon leading-twist Sivers, transversity, and pretzelosity transverse-momentum dependent (TMD) parton distribution functions (PDFs). The other two are induced by subleading effects. These TSAs provide unique new inputs for the study of the nucleon TMD PDFs and their universality properties. In particular, the Sivers TSA observed in this measurement is consistent with the fundamental QCD prediction of a sign change of naive time-reversal-odd TMD PDFs when comparing the Drell-Yan process with semi-inclusive measurements of deep inelastic scattering. Also, within the context of model predictions, the observed transversity TSA is consistent with the expectation of a sign change for the Boer-Mulders function.

(to be submitted to Phys. Rev. Letters)

190 GeV π^- on a NH_3 transv. pol target

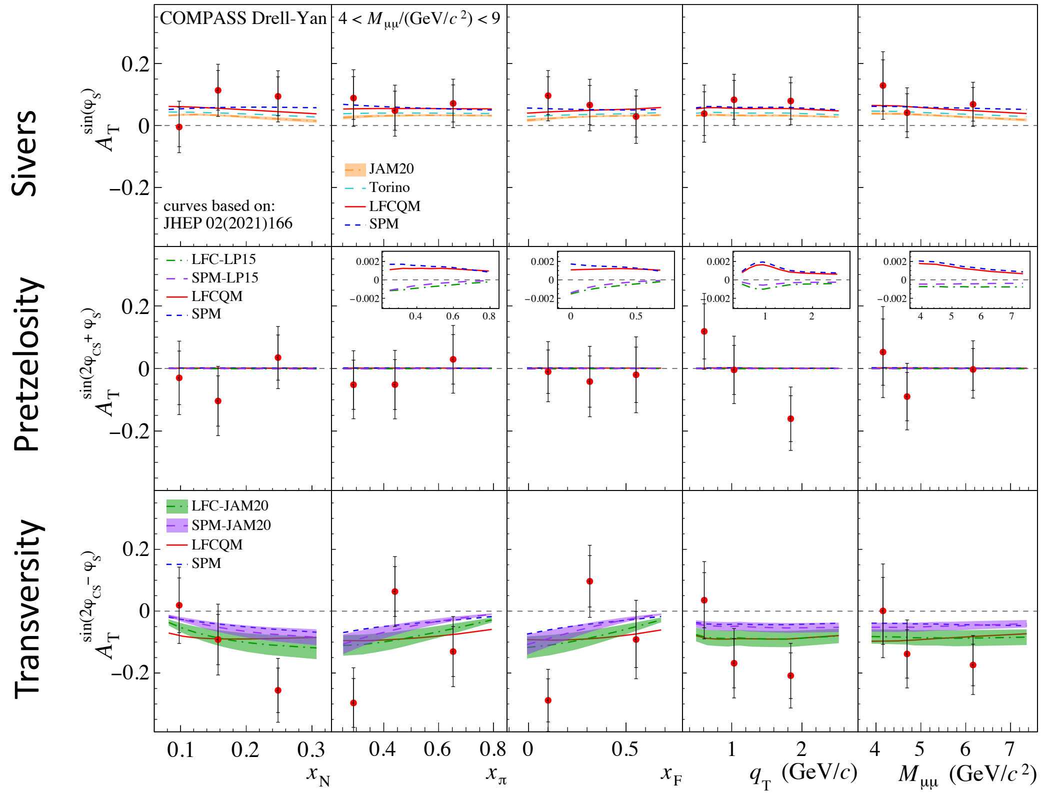

> 0

≈ 0

< 0

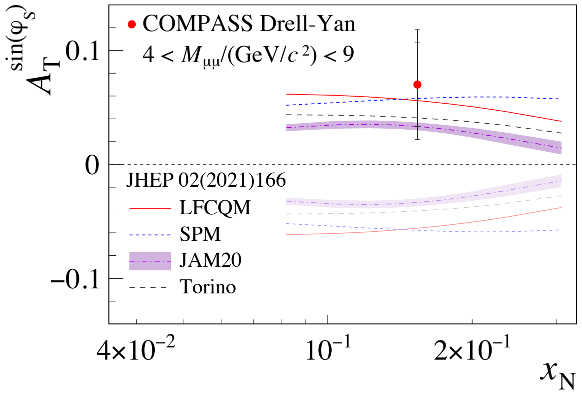

Checking TMD Universality!
Integrated Sivers amplitude consistent with models including the expected **sigh-change hypothesis (w.r.t. SIDIS)**

The main ingredients from theory

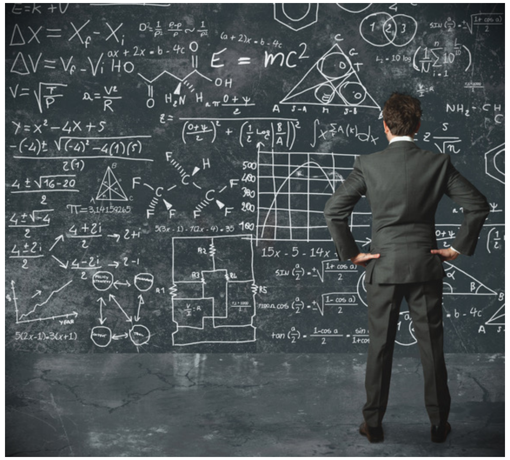

- **Factorization:** proved for SIDIS & DY (milestone!) $\rightarrow$ allows interpretation of cross-section
- **Universality:** essential to interpret underlying physics in different processes;
  - can be tested by comparing TMDs from different processes
  - predicted sign change for T-odd TMDs in SIDIS/DY awaits solid experimental check!
- **TMD Evolution:** different schemes/implementations now available;
  - Hard to apply to SIDIS data (low energy) where non-perturbative behaviour is dominant
  - can be tested by comparing results from experiments at different energies:

    $\langle Q^2\rangle_{Hermes,Compass,JLab12} \sim 2-5\ GeV^2;\ \langle Q^2\rangle_{BesIII} \sim 15GeV^2;\ \langle Q^2\rangle_{Belle/Babar} \sim 100GeV^2$
- **Phenomenological models:** L-C constituent quark models, spectator models, $\chi QSM, etc$
- **Lattice QCD:** recent results on Transversity, Sivers, B-M, worm-gear, tensor charge, ...

The main ingredients from phenomenology

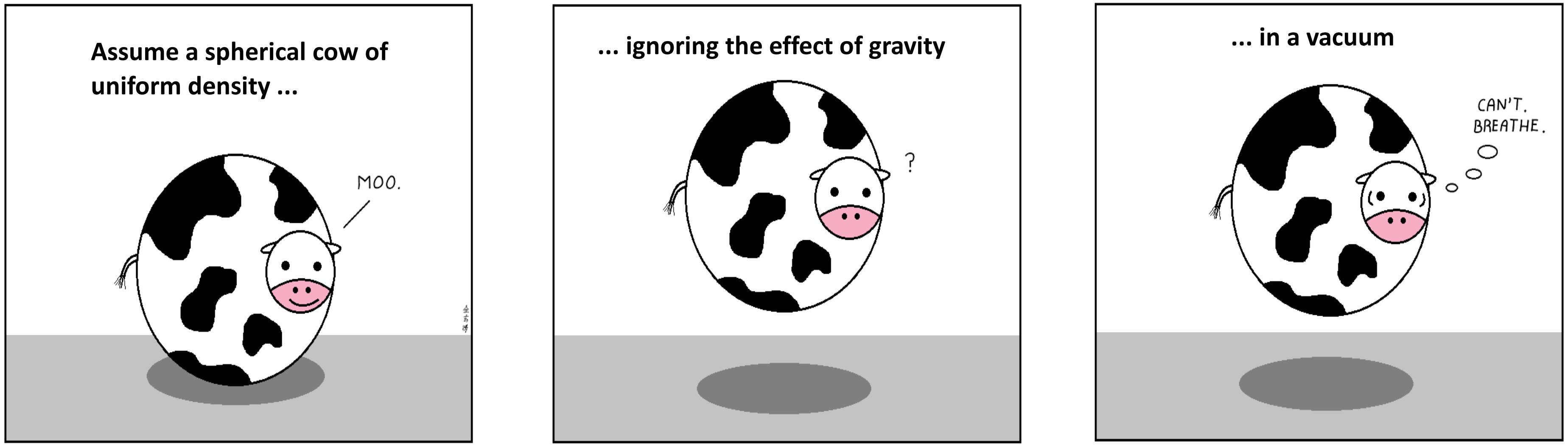

- Sofisticated **global analyses** of SIDIS and e^+e^- data (multi-D) based on **TMD-evolution**
- **Careful error propagation and advanced statistical tools**
- **Deconvolution of PDF & FF**: educated guess on $k_\perp$ distribution, $\boldsymbol{P_{h\perp}}$/Bessel-weighting
- **Knowledge of higher-twist** contributions is crucial to interpret leading-twist observables
- Separation between **CFR & TFR** (Fracture Functions, Berger criterion, x_F, ...)